Universidade do Minho
Escola de Engenharia

Maria Inês Bacelar Junqueira Braga

# VIBRATION SENSOR FOR IN-SITU MONITORING DURING ROBOT BASED COMPUTER POLISHING CCP

Master Dissertation
Master's degree in Product Engineering

Dissertation supervised by
**Prof. Dr. Antonio J. Pontes**
**Prof. Dr. Rainer Börret**
**Dr. Rui Almeida**

August 2021

## Acknowledgements

This master thesis was done in collaboration with the Aalen University and Minho University. For the realization of this thesis there are some people to whom I would like to express my appreciation for their help throughout the project.

Firstly, I would like to thank to my supervisor in Aalen university, Prof. Dr. Rainer Börret and to my supervisor in Minho university Prof. Dr. António Pontes.

I would especially like to thank Dr. Rui Almeida for all the support throughout the project, for the constructive comments and for all the help during the thesis work. I would also like to thank Max Schneckenburger for the suggestions and tips during the project and also Sven Höfler for the help and advice.

A special thanks to my family for all their support and especially to my mother, for without her the realization of this thesis would not have been possible.

I would also like to thank my friends Luis Gomes and Joana Carvalho for all their support and immeasurable friendship throughout the years.

I would also like to thank my family in Aalen for giving me the motivation to do the thesis and I would also like to thank my new friend from the Erasmus period Sónia Machado for the help and motivation during this project.

Finally, I would like to thank the attribution of the Erasmus+ scholarship, and thanks to this financial support it was possible to carry out this project at the University of Aalen in Germany.

## Statement of Integrity

I hereby declare having conducted this academic work with integrity. I confirm that I have not used plagiarism or any form of undue use of information or falsification of results along the process leading to its elaboration.

I further declare that I have fully acknowledged the Code of Ethical Conduct of the University of Minho.

## Abstract

The current polishing process, computer controlled polishing, parameters are set before the process start and are assumed constant throughout the entire process. However, these are just assumptions that can only be proven when sensors are mounted on a polishing head.

The aim of this research is access if the machine is working properly throughout the analysis of the vibrations, more specifically the vibrations of the bearings, to predict incoming maintenance of the polishing head before it even stops running and when the bearings needs to be changed in order to achieve the best performance of the machine. A sensor that will help to investigate the process is a vibration sensor. This sensor can help to get information about abnormal vibrations from the polishing head. A vibration sensor could help to predict the lifetime of bearings or from the V-belt pulley.

The function of monitoring and controlling the vibration caused on the polishing head is important because with this analysis is possible to discover abnormal vibrations and maybe correct them allowing to have more control over the surface that is being polished. This optimizes the operation of the polishing machine, since the precision of the machine is one of the most important factors, as it has a great impact on the polishing performance of the final part.

A research was done in order to know which polishing parameters could be measured using a vibration sensor as well as position and assembly on the polishing head and then conclusions were made where it was possible to see that in fact it was possible to condition monitoring with this sensors and to identify the damages on the bearings throughout the vibrations.



**Keywords:** Vibration sensor, Polishing head machine, Vibration analysis, bearing analysis, condition monitoring.

## Resumo

No processo de polimento atual, polimento controlado por computador, os parâmetros são definidos antes do início do processo e são assumidos constantes ao longo de todo o processo. Contudo, estes são apenas suposições que só podem ser provadas quando os sensores são montados numa cabeça de polimento e o seu comportamento é monitorizado.

O objetivo desta investigação é verificar se a máquina está a funcionar corretamente através da análise das suas vibrações, mais especificamente as vibrações dos rolamentos, para prever a manutenção da cabeça de polir antes mesmo de esta parar de funcionar e também perceber quando os rolamentos precisam de ser mudados para se obter o melhor desempenho da máquina. Um sensor que irá ajudar a investigar o processo é um sensor de vibração. Este sensor pode ajudar a obter informações sobre vibrações anormais da cabeça de polimento. Um sensor de vibração pode ajudar a prever a vida útil dos rolamentos pois através do seu desempenho pode-se observar o seu desgaste através da diminuição da sua performance.

A função de monitorizar e controlar a vibração causada na cabeça de polimento é importante porque com esta análise é possível descobrir vibrações anormais e talvez as corrigir, permitindo ter mais controlo sobre a superfície que está a ser polida. Isto otimiza o funcionamento da máquina de polir, uma vez que a precisão da máquina é um dos fatores mais importantes, uma vez que tem um grande impacto sobre o desempenho no processo de polimento da peça final.

Foi feita uma pesquisa para saber quais os parâmetros de polimento que podiam ser medidos utilizando um sensor de vibração, bem como a posição e montagem na cabeça de polimento, e depois foram tiradas conclusões onde era possível ver que, de facto, era possível monitorizar o seu estado com estes sensores e identificar os danos nos rolamentos através das suas vibrações.

**Palavras-chave:** Sensor de vibração, Máquina de cabeça de polir, Análise de vibração, análise de rolamentos, monitorização do estado.

## Abbreviations

AI- Analog Input

BCM- Balluff Condition Monitoring

CAD- Computer Aided Design

cDAQ- Compact DAQ

CSV- Comma-separated values

DAQ- Data Acquisition

DOE- Design of Experiments

FFT- Fast Fourier Transform

IO- Input/Output

IODD- Input/Output Device Description

MATLAB- Matrix Laboratory

MEMS- Micro-Electro-Mechanical System

NI- National Instruments

PLC- Programmable logic controller

RMS- Root mean square

TCP- Tool Center Point

ZOT- Zentrum für Optische Technologien/ Centre for Optical Technologies

# Index

## List of Figures

## List of Tables

# 1. Introduction

In this first chapter a brief contextualization of the project will be made, then the objectives and the aim of the project will be addressed, as well as the challenges and problems it presents.

## 1.1 Contextualization

This project is based on the integration of a vibration sensor in a polishing head robot. The function of monitoring and controlling the vibration caused on the polishing head is important because with this analysis is possible to discover abnormal vibrations and maybe correct them allowing to have more control over the surface that is being polished. This optimizes the operation of the polishing machine, since the precision of the machine is one of the most important factors, as it has a great impact on the polishing performance of the final part. The more precise the machine, the better the results will be for the part being polished.

## 1.2 Objectives and aim of the project

This project was carried out in the Centre for Optical Technologies (ZOT – Zentrum für optische Technologien) in the Aalen University. This project aims to use vibration sensors to analyze the polishing head machine from the company Carl Zeiss and understand how it operates or behaves. During this project some of the objectives were to perform a market research and find the most appropriate and suitable vibration sensor for this application. So that later on when the vibration sensor is installed on the robot it will be possible to understand or analyze what would be the most appropriate place to fit the sensor in order to obtain/collect the best data results and also to understand what can be monitored with this sensor. Another objective was to test the bearings that were used in the machine, in order to obtain knowledge about the current condition of the bearings and then after to test the vibration sensors directly on the polishing head machine. And last but not the least to read the results obtained and draw conclusions.

1.3 Challenges/Problems

This project presented some challenges such as fitting the sensor to the polishing machine, because this factor has a big impact on the data obtained by the sensor. The better the sensor is installed the better and more accurate will be the obtained results. The other challenge of this project would be how to transfer the data to the PLC (Programmable logic controller) or directly to a computer, i.e. how this connection would be made or if another type of intermediate device would be needed to make this connection.

Another problem with this project is the connection between the sensor and the PLC or computer, as there may be a risk of the cables being damaged in use. With this problem then comes another challenge for this project which is how to solve this problem of the cables so that there is no risk of them breaking. The challenge of this project is also to understand what can be monitored with the sensor and how to use the information obtained to improve the operation of the polishing machine, and finally, how to read the data obtained from the tests with the sensor.

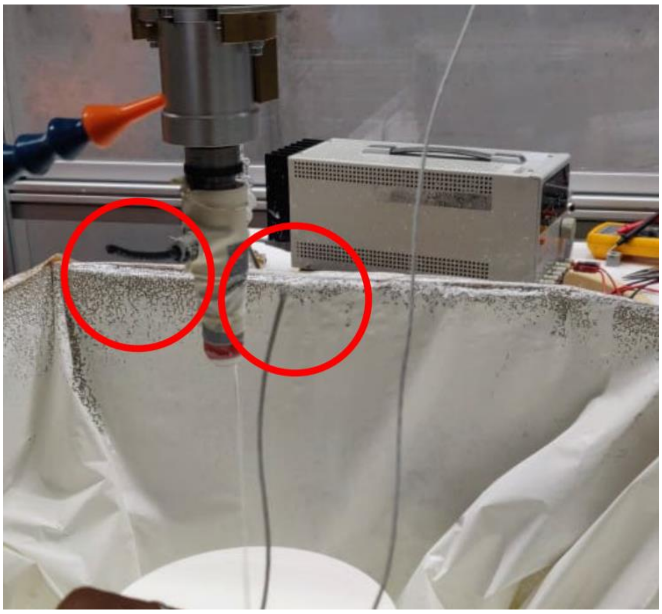

*Figure 1 – Cable damaged on previous trials*

## 2. Polishing Process in the ZOT

### 2.1 Polishing

Polishing is one of the oldest methods of removing material, invented several decades ago. This is a process used to generate surfaces with very high tolerances in geometry and roughness characteristics. This process remains one of the most important finishing methods.

In this process a small portion, particle sizes ranging from one to hundred micrometers, of the material is removed in order to obtain a smoothing surface. This process works in the following way, by means of a rotating disk which is rubbered with polishing particles to obtain a smooth surface.

The polishing process generates a reflective surface. Most polishing processes use a pad that contains an abrasive surface, and this pad is smoother than the part being polished. That is, the workpiece is the hard component and the pad is the soft component. During this polishing process micrometers of material are removed. Usually polishing is achieved by using a fine-micron or sub-micron abrasive particle in conjunction with a liquid, such as polishing slur. In the polishing process a polishing pad and a water-base slur are then used to generate a reflective and clear surface. Usually, there are some dirt stains or a few cracks present on the workpiece that are not visible to the naked eye, and this dirt can then be removed by the polishing process.

### 2.2 Computer controlled Polishing

CCP stands for Computer-Controlled polishing and is a process used to obtain a high-quality surface finish, for example in optical lenses, because high accuracy can be obtained when robots are used. As already mentioned, the main purpose of the polishing process is to obtain an even and polished surface on the workpiece.

Nowadays, robots are implemented for the polishing process as they are more efficient in terms of speed, safety, and can also be used for mass production. In other words, the polishing process has improved significantly through the use of robots, because they have precision and repeatability. In addition, the robot has the advantage that it is flexible and can polish easily curved surfaces that are complex to polish. Another advantage of using the robot is that you can improve safety, consistency, and quality.

Computer-Controlled polishing has more advantages than traditional polishing methods or techniques, because it allows you to easily finish polishing in less time and its accuracy is much higher compared to traditional polishing.

### 2.3 Polishing Robot in the ZOT

In the ZOT (Centre for Optical Technologies or Zentrum für Optische Technologien) there are several robots from the company ABB [1]. These robots have different sizes and accuracies. The robot used in this work was the ABB IRB 4400 robot that is used for plastic and glass polishing.

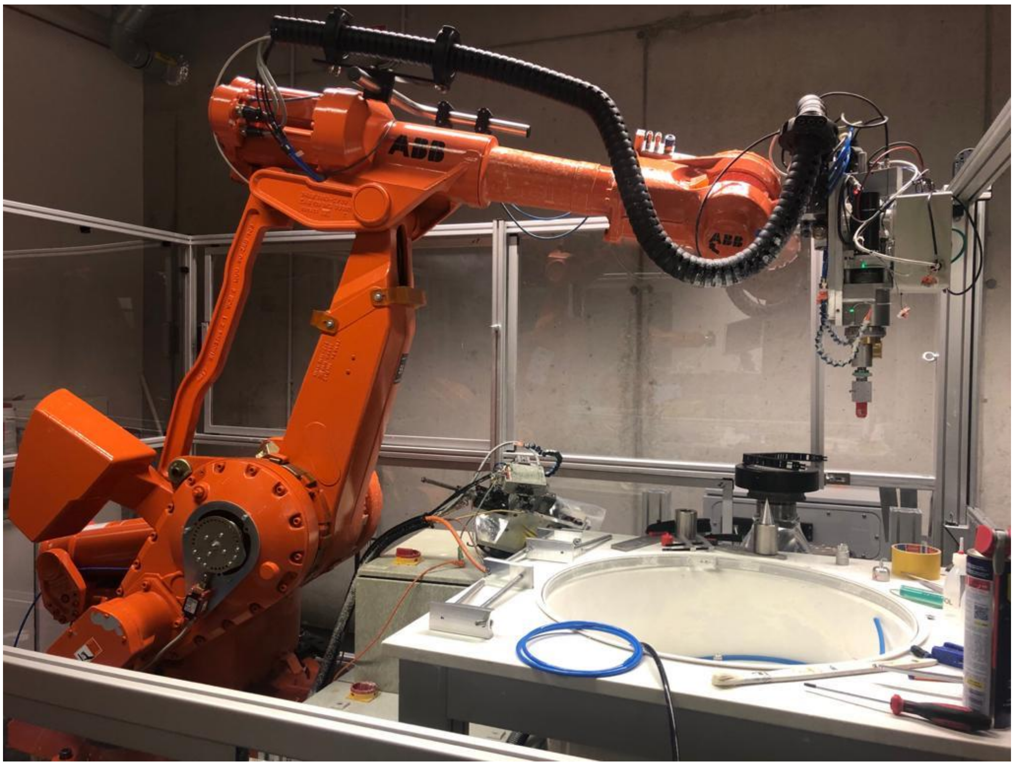


*Figure 2 – Robot ABB IRB 4400 with polishing head from Zeiss company*

This is a large-sized robot that is versatile and fast. This robot can support loads up to 60 Kg and has a range of 1,96 meters.

The robot is then responsible for the accurate motion system of the polishing tool on the surface. This is a 6-axis industrial robot. The most important polishing parameters of this robot are the speed of rotations applied from the electric motor to the polishing tool and the pressure applied from the pneumatic cylinder to the polishing tool.

Basically, this robot is composed of a polishing head, from Zeiss, which is located at the end of the robotic arm, and that polishing head has a polishing tool at the end, which will remove material by rotating the polishing tool tip onto the part to be polished. The part to be polished is fixed on a worktable so that it does not move during the process using a zero-point clamping system. The polishing slur consists of sand and water particles, and then is added to the part. Without his liquid agent no material would be removed in the polishing process. In figure 3 it can be observed the workpiece with polishing slur, white liquid on top of the workpiece.

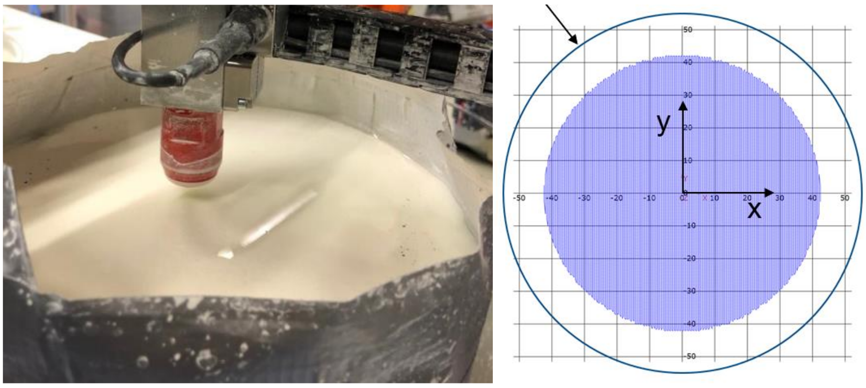


*Figure 3 - Polishing slur on the workpiece; Polishing track on the Zaphod program (Units in mm)*

To control and program the robot a program was created where the duration of the polishing process, the force to be applied, and the rotations per minute were defined. For the creation of this program the software "Zaphod", that was created in ZOT, was used. Through this program is created the code that guides the robot during the polishing process according to the area of the part to be polished. For a correct operation of the robot, it is also necessary to calibrate. This calibration is done in order for the polishing robot to know where is located the workpiece and where the TCP of the robot is. For this process the TCP is recorded and the part to be polished is measured. Then these values are integrated into the code that commands the robot operation.

# 3. Research

At an early stage of the project, research was conducted where the various types of sensors were studied, and why it is important to analyze and monitor vibrations. This chapter also discusses the sensors that were considered for use in this project, and finally a comparison of the various sensors is made, and some conclusions are drawn.

## 3.1 Vibration analysis and Monitoring vibration

Vibration can be defined as a mechanical oscillation about an equilibrium position of a machine or component, or simply the back-and-forth motion of a machine or component. Vibration or oscillation is any motion that repeats itself, regularly or irregularly within a time interval.

"Vibration is an oscillating motion about an equilibrium so most vibration analysis looks to determine the rate of that oscillation, or the frequency. The number of times a complete motion cycle occurs during a period of one second is the vibration's frequency and is measured in hertz (Hz). For simple sine waves the vibration frequency could be determined from looking at the waveform in the time domain; but as we add different frequency components and noise, we need to perform spectrum analysis to get a clearer picture of the vibration frequency." (by Steve Hanly)[2]

It is important to analyze vibration because many of the common vibration problems are misalignment, defective bearings, looseness or unbalance. As mentioned before and further again, analyzing the vibration of the machine's bearings allows us to get information about abnormal vibrations in the polishing machine. With this information it is possible to predict the next maintenance of the polishing machine before it has to stop working.

As mentioned before, the most common problems with vibration are misalignment, defective bearings, unbalance or looseness and by analyzing the machine's bearing vibrations, it was possible to obtain information regarding abnormal vibrations of the polishing head. Because normally vibration in a machine or industrial equipment is part of normal machine operation, but sometimes it can also be a sign of machine problems.

Through vibration analysis it is possible to perform a machine screening, after which it is possible to diagnose or analyze a possible failure. With this data obtained it is possible to take the right action at the right time to be able to correct the machine before the machine error or failure gets worse.
The actual process parameters of the polishing machine are defined before starting the process and are assumed to be constant during the entire process.

By installing a vibration sensor on the machine this allows to spend less time taking manual readings on the machine that may be working properly. Machine vibration analysis is a cost-effective way to monitor machine elements and automatically receive data collection, which helps to understand when it is really necessary to intervene and perform preventive maintenance on the machine. In other words, monitoring vibration over time helps predict problems before any more serious risks occur. Because if the machine has an unforeseen problem this will delay production and therefore increase costs, which could be predicted by analyzing its vibration. When these kinds of problems are detected early there is the opportunity to schedule maintenance, thus reducing machine downtime, thus reducing the increased costs.

In addition to being able to tell when the machine needs maintenance and to reduce costs, vibration analysis also has the advantage of being able to determine the current condition of the machine and what the specific cause or location of the machine problem is.

When it comes to types of vibration and vibration analysis of a bearing, in terms of machine monitoring there are two types of vibrations: axial vibration and radial vibration. Axial vibration is a vibration longitudinal to the shaft or parallel to the motor shaft. Radial vibration occurs when a force is applied off the shaft. For example, a misalignment of the shaft can cause axial vibration.

## 3.2 Graphics for analysis

The acquisition of vibration data is only one part of the challenge of vibration measurement, the other major part is the analysis of the data that is acquired, as it is important to understand the types of waveforms associated with vibration analysis, what the important differences are between them, and when it is most appropriate to use each type of vibration analysis tool. In order to later be able to analyze the results that will be obtained, and by doing this research it was possible to realize that there are different types of graphics that allow to get different readings of different aspects of vibration. Usually, when analyzing the vibration data in time domain, i.e. acceleration/vibration amplitude plotted against time, one is limited to a few parameters in quantifying the strength of the vibration, such as amplitude, peak-to-peak value and RMS.

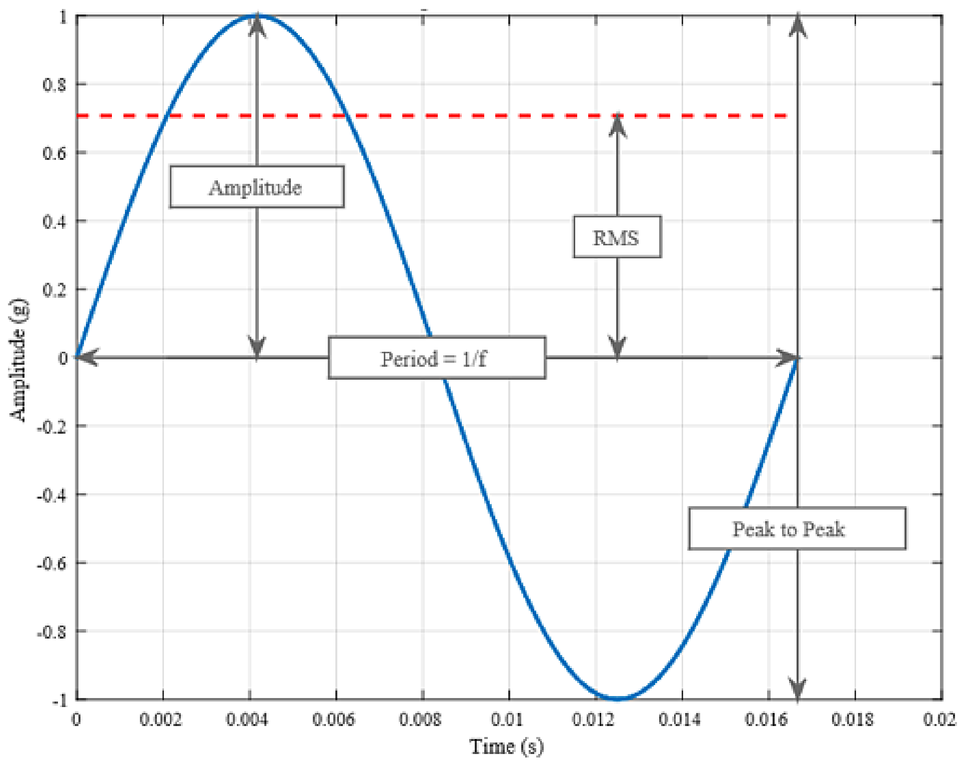


*Figure 4 - Example of a simple 60 Hz sine wave*
*Source: https://www.researchgate.net/figure/A-simple-60-Hz-sine-wave-is-shown-with-the-amplitude-peak-to-peak-RMS-frequency-and_fig8_318827258*

In figure 4, it can be observed an example of a simple 60 Hz sine wave, where it can be seen the amplitude of the wave, the RMS and the peak to peak.

The RMS, which stands for Root Mean Square, is a value that is generally very useful because it is directly related to the energy content of the vibration profile. That is, the RMS value of a periodic waveform is the same as the effective value of the waveform, and this is obtained by taking the square root of the mean of the square waveform.

“The peak amplitude of a sinusoidal waveform is the maximum positive or negative deviation of a waveform from its zero-reference level.” (John Clayton Rawlins M.S., in Basic AC Circuits (Second Edition), 2000)

Any waveform is really just a set of series of single sinusoids or sinusoids of different amplitudes, frequencies or phases.

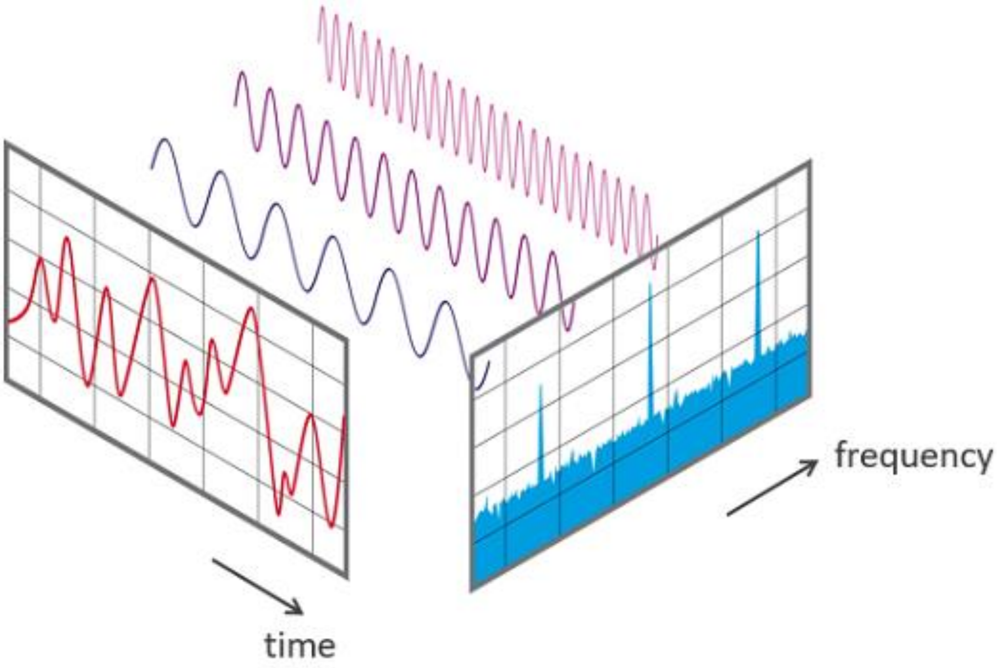


*Figure 5 - View of a signal in the time and frequency domain*
*Source: https://www.nti-audio.com/en/support/know-how/fast-fourier-transform-fft*

Therefore, the Fourier series is a series of sinewaves and is used for spectrum analysis to deconstruct a signal into individual sine waves components and the result is the amplitude of the acceleration/vibration as a function of frequency, which then allows to perform analysis in the frequency domain to gain a deeper understanding of the vibration profile. In order to better understand and visualize a Fourier transform it can be observed in figure 5 how it works.

## 3.3 Types of sensors

In an initial phase a research about vibration sensors was carried out to understand how they work and what were the different types of sensors, as it can be seen in the scheme of figure 6. In this research it was possible to conclude that there are three main types of vibration sensors, them being: accelerometers, strain gauge and Eddy-Current.

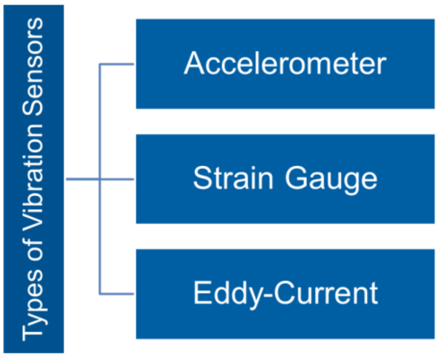


*Figure 6 - Types of vibration sensors*

Accelerometers are devices that measure the vibration or acceleration of a moving structure. Within the category of accelerometers there are several types available on the market. Accelerometers are devices that, as the name implies, measure acceleration, which is the rate of change of the velocity of an object.

Acceleration measures the change in velocity with respect to time. In other words, acceleration is the physical quantity that measures the change in velocity of a mobile object as a function of time. The unit of acceleration according to the International System of Units (SI) is the $m/s^2$ (meter per square second), but it can also be measured in G-Forces (g). One G-Force here on planet earth is equivalent to 9.8 $m/s^2$. The sensors that measure this physical quantity are called accelerometers. Usually, the acceleration is given as a part or multiple of the gravitational average acceleration g.

Strain gauge sensors are devices that as the name implies measure the strain of a machine component. A strain gauge is a sensor to which resistance varies with the force applied. Basically, this sensor converts a force, pressure or voltage into an electrical resistance difference that can then be measured. For when external forces are applied to a stationary object, stress and strain are the result.
In practice this sensor works as when there is a strain applied to any metallic cable, the length of this cable increases and its diameter decreases. This increase in length and decrease in diameter will change the resistance of the cable, which then provides our measurement of the strain of the component or machine.

An eddy-current sensor or capacitive displacement sensor are devices that are not in contact with surfaces and measure the position and or change of position of a conductive component. Basically, these sensors operate with magnetic fields. The sensor contains a probe that creates an alternating current at the tip of the probe. This alternating current that creates small currents in the component being monitored is called eddy-currents. In other words, the sensor monitors the interaction of these two magnetic fields.

As these two fields interact, the sensor produces a voltage proportional to the change in the interaction of the two fields.

When using this type of sensor, it is important to keep in mind that the component to be monitored must be three times the diameter of the sensor in order for it to operate normally otherwise advanced sensor calibration is required.

The most common and most accurate of these three types of vibration sensors are the accelerometers. And it was on this type of sensors that the research was most focused, because this sensor has a good frequency range, which means that it can sense/measure fast or slow applications. In addition to this frequency range these accelerometers are also more affordable and more durable. These sensors must be mounted directly on the machine.

Strain gauges, on the other hand, are versatile and accurate while being suitable for inconvenient to reach locations because of their thin thickness. However, these sensors can be difficult to install correctly and to get the data correctly. Usually amplifiers are needed, which will increase the cost.

Finally, eddy-current or capacitive sensors have a medium accuracy and are not ideal for high resolution applications. But they are very durable which makes them perfect for dirty environments. And just like accelerometers they must be mounted directly on the machine to be monitored.

### 3.4 Vibrations sensors

A sensor is a device that detects and responds to one type of input from a physical environment. This physical input can be light, heat, pressure, or others. And the output is usually a signal that is converted to a readable display where the sensor is located or is transmitted in electronic form to a reading or processing network.

During the research, sensors of different brands were analyzed and compared. Some of the brands are as follows: Balluff, SKF, ASC, Althen Sensors, Advantech, Fluke, Emerson, IFM, MMF, GP systems, SDT Ultra sound among others.

To select a vibration sensor for this specific project it was important to take into consideration some of the following factors, such as range and accuracy, environmental conditions, and the shape of the surface to be measured. The most important factors in deciding on the sensor were its shape and size, since it had to be relatively small, and whether its range and accuracy fit the specific needs of this work.

Its range and accuracy are decisive factors, because the proportionality of its offset, acceleration, or deviation depends on the frequencies of interest and the level of signals involved/intended. By range and precision it is meanted measuring range, frequency range and accuracy of the data.

The type of mounting of these sensors was also taken into consideration because their correct installation is a determining factor to obtain a good and accurate diagnosis/reading of the machine condition results.

To simplify this research, tables were developed with the most relevant sensor specifications in order to simplify the analysis and comparison between them. In table 1 and table 2 below, we can observe the comparison between the sensors.

*Table 1 – Vibration sensors research*

| Brand | | BALLUFF | BALLUFF | IFM | SKF | ASC |
|---|---|---|---|---|---|---|
| Model | | BCM0001 | BCM0002 | VSM101 | CMSS 2100 | OS-325MF-PG |
| Size | Height | 3,2 cm | 3,2 cm | 4,73 cm | 5,3 cm | 2,7 cm |
| | Width | 2 cm | 2 cm | 2,62 cm | 2,46 cm | 2,7 cm |
| Mass | | 30 g | 30 g | 187,2 g | 90 g | 68 g |
| Measuring axes | | 3 | 3 | 3 | 3 | 3 |
| Frequency range | | 2 to 3200 Hz | 2 to 3200 Hz | 0 to 4500 Hz | 0,5 to 14 000 Hz | ±2 to ±200 g |
| Working temperature | | 0 to 70 °C | 0 to 70 °C | -35 to 85 °C | -50 to +120 °C | -55 to +125 °C |
| Price | | 255 € | 319 € | 448,50 € | ~450 € | - |
| Material | | Stainless steel | Stainless steel | Stainless steel | Stainless steel | Stainless steel |
| Wireless | | no | no | no | no | No |

In table 1 it can be seen different vibration sensors with cables. Of the various characteristics of the sensors, the most relevant for the decision to choose a sensor was the size of the sensor, since it should not be too large, its price, and also the type of sensor, i.e. whether the type of sensor met the characteristics needed for the project or which one would fit better within the scope of the project.

The sensor of the company BALLUFF, model BCM0001 is easy to parameterize and it is easy to match the processing of the sensor to a specific application. This sensor has the functions vibration velocity, vibration acceleration and contact temperature. Another advantage of choosing this sensor is the fact that the university has this sensor, thus bringing no added cost to the project. The BCM0002 sensor, from the same company, is basically the same sensor but is a newer version, and besides measuring vibration velocity, vibration acceleration and contact temperature, it can also measure vibration severity zone, relative humidity and sensor self-awareness. Since the BCM0001 sensor fits the project parameters and the most updated version of this sensor is not necessarily more beneficial for this project, there is no need to invest in this sensor for this reason the BCM0001 sensor was one of the selected sensors.

The sensor of the company IFM, model VSM101 is a robust sensor with high mechanical overload protection. For easier installation the company offers an adapter or a magnet, but it is not included with the sensor.

The sensor from SKF company, model CMSS 2100 is hermetically sealed for installation in high humidity areas. This sensor contains a small physical size for small bearings or hard-to-reach areas.

Finally, another of the sensors selected was the sensor from the company ASC, model OS-325MF-PG. This sensor is a MEMS capacitive accelerometer with a good frequency range, it has a robust and reliable design that is why it has a very high shock resistance. This was one of the sensors selected since the frequency range fits the needs of the project.

### 3.5 Wireless vibrations sensors

*Table 2 – Wireless vibration sensors research*

| | | | | | | | |
|---|---|---|---|---|---|---|---|
| **Brand** | | FLUKE | ALTHEN and TREON | PCE | PCB Piezotronics | Yokogawa | iQunet |
| **Model** | | 3561FC | Iot Vibration Node | VMS 501 | 670A01 | Sushi XS770A | IVIB161010-ACC3-016 |
| **Size** | **Height** | 6,15 cm | ~7,5 cm | 8 cm | 11,18 cm | 9,7 cm | 5,7 cm |
| | **Width** | 2,41 cm | 2,8 cm | 4 cm | 3,49 cm | 4,6 cm | 4,7 cm |
| **Weight** | | 40 g | 129 g | 217 g | 454 g | 260 g | 35 g |
| **Measuring axes** | | 3 | 3 | - | - | 3 | 3 |
| **Frequency range** | | 10 to 1000 Hz | 10 to 1000Hz | 5 Hz to 10 KHz | 4 to 2300 Hz | 10 to 1000 Hz | 12 to 3200 Hz |
| **Working temperature** | | -30 °C to +80 °C | -40°C to +85 °C | -20 to +120 ° C | -20 to +70 °C | -20 to 85°C | -20°C to +70°C |
| **Price** | | 928,57 € | - | 1 190,23 € | ~500 € | - | 357,14 € |
| **Material** | | Plastic | Stainless Steel | Stainless Steel | Stainless Steel | Plastic, Stainless steel | Thermoplastic (case) |
| **Accuracy** | | - | +/- 2°C | - | - | - | - |
| **Wireless** | | yes | yes | yes | yes | yes | yes |
| **Gateway included** | | yes | no | no | no | no | no |

The table 2 has also been developed for the wireless vibration sensors for the same purpose, to facilitate the overview of the different sensors. In the following it will be briefly explained some of the general advantages or disadvantages of each wireless sensor.

The company FLUKE's sensor, model 3561FC has the advantage of being easy to use, as it is intuitive in the sense that it is not necessary to be an expert to be able to operate this sensor. It is easy to install, but a disadvantage is that it is difficult to remove because it uses glue to attach it. On the other hand, as it is a wireless sensor it doesn't need cables. This sensor also has the great advantage that it already includes a gateway, so there is no need to buy this one afterwards. This sensor is sold in a pack, this includes 4 sensors, a gateway, plus one year of using its software. This sensor is versatile, can have several applications and allows remote vibration monitoring. This sensor allows you to get real-time information about the date history. It has a battery life of three years. And finally, it is good for remote monitoring in dangerous places or places that are difficult to access.

The sensor of the companies Althen and Treon, model IOT vibration sensor node is designed for demanding industrial conditions. It is dust and water resistant. But unfortunately, it is necessary to buy the gateway separately, which brings an extra cost. The mounting method for this sensor is via a M8 thread.

The sensor of the company PCE, model VMS 501 has a long battery life, and is easy to connect to the machine, as it is attached with a magnetic base. This sensor is easy and quick to install. This sensor can save the measurements temporarily when the connection to the server is interrupted.

The sensor of the company PCB Piezotronics, model 670A01 has the major advantage of being easy to remove or change its battery. A small aside is that accelerometers are better in the sense that they can measure DC acceleration as opposed to piezoelectric ones. This sensor comes with a mounting stud, a long stainless-steel screw with hex socket and brass tip. It is not recommended to mount the sensor with a magnet due to the size and mass of the sensor. The mounting pad can be epoxied onto the machine with an Epoxy Kit to attach it to the machine.

The sensor of the company Yokogawa, model Sushi XS770A can be installed in areas where flammable gas or steam is present. It has a long-distance communication (more than 10km). Configuration and monitoring status can be done via a smartphone which makes this sensor simpler and more intuitive to use. Using an Android-based smartphone with NFC (Near Field Communication) it is possible to send the date to a cloud. The XS770A can be mounted easily by a screw or a magnet.

Finally, the sensor from the company iQunet, model IVIB161010- ACC3- 016 has a long battery life but does not include the server/gateway which is expensive. The parameters of this sensor can be set remotely, such as the sampling rate, samples number, dynamic range e automatic measurement interval. This sensor can be installed with M3 screws or epoxy adhesive for permanent mounting.

## 3.6 Advantages and disadvantages

After analyzing each sensor, it was possible to see more generally the advantages and disadvantages of the different types of sensors.

The wireless vibration sensors have a great advantage in that there is no need for cables, thus solving one of the initial problems of the project, which was the wear and tear or the chance of cables becoming damaged due to the high revolutions of the machine causing such possible damage. Since the machine works at high revolutions per minute continuously, it is natural that with the passage of time and with the vibrations to which the cables are subjected, they start to wear out, leading to their breakage.

Normal (cabled) vibration sensors have the advantage of being more affordable, smaller and more compact, and versatile, meaning that they can be applied in a variety of situations. Wireless vibration sensors, on the other hand, are easy to install, have the great advantage of not needing a connecting cable, but the disadvantage is that they require an additional device to receive the information and send it to a receiver - in this case a computer - where the data can later be stored and analyzed. The biggest disadvantage of these wireless sensors is that the additional device usually ends up being more expensive than the sensor itself, which is already expensive compared to normal sensors.

### 3.7 Overall comparisation and conclusions

After careful consideration of the various sensors and taking into account the needs of the project, the sensors selected were the BCM0001 sensor from BALLUFF and the OS325-PG sensor from ASC. The BALLUFF sensor is a sensor that the university already owned and is useful for the project since it is an intelligent sensor that already provides processed data. One of the sensors that could also fit in the project would be the BCM0002 sensor which is an improved version with more qualities than the BALLUFF (BCM0001) sensor, but after a quick analysis it was possible to realize that these new qualities would not be so relevant for this project and that the sensor that the university already had was sufficient for the job, so there was no need for extra costs. Since there is already a smart sensor it was thought that it would also be useful to get a sensor that can provide raw data so that there would be more freedom to work with the results obtained and also be able to compare the results between the two sensors. For this the ASC-325 sensor was selected and purchased, as this is a sensor that reads and provides raw data.

## 4. Programming

For this project it was necessary to use programming to be able to obtain graphics and to be able to process and manipulate the data obtained from the trials conducted in the workbench and on the polishing head. It was also necessary to design an app using MATLAB [6] for the ASC-325 sensor.

### 4.1 MATLAB

One of the programs used in this project was MATLAB. MATLAB is a program developed by an American company called MathWorks. This program specializes in matrix calculations and also for optimizing and solving mathematical problems in science and engineering. This software also provides the possibility to simplify the implementation of hardware, such as a DAQ device. DAQ stands for data acquisition, and data acquisition is the process of sampling signals that measure real world physical conditions and convert the sample results into digital numeric values that can be manipulated with a computer. This will be important later on when connecting the OS-325MF-PG sensor.

#### 4.1.1 Basics in MATLAB

For this work it was necessary to use the MATLAB program for the programming part. In the beginning it was necessary to learn how to use this program and understand how to program for this project. Initially basic commands were used to perform basic functions such as importing the data into the program or plotting the data. Some of the basic commands used can be seen in figure 7.

```
flange=importdata('Filename.txt');
time=flange.data(:,1);              %Exports first collumn and stores it in time
xdata1=flange.data(:,2);            %Exports second column and stores it in xdata1
xdata2=flange.data(:,5);
plot(time, xdata1);                 %Time=x axis and xdata1=y axis
hold on;                            %keeps working on the same plot
plot(time, xdata2);
title('Inserttitle');
xlabel('X-axis name');
ylabel('Y-axis name');
hold off;
clf;                                %clear figure
clear;                              %clear variables
```

*Figure 7 - Example of simple commands on MATLAB*

To know how to analyze the data obtained with the trials, some basic coding experiments were carried out in MATLAB to learn how to work with this program and how to work with the data that will be obtained later on.

### 4.1.2 Plotting graphics with MATLAB

Some graphs were made using data from old vibration sensor tests, and with that data graphs of the different axes, xyz, and also a FFT of that data were made. To run these graphics, it was necessary to gain basic knowledge of coding. It was necessary to understand which commands were needed and which functions were in each line of code, and what these functions changed in the results or in the parameters of the graphics. In figure 8, it can be observed the commands used and the graphic result.

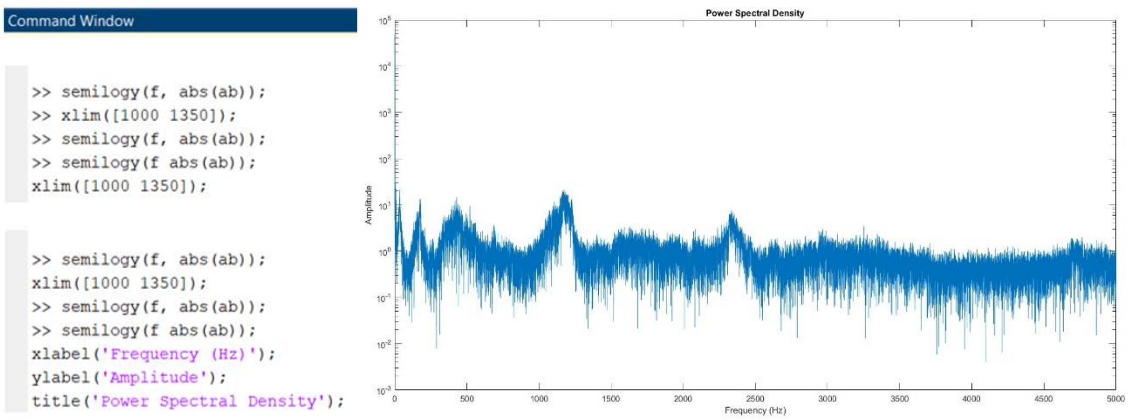


*Figure 8 - Example of a FFT plotted using MATLAB*

### 4.1.3 Software programming

To use the OS-325MF-PG sensor it was necessary to develop an app using MATLAB software, through the App designer option. This program creates data logs of DAQ hardware. For the logging procedure a graphical user interface is created. This allows the user to easily perform the measurement and also provides the possibility to see in real time the data being saved. In figure 9 it is possible to observe the display of the app created for the measurements.

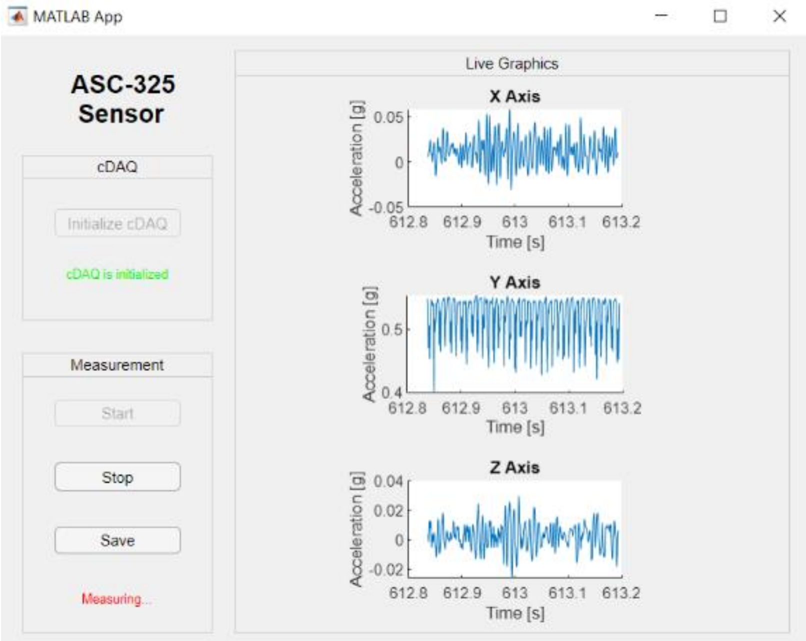


*Figure 9 - ASC-325 Sensor App designed with App Designer in MATLAB*

The first step to use this app is to open MATLAB and inside this program open the app, after this it will be showed the interface, as can be seen in the figure 9. This app has three different menus. In the first menu titled cDAQ this contains a button that when clicked starts the DAQ device, and when it is initialized appears the app gives feeback as it can be seen in green letters in figure 8. This action calls a subprogram "Init_DAQ" where all settings for the hardware DAQ are made. The calibration parameters for this sensor have been entered into the code, corresponding to the calibration protocol provided by the sensor manufacturer.

Another menu is the Live Graphics menu where it can be observed in real time the data being taken on the various axes.

There is also a menu called Measurements, which contains three commands. The command to start recording the data, to stop recording data and the command to save the data read by the sensor. If no error occurs during the initialization of the DAQ device, then the "Start" button is enabled and the measurement can be started by pushing the button. This starts the data acquisition and calls the subprograms "Save_Data" and "Plot Data". These programs write the acquired data to a logging file and plots the live sensor data on the graphs in the Live graphics menu. These commands continue to run until the "Stop" button is pressed, which will then stop the measurement. After this the user can finally click on the "Save" button, which will open the dialog for entering the name and destination path of the obtained file. Afterwards the data is written in ASCII file with additional information about the measurements, for example the data or time. In this menu feedback is received as to when the vibrations are being measured, as it can be seen in red letters on the figure 8. Finally, just close the application after it has been used and the data has been recorded properly.

## 4.2 Plotting graphics with Anaconda/Jupyter

To plot the obtained results the Jupyter Notebook application from the Anaconda [7] software was used. Anaconda is a Python distribution software, pre-built and preconfigured with a collection of packages, which are commonly used for data science. The Anaconda browser is a GUI tool that is included in Anaconda distribution and makes it easy to configure, install and launch tools such as the Jupyter Notebook.

Jupyter Notebook is an open-source web application that allows you to create and share documents that contain live code, equations, narrative text or visualizations. Some of the uses of this application are data transformation and cleaning, statistical modeling, numerical simulation and data visualization and much more. In this case this application was used for data visualization.

## 5. Vibration sensors

In this chapter it will be approached which sensors were selected, and it will be explained in more detail how they work and their specifications.

### 5.1 BALLUFF (BMC0001)

#### 5.1.1 Specifications of the sensor

One of the sensors used in this project was the BCM0001 sensor from BALLUFF, as seen in figure 10, since the university already had this vibration sensor. This sensor is an IO-Link sensor, which means that the connection type is IO-Link. IO-Link is a serial, bi-directional point-to-point connection for signal transmission and energy supply under any network. An IO-Link connection is a standardized uniform interface for sensors and actuators irrespective their complexity (measuring, switching, mixed signal, multi-channel binary, etc.).

This sensor can measure vibration (velocity/acceleration), the contact temperature and has 3 measurement axes. In table 3 it can be seen with more detail some specifications of this sensor.

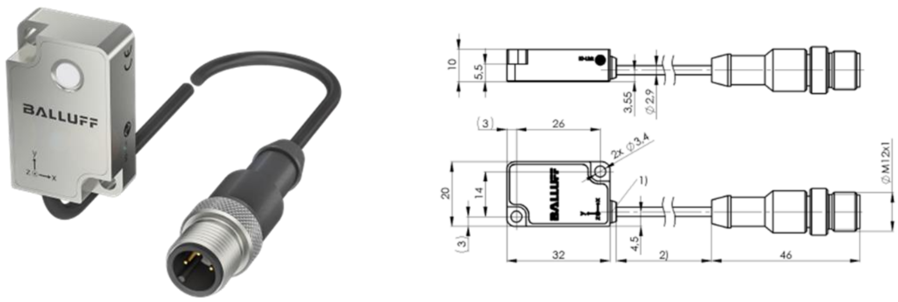


*Figure 10 - BCM0001 sensor from BALLUFF*
*Source: https://my.balluff.com/de-de/products/BCM0001?gclid=CjwKCAjwpMOIBhBAEiwAy5M6YP51MCmUzGOK3-URmTsOCM9BGGb0Lo00adxIVVLhprhkbxYBmc8yWBoCQyIQAvD_BwE*

*Table 3 – BALUFF sensor specifications*

| | |
|---|---|
| **Vibration frequency range** | 2 to 3200 Hz |
| **Price** | 255 € |
| **Vibration acceleration, measuring range RMS** | 0 to 16 g |
| **Contact temperature, measuring range** | 0 to 70 °C |
| **Interface** | IO-Link 1.1 |
| **Connection** | Cable with connector, M12x1-Male, 3-pin, 1.5m |
| **Housing material** | Stainless steel (1.4404) |
| **Ambient temperature** | 0 to 70 °C |

The sensor has multiple measurements in one device, which means that it detects various physical variables. The Balluff condition monitoring sensor detects vibration and temperature, then processes them and provides the desired data to a host system via IO-Link.

The sensor has integrated processing circuitry with configurable data processing and also it has configurable events and status indicators. One of the biggest advantages of this sensor is the fact that it has a fast and simple connection through the IO-Link. This sensor has a compact form which is good for restricted spaces. The standardized IO-Link protocol allows to easily parameterize the sensor and match the processing in the sensor to a specific application.

### 5.1.2 Connection and reading

The connection in this case is made with an IO-Link Master which is the IO-Link interface AL1060 showed in the figure 11 and the IO-Link device which is the BALLUFF BCM0001 sensor.

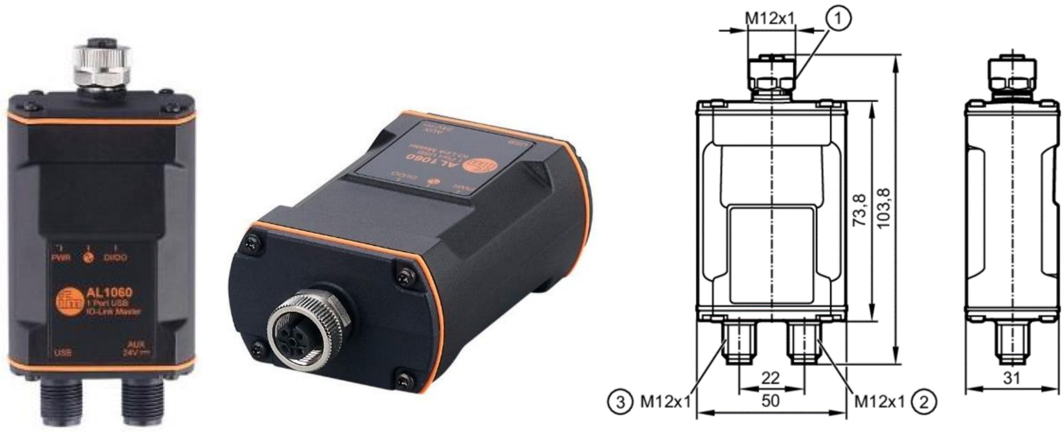


*Figure 11 – IO Link interface AL1060*
*Source: https://www.ifm.com/pt/pt/product/AL1060*

The IO-Link USB master establishes the connection between the IO-Link sensor and the automation system. As a component of an I/O system, the IO-Link USB master is installed in the computer. The name of the software installed is “LR device”.

It is possible to observe, in figure 12, the layout of the LR device software. This software has two main menus, the “Setup” and the “Cockpit” on the left upper corner. The first step is to connect the devices to the application, after which it is necessary to adjust the devices' setups accordingly. One of the sensor parameters that were changed was Process Data Profile Configuration. Since this sensor only lets you set 4, in the first slot the X-axis RMS was set and in the second slot the Z-axis RMS. Since there is an axial and two radial axis there is no need to retain information from all 3 axes, since the Y-axis and the Z-axis are radial. In slot 3 the Peak-to-Peak of the X-axis has been set and in slot 4 the Peak-to-Peak of the Z-axis.

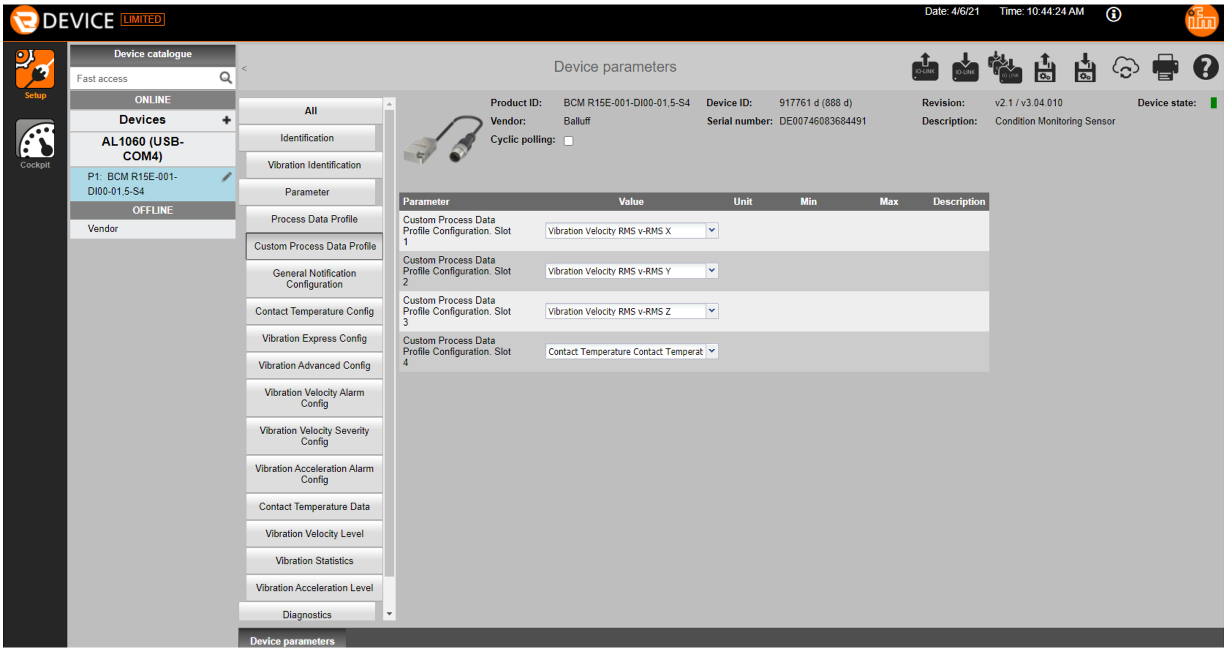


*Figure 12 - LR software in the setup menu*

In the "Cockpit" menu, figure 13, the four slots previously defined as features to be measured in the diagram were set and a time interval was set. After the vibration is measured by the sensor the data is saved as a .CVS file. CVS stands for comma-separated values and this type of text file has a specific format that allows the data to be saved in a table structured format.

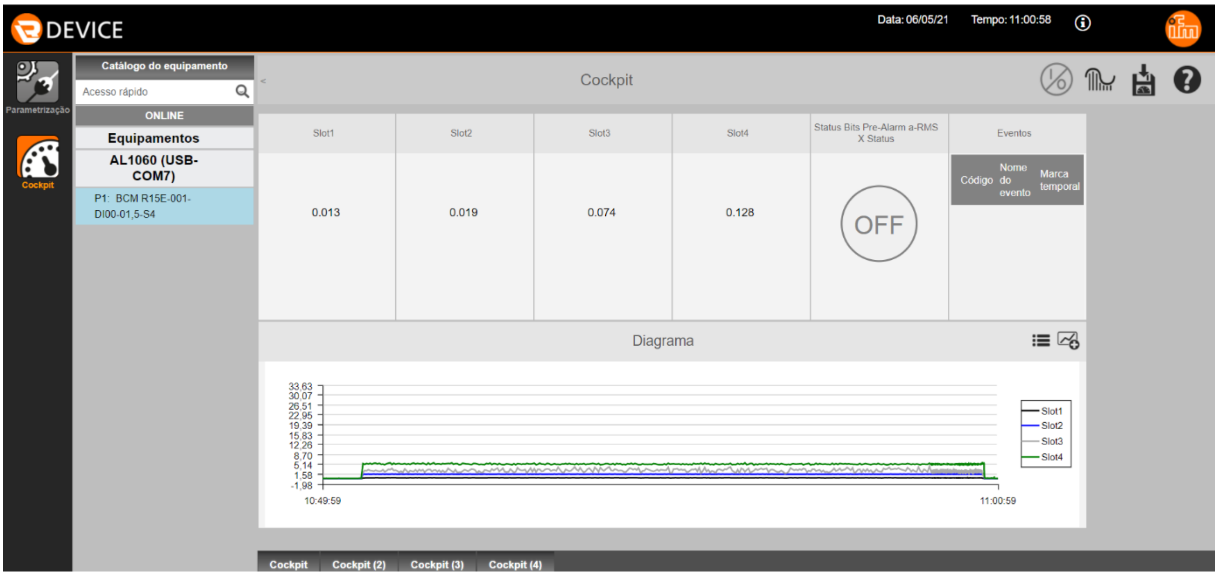


*Figure 13 - LR software in the cockpit menu*

## 5.2 ASC-325

### 5.2.1 Specifications of the sensor

The second sensor used in this project is the ASC-325 sensor. This sensor is applicable for condition monitoring. This sensor is a MEMS capacitive accelerometer. MEMS is short for "Micro Electromechanical System". These are systems with electrical and mechanical components that have microscopic dimensions. The key components of capacitive accelerometers are high-quality MEMS that feature excellent long-term stability and reliability. This technology allows measuring static (DC) and constant accelerations, which is used to calculate the speed and displacement of moving objects.

This accelerometer has the advantage of having a frequency response from 0 Hz to 7 kHz and is best suited for low to medium frequency measurements. This accelerometer can also work with low voltages as +5VDC.

These MEMS capacitive accelerometers consist of a mass that is located in the middle of two parallel plates. The principle of operation is as follows, it is to form two capacitors between the mass and the outer fixed plates. In the event of an acceleration impact on the sensor, the value of the capacitors is being changed due to the moving proof mass, resulting in a capacity change that is proportional to the acceleration.

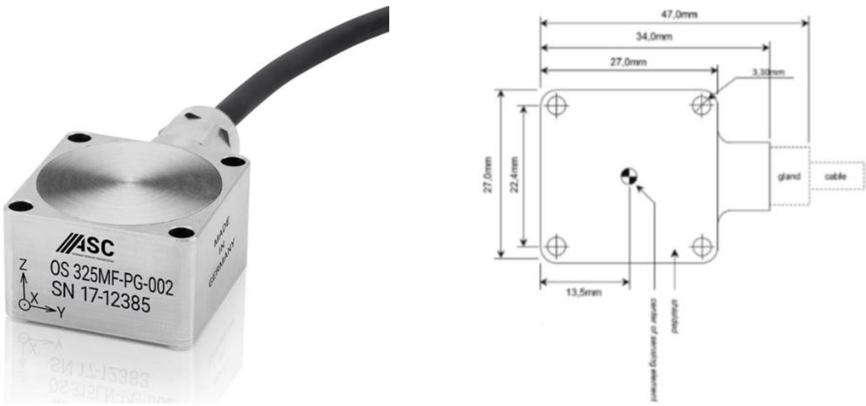


*Figure 14 - OS 325MF-PG-002 sensor from ASC*

This sensor features an extremely robust design with shock resistance up to 6.000 g. These accelerometers are hermetically sealed which makes them ideal for any kind of harsh environmental condition. [12]

Some of the features of this sensor are as follows, Low Noise Differential Voltage Output, very high shock resistance, excellent Offset and scale factor stability. Normally, sensors internally convert the capacitance signal into a current or voltage signal to send the data.

This capacitive accelerometer also has the advantages of outstanding temperature stability and excellent behavioral response.

*Table 4 – ASC-325 sensor specifications*

| | |
|---|---|
| **Measuring axis** | 3 |
| **Sensor type** | Accelerometer |
| **Sensor technology** | MEMS capacitive |
| **Output signal** | Voltage |
| **Measuring range** | up to 5g |
| **Temperature** | -20 °C to +100 °C |
| **Housing material** | Stainless steel (IP68) |
| **Noise Density** | 10 to 680 µg/√Hz |

In the table 4 it is possible to easily see some of the main specifications of this sensor. To see more specific details about this sensor check the appendices' part.

### 5.2.2 Connection and reading (Matlab app)

This sensor was connected directly to the computer throughout a DAQ USB Device. DAQ stands for data acquisition. The device used was a NI USB-6001, from the company National Instruments. [38] When it comes to pinout terminology, the pin type AI, that stands for analog input and then a number that corresponds to a channel number. To connect the sensor to the DAQ USB device the white cable was connected to AI 0, the gray cable to AI 4, the yellow cable to AI 1, the pink cable to AI 5, the green cable to AI 2 and finally the blue cable to AI 6. In addition to the NI USB-6001 a power supply was also used, in this case it was the DC Multi-Output Power supply 6040. To this device was connected the red cable to the positive signal and the brown cable to the negative signal, 5V/500mA, and the ground cable to the ground signal. Finally, the DAQ USB device was connected to the computer via a USB input. To be able to make these connections the table of the cable code/pin configuration in figure 15 was used.

| | Pin | Color Code Cable Type K3 | Color Code Cable Type K4 | Description | |
|---|---|---|---|---|---|
| 1 | Supply + | Blue | Red | Power: | supply voltage +5 to +40 VDC |
| 2 | Supply - | Brown | Black | Power: | GND |
| 3 | Signal + | White | Green/Purple | X-Axis: | positive, analog output voltage signal for differential mode |
| 4 | Signal - | Grey | White/Purple | X-Axis: | negative, analog output voltage signal for differential mode |
| 5 | Signal + | Yellow | Green/Grey | Y-Axis: | positive, analog output voltage signal for differential mode |
| 6 | Signal - | Pink | White/Grey | Y-Axis: | negative, analog output voltage signal for differential mode |
| 7 | Signal + | Green | Green | Z-Axis: | positive, analog output voltage signal for differential mode |
| 8 | Signal - | Blue | White | Z-Axis: | negative, analog output voltage signal for differential mode |

*Figure 15 - Cable code/ Pin configuration of the ASC-325 sensor*

## 5.3 Sensors comparison

The most significant difference between these two sensors is the fact that the Balluff sensor is an intelligent sensor that can already provide RMS and Peak-to-Peak values while the ASC sensor is a sensor that provides raw data that later has to be analyzed and processed. The added value of getting raw data is that it can be worked on as needed, it gives the opportunity to create FFT graphics which will allow to extract more information, while with the other sensor we can only get already processed information. When compared the ASC-325 sensor has a much lower frequency range than the BCM0001.

# 6. Trials with the bearings (testbench)

In this chapter it will be explained which bearings were tested, the trial procedure and it will be showed the trials results and analysis.

## 6.1 Bearings

The polishing head machine contains the bearings 6001 (Deep groove ball bearings) from the SKF company. The reason why this bearing was select is because, as it can be observed in figure 16 that represents the bearings located in the polishing head robot, it is the easiest bearing to access without having to demount the whole polishing head in order to change the bearings.

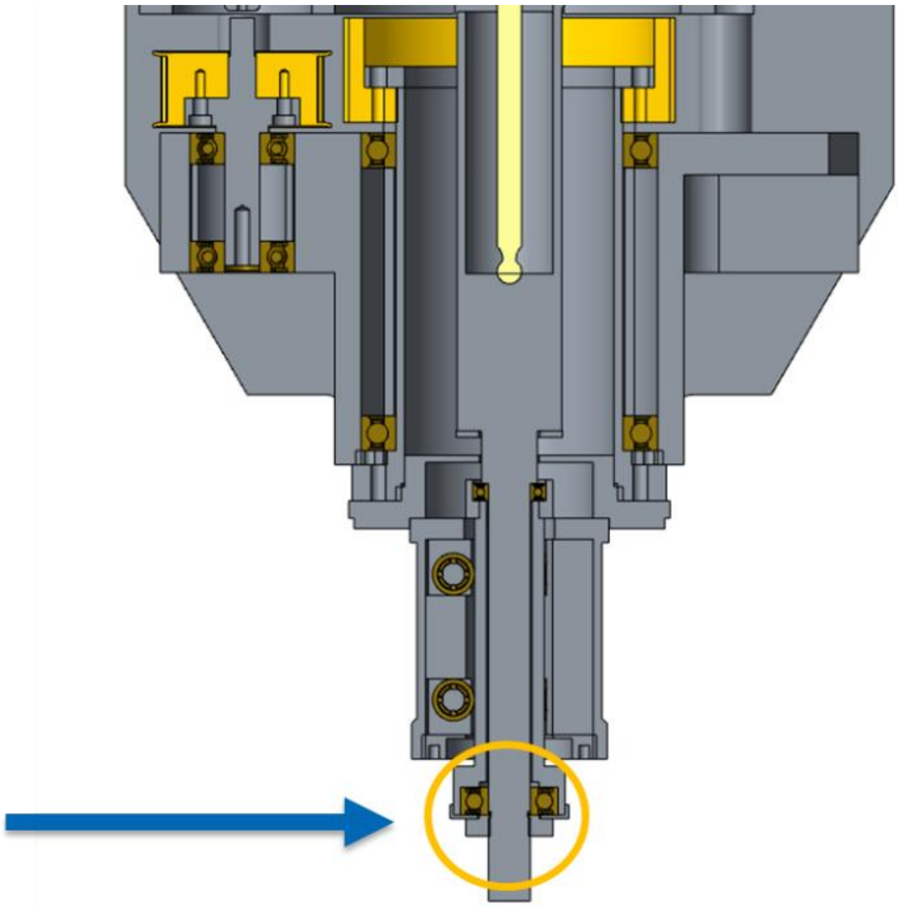

*Figure 16 – CAD model of the location of the bearings in the polishing head*

For this reason, these bearings, figure 17, were used for testing in the testbench.

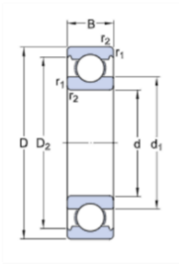

DIMENSIONS

| | |
|---|---|
| d | 12 mm |
| D | 28 mm |
| B | 8 mm |
| $d_1$ | ≈ 17 mm |
| $D_2$ | ≈ 24.72 mm |
| $r_{1,2}$ | min. 0.3 mm |

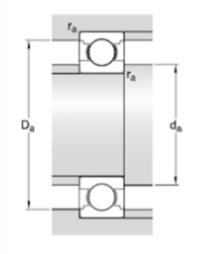

ABUTMENT DIMENSIONS

| | |
|---|---|
| $d_a$ | min. 14 mm |
| $D_a$ | max. 26 mm |
| $r_a$ | max. 0.3 mm |

*Figure 17 – Bearing 6001 from SKF*
*Source: [https://www.skf.com/de/products/rolling-bearings/ball-bearings/deep-groove-ball-bearings/productid-6001](https://www.skf.com/de/products/rolling-bearings/ball-bearings/deep-groove-ball-bearings/productid-6001)*

For these tests a new, a corrosive and a milled bearing were used, to understand the different behavior in the results. The milled bearing was drilled with a milling cutter diameter of 1.5mm. After seeing how they behave, it will be possible to see in the polishing machine when a bearing is in good condition, when it starts to wear out, or when it must be replaced in order to obtain the best efficiency from the robot. In the figure 18 we can see the 3 types of bearings used in these trials. The goal was to test the different bearings and the different sensors in the test bench to see if they work. And if they worked in the test bench then the goal is to get the same results in the polishing head robot.

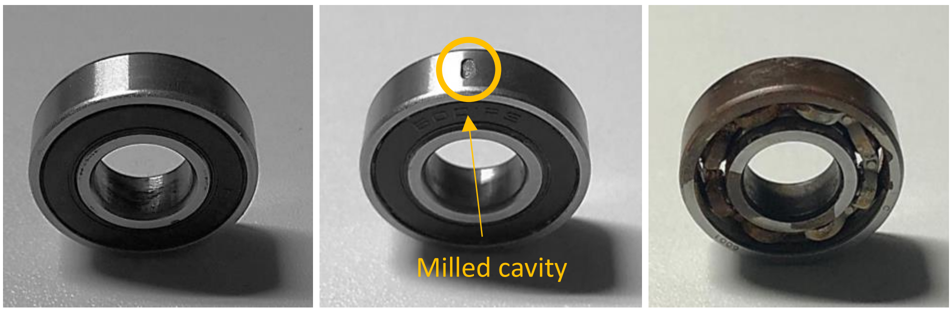


*Figure 18 – New bearing, milled bearing and corrosive bearing*

## 6.2 Component for the bearings

Before conducting tests on the polishing head machine, tests were conducted on the bearings that are used in the polishing head robot. Since the university already had a test bench where it was possible to test bearings, it was necessary to develop components to test specifically the bearings mentioned before in this test bench machine. For these trials, 3 different components were used. The first component, showed in figure 19, is the piece where the bearing is attached, and this component is attached to the testbench with 6 nuts and 6 M6 screws. This component is made of steel.

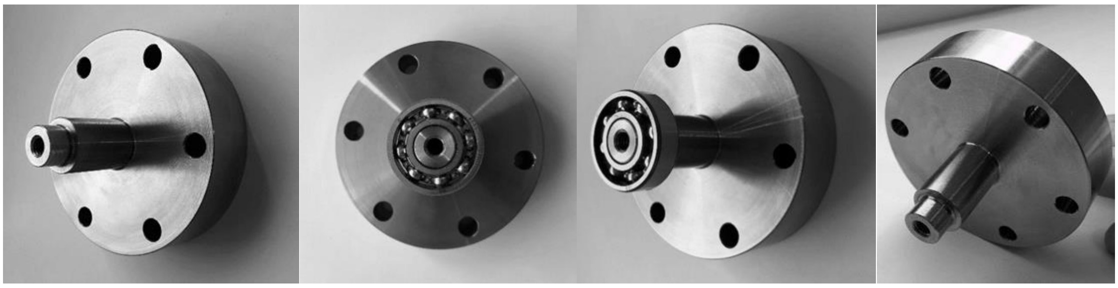

*Figure 19 – Component designed to mount the bearing in the testbench*

The second component has the purpose to attach the BALLUFF sensor (blue square in figure 20) on the top. This component fits onto the bearing and two cable ties are inserted on the side holes (yellow circles in figure 20). Then a weight is applied creating a down force (the thick blue arrow represents the direction of the force in the middle of figure 20).

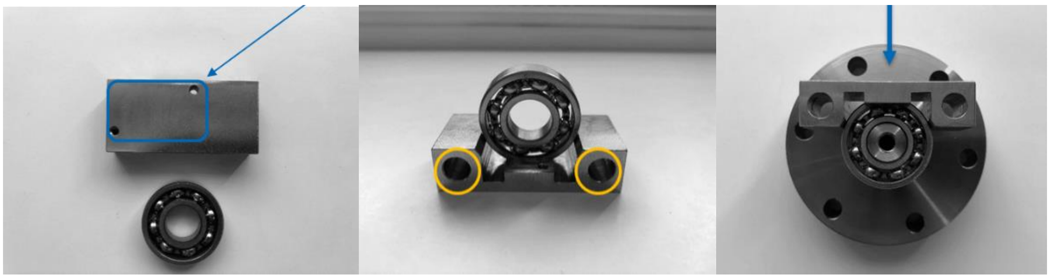

*Figure 20 – Components designed for the trials in the testbench*

The third component is the same as the second component, it has the same purpose, and it works the same way with the difference that this one is used to attach specifically the ASC-325 sensor.

## 6.3 Trial procedure

This test bench works as follows: the bearing adapter is fitted and secured to the test bench using 6 screws and 6 nuts, then the bearing is fitted into the adapter and secured with a screw and 2 washers. This test bench consists of a motor connected to a shaft and weights to be applied to the component to be tested. The weight on the bearings was applied as follows, first the part where the sensor is attached was attached using M3 screws, then some cable ties were added to the component and to these cable ties a carabiner was attached that applies the weight that was placed/set. Regarding the weight, it should be noted that the weight applied to the left side (see figure 21) is not the same weight that is being applied to the bearing.

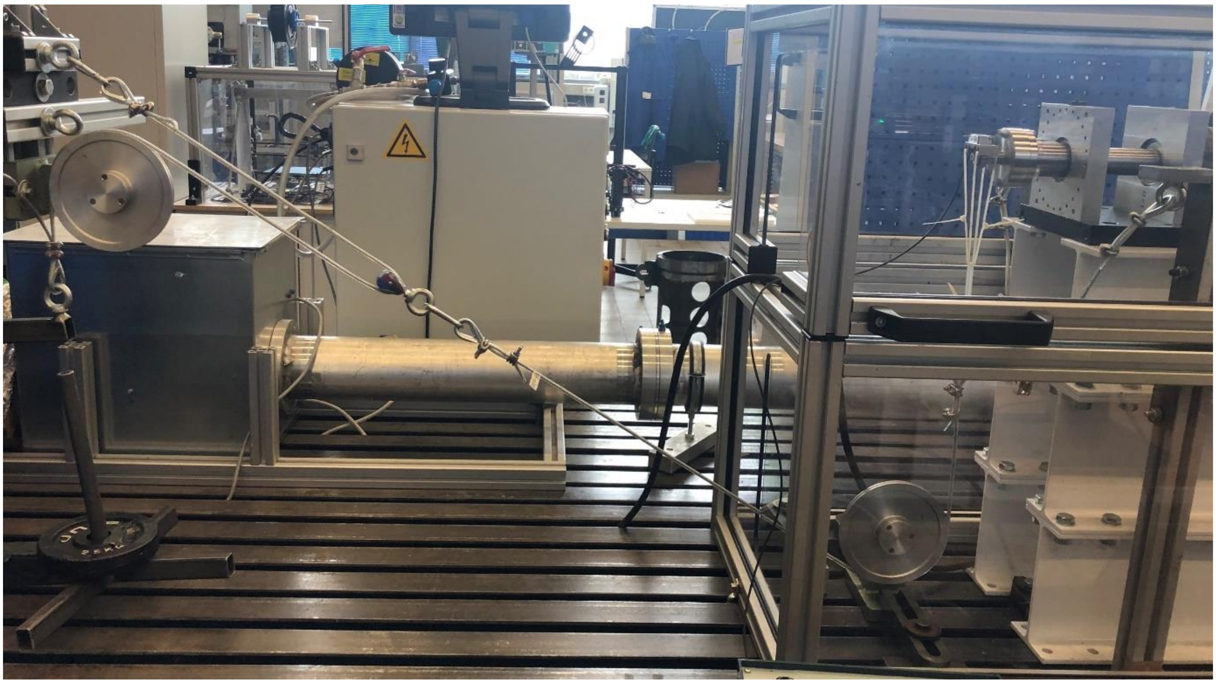

*Figure 21 – Testbench in the Aalen University*

Regarding the revolutions per minute of the machine, these can be defined by the user. In the trials performed on the bearings were used 600 rpm and 1200 rpm. This machine is relatively easy to use, as it has an intuitive and simple menu. After starting the machine, the revolutions per minute are set and then click "Hand On" and the machine starts working. To stop the machine later, it is only necessary to just click "Off".

## 6.4 Trials with the BALLUFF sensor

To perform the tests with the Balluff sensor the testbench bearing adapter was placed onto the testbench and then the bearing was placed. Since the adapter was not produced to the correct tolerances, another adapter was produced. While this adapter was being produced, and to make sure that the first adapter was used optimally, a measuring needle was used to try to minimize as much as possible the unevenness of the part, has it can be seen in figure 22 on the top right image.

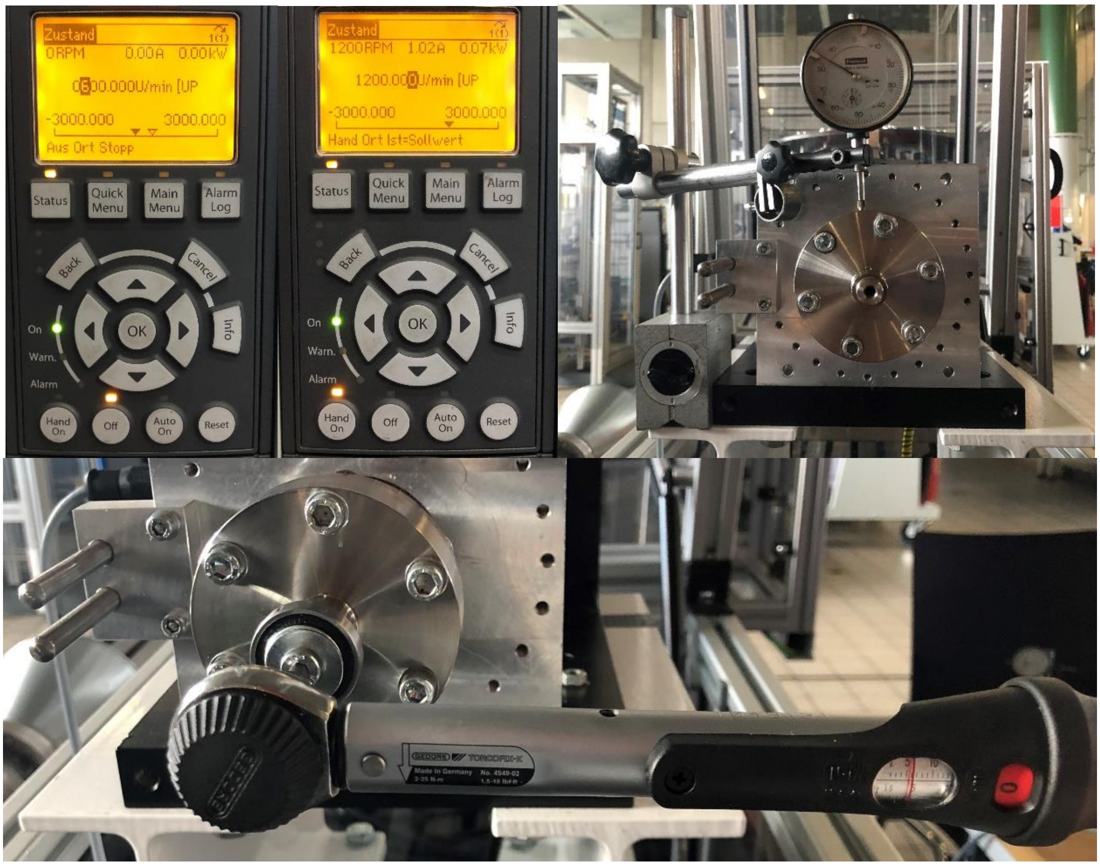


*Figure 22 – Testbench controller; adapter being set-up*

After this the Balluff sensor was fitted to the designed part by means of two M3 screws to embed it, and then the part was fitted to the bearing and fixed with a screw and two washers so that there was no gap between the bearing and the fixing screw. To tighten this screw, a torque key was used to confirm that it was not being tightened too tightly and more importantly to make sure it was used always the same torque and the same mounting conditions on each trial, has it can be observed in figure 22 bottom image. After checking the parameters for what force should be applied in this situation, this corresponding force was then applied. Afterwards, cable ties and a carabiner are added to apply downward force. After the force is applied, a spirit level ruler is used to check that the part is leveled, figure 23 right side.

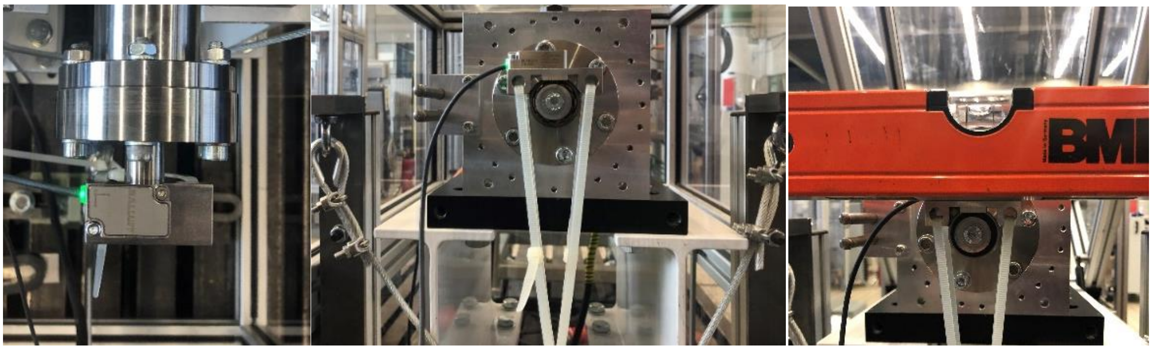

*Figure 23 – Set-up process (top view; front views)*

Then the sensor was connected to the IO-Link USB Master and this device was connected to the computer via the USB input. After all these steps the trials started.

### 6.4.1 Trials (DOE)

To start the trials a DOE was created. This first DOE is composed of 25 runs and the variables are the following: the force to be applied, which had a lower limit of 0,5Kg, a middle limit of 1Kg and an upper limit of 2,5Kg. The revolutions per minute, had a lower limit of 600rpm and an upper limit of 1200rpm. The runtime in minutes, had a lower limit of 5 minutes and an upper limit of 10 minutes. And finally, the condition of bearings used in the trials, new, milled or corrosive. The goal with this first DOE was to understand the different variants and their respective impact on the results. For this first DOE a software was used. The software used was Design expert from the company Stat ease. [39] For the following DOEs they were made without the software, and they were made according to the needs of project.

*Table 5 – First trials in the testbench DOE*

| Run | Weight (Kg) | RPM (rpm) | Time (min) | Bearing type | New mounted ? | Mounting | Measured axis |
|---|---|---|---|---|---|---|---|
| 8 | 1 | 1200 | 10 | New | Yes | Air | X-axial; Z-radial |
| 11 | 0,5 | 600 | 10 | New | No | Air | X-axial; Z-radial |
| 12 | 1 | 600 | 5 | New | No | Air | X-axial; Z-radial |
| 14 | 2,5 | 1200 | 10 | New | No | Air | X-axial; Z-radial |
| 16 | 1 | 600 | 5 | New | No | Air | X-axial; Z-radial |
| 18 | 0,5 | 1200 | 5 | New | No | Air | X-axial; Z-radial |
| 20 | 2,5 | 1200 | 5 | New | No | Air | X-axial; Z-radial |
| 23 | 2,5 | 600 | 10 | New | No | Air | X-axial; Z-radial |
| 1 | 0,5 | 1200 | 10 | Corrosion | Yes | Air | X-axial; Z-radial |
| 5 | 2,5 | 600 | 5 | Corrosion | No | Air | X-axial; Z-radial |
| 6 | 2,5 | 1200 | 5 | Corrosion | No | Air | X-axial; Z-radial |
| 7 | 2,5 | 1200 | 10 | Corrosion | No | Air | X-axial; Z-radial |
| 9 | 0,5 | 1200 | 5 | Corrosion | No | Air | X-axial; Z-radial |
| 15 | 0,5 | 600 | 10 | Corrosion | No | Air | X-axial; Z-radial |
| 21 | 1 | 600 | 5 | Corrosion | No | Air | X-axial; Z-radial |
| 24 | 2,5 | 1200 | 10 | Corrosion | No | Air | X-axial; Z-radial |
| 2 | 0,5 | 600 | 5 | Milled | Yes | Air | X-axial; Z-radial |
| 3 | 2,5 | 600 | 10 | Milled | No | Air | X-axial; Z-radial |
| 4 | 2,5 | 600 | 5 | Milled | No | Air | X-axial; Z-radial |
| 10 | 2,5 | 1200 | 10 | Milled | No | Air | X-axial; Z-radial |
| 13 | 0,5 | 600 | 10 | Milled | No | Air | X-axial; Z-radial |
| 17 | 2,5 | 1200 | 10 | Milled | No | Air | X-axial; Z-radial |
| 19 | 0,5 | 1200 | 5 | Milled | No | Air | X-axial; Z-radial |
| 22 | 0,5 | 1200 | 5 | Milled | No | Air | X-axial; Z-radial |
| 25 | 0,5 | 600 | 10 | Milled | No | Air | X-axial; Z-radial |

### 6.4.2 Results analysis

After these first tests in the testbench it was observed that, in fact, it is possible to distinguish between the different bearing types by their vibrations. In the new bearing, figure 24, it can be seen that the values are around 1g which is much less compared to the other two bearings. In the case of the milled bearing, it already presents higher values and its vibration amplitude remains constant and not very high. In the case of the bearing with corrosion, it presents high values and also presents a large vibration amplitude, between almost 4g and 7g, which was already expected. Depending on the measurement axis, speed or normal force have the main influence on the vibrations of the bearing. With these trials, it can be seen that this sensor is good for condition monitoring, since it can be distinguished the different bearings by their vibrations. The x axis represents the axial direction and the y and z axis represent the radial direction.

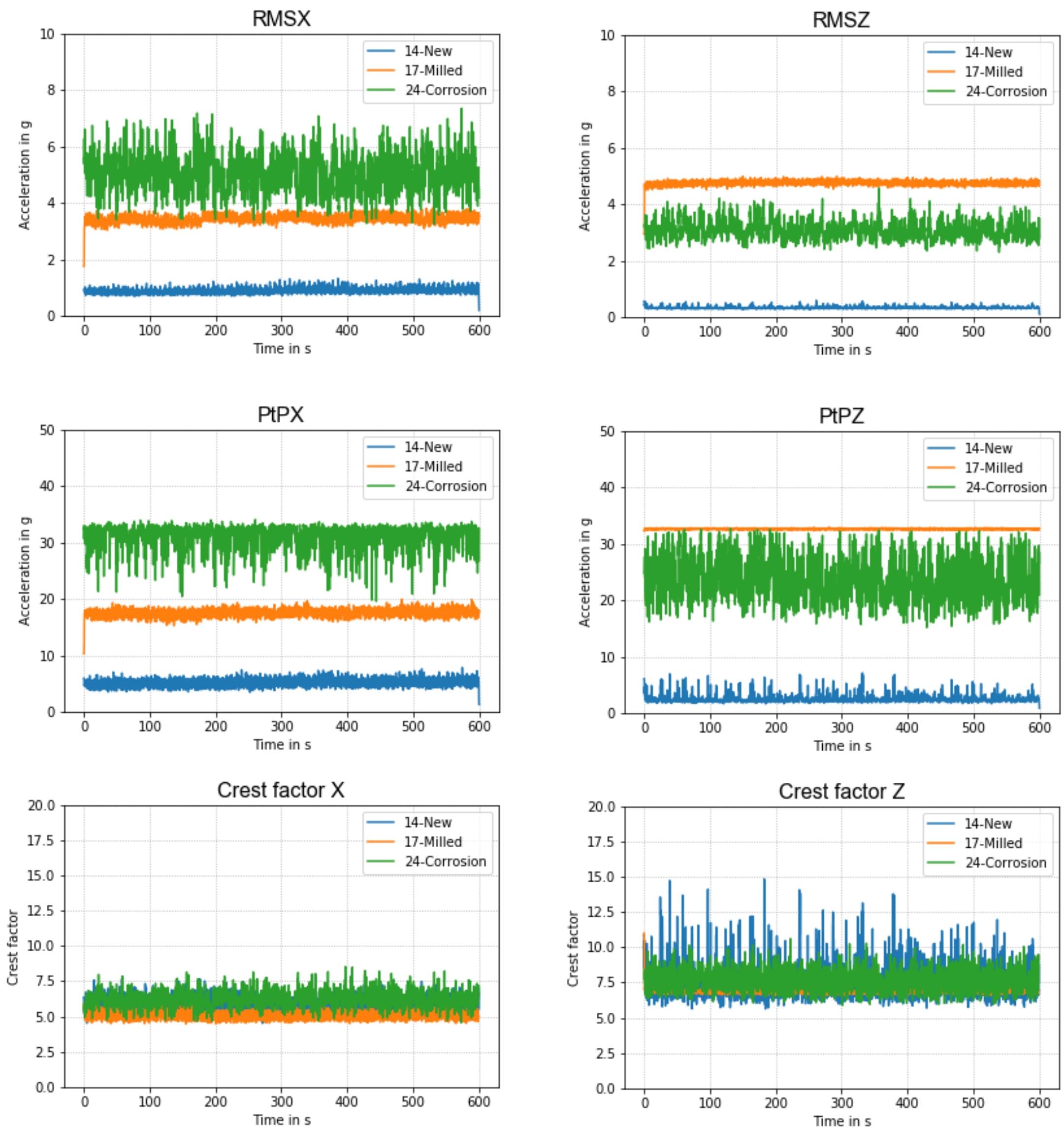


*Figure 24 – Results from the comparison of the new, milled and corrosive bearings*

To have another analysis of the results, a statistical software was used and it was possible to see that in the RMS, in the x axis, that the force and the rotations per minute are the variables with more influence in the results, as it can be seen in the graphics in figure 25.

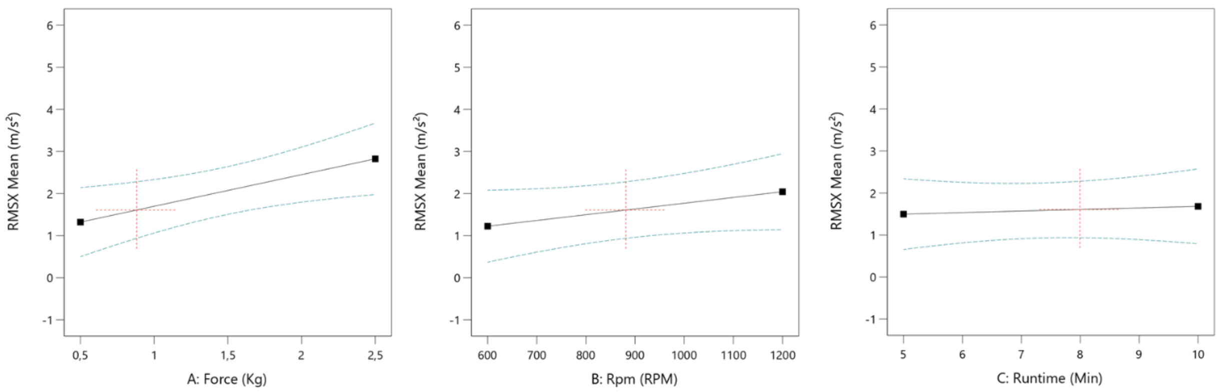


*Figure 25 – Graphics from the statistical software RMS*

With the use of a statistical software it was possible see that in the case of the peak to peak, in the x axis, the factor that has the more influence is the force applied, as it can be seen in the graphics of figure 26.

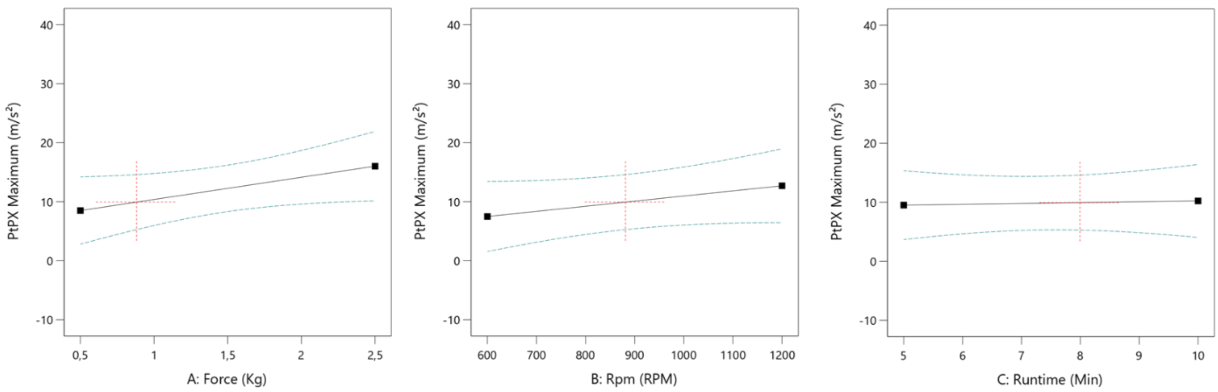


*Figure 26 – Graphics from the statistical software Peak-to-Peak*

But for example, in the case of the RMS of the z axis the factor that has the main influence is the angular frequency, as can be observed in figure 27.

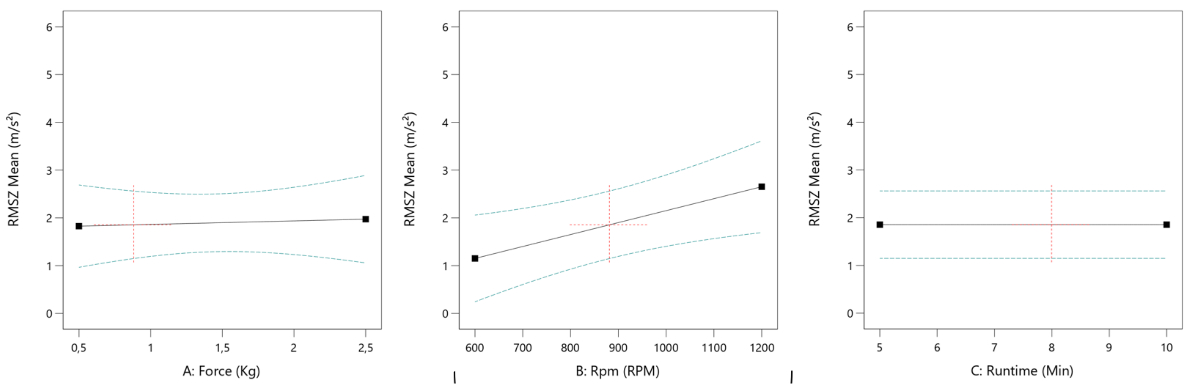


*Figure 27 – Graphics from the statistical software RMS z axis*

With this software it was possible to identify which factor had more influence on the results and with this information the next trials were designed taking this into account, in order to obtain the best results.

With these trials it was also possible to see that there is a correlation between speed and vibration measured. With increase in speed, there is increase in vibration and vice versa. And there is also a correlation between force and vibration that is also measurable as well. With increase in normal formal, there will be increase in vibration and vice versa.

### 6.4.3 Second Trials (DOE)

After the first trial a second DOE was developed. This second DOE was intended to understand if the way the sensor was mounted had an impact on the results or not. Since air bubbles can exist between the sensor and the contact surface, different liquids were used in order to reduce them. The reason why this was done was because air can damp a lot of vibrations and the question was if in this case, air was damping on the results or not. Soap, oil and beeswax were the liquids used for these trials. Several trials with the same characteristics were performed to test the reproducibility of the results. And also to see that if air would be damping the results, then it would have less vibrations with air and more with the other mounting methods.

*Table 6 – Second trials in the testbench DOE*

| Run | Force (Kg) | RPM (rpm) | Run time (min) | Bearing | New mounted? | Mounting | Measured Axis |
|---|---|---|---|---|---|---|---|
| 26 | 2,5 | 1200 | 5 | New | Yes | Air | X-axial; Z-radial |
| 27 | 2,5 | 1200 | 5 | New | No | Air | X-axial; Z-radial |
| 28 | 2,5 | 1200 | 5 | New | No | Air | X-axial; Z-radial |
| 29 | 2,5 | 1200 | 5 | New | No | Air | X-axial; Z-radial |
| 30 | 2,5 | 1200 | 5 | New | Yes | Air | X-axial; Z-radial |
| 31 | 2,5 | 1200 | 5 | New | No | Air | X-axial; Z-radial |
| 32 | 2,5 | 1200 | 5 | New | No | Air | X-axial; Z-radial |
| 33 | 2,5 | 1200 | 5 | New | No | Air | X-axial; Z-radial |
| 34 | 2,5 | 1200 | 5 | New | Yes | Soap | X-axial; Z-radial |
| 35 | 2,5 | 1200 | 5 | New | No | Soap | X-axial; Z-radial |
| 36 | 2,5 | 1200 | 5 | New | No | Soap | X-axial; Z-radial |
| 37 | 2,5 | 1200 | 5 | New | No | Soap | X-axial; Z-radial |
| 38 | 2,5 | 1200 | 5 | New | Yes | Beeswax | X-axial; Z-radial |
| 39 | 2,5 | 1200 | 5 | New | No | Beeswax | X-axial; Z-radial |
| 40 | 2,5 | 1200 | 5 | New | No | Beeswax | X-axial; Z-radial |
| 41 | 2,5 | 1200 | 5 | New | No | Beeswax | X-axial; Z-radial |
| 42 | 2,5 | 1200 | 5 | New | Yes | Oil | X-axial; Z-radial |
| 43 | 2,5 | 1200 | 5 | New | No | Oil | X-axial; Z-radial |
| 44 | 2,5 | 1200 | 5 | New | No | Oil | X-axial; Z-radial |
| 45 | 2,5 | 1200 | 5 | New | No | Oil | X-axial; Z-radial |

## 6.4.4 Second trials results analysis

After these second trials and after analyzing the graphics on figure 28, it was possible to see that oil was the mounting method that best captured the vibrations.

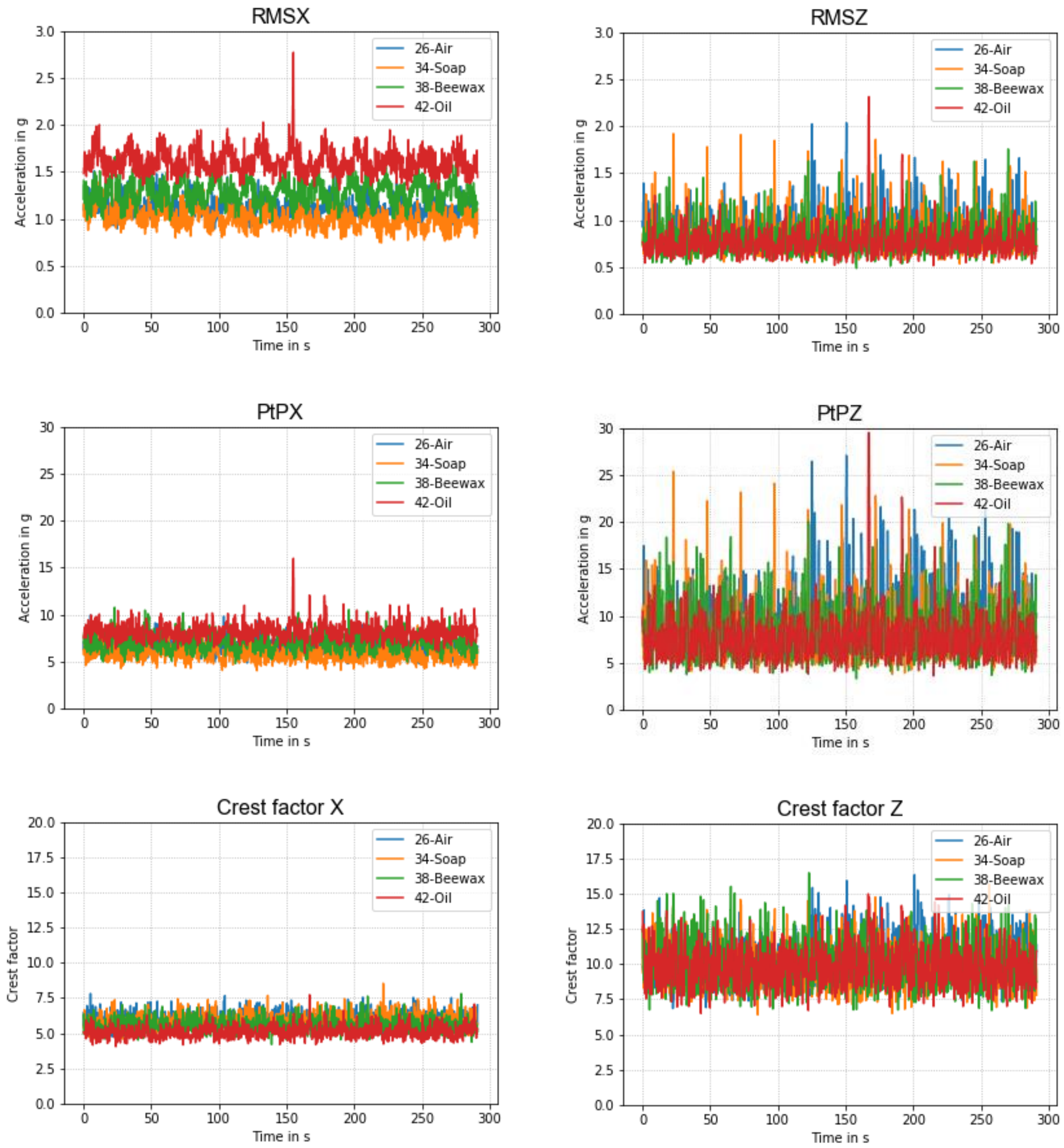


*Figure 28 -Results from the comparison between air, soap, beeswax and oil*

## 6.4.5 Last Trials (DOE)

After the previous DOE another one was created in order to see if the difference in which of the liquids was applied first showed any difference in the results, and also to see if the results were reproducible in terms of repeatability. The purpose of testing their repeatability is to verify that if in fact the results are constants or not, to verify their reliability.

*Table 7 – Last trials in the testbench DOE Part 1*

| Run | Weight (Kg) | RPM (rpm) | Time (min) | Bearing type | New mounted ? | Mounting | Measured axis |
|---|---|---|---|---|---|---|---|
| 47 | 2,5 | 1200 | 5 | New | Yes | Oil | X-axial; Z-radial |
| 48 | 2,5 | 1200 | 5 | New | No | Oil | X-axial; Z-radial |
| 49 | 2,5 | 1200 | 5 | New | No | Oil | X-axial; Z-radial |
| 50 | 2,5 | 1200 | 5 | New | No | Oil | X-axial; Z-radial |
| 51 | 2,5 | 1200 | 5 | New | Yes | Beewax | X-axial; Z-radial |
| 52 | 2,5 | 1200 | 5 | New | No | Beewax | X-axial; Z-radial |
| 53 | 2,5 | 1200 | 5 | New | No | Beewax | X-axial; Z-radial |
| 54 | 2,5 | 1200 | 5 | New | No | Beewax | X-axial; Z-radial |
| 55 | 2,5 | 1200 | 5 | New | Yes | Soap | X-axial; Z-radial |
| 56 | 2,5 | 1200 | 5 | New | No | Soap | X-axial; Z-radial |
| 57 | 2,5 | 1200 | 5 | New | No | Soap | X-axial; Z-radial |
| 58 | 2,5 | 1200 | 5 | New | No | Soap | X-axial; Z-radial |
| 59 | 2,5 | 1200 | 5 | New | Yes | Air | X-axial; Z-radial |
| 60 | 2,5 | 1200 | 5 | New | No | Air | X-axial; Z-radial |
| 61 | 2,5 | 1200 | 5 | New | No | Air | X-axial; Z-radial |
| 62 | 2,5 | 1200 | 5 | New | No | Air | X-axial; Z-radial |

A last DOE was also developed for the testbench with the BALLUFF sensor. This DOE came about after the first tests were performed on the Robot. Basically, after the first tests on the robot it was noticed that the bearing with a few hours of operation showed better results than a completely new bearing. See chapter 8 for more details.

*Table 8 – Last trials in the testbench DOE Part 2*

| Run | Weight(Kg) | RPM (rpm) | Time (min) | Bearing type | New mounted ? | Mounting | Measured axis |
|---|---|---|---|---|---|---|---|
| 63 | 2,5 | 600 | 5 | 50h | Yes | Air | X-axial; Z-radial |
| 64 | 2,5 | 600 | 5 | 50h | No | Air | X-axial; Z-radial |
| 65 | 2,5 | 600 | 5 | 50h | No | Air | X-axial; Z-radial |
| 66 | 2,5 | 600 | 5 | 50h | No | Air | X-axial; Z-radial |
| 67 | 2,5 | 1200 | 5 | 50h | No | Air | X-axial; Z-radial |
| 68 | 2,5 | 1200 | 5 | 50h | No | Air | X-axial; Z-radial |
| 69 | 2,5 | 1200 | 5 | 50h | No | Air | X-axial; Z-radial |
| 70 | 2,5 | 1200 | 5 | 50h | No | Air | X-axial; Z-radial |
| 71 | 2,5 | 600 | 5 | New (1) | Yes | Air | X-axial; Z-radial |
| 72 | 2,5 | 600 | 5 | New (1) | No | Air | X-axial; Z-radial |
| 73 | 2,5 | 600 | 5 | New (1) | No | Air | X-axial; Z-radial |
| 74 | 2,5 | 600 | 5 | New (1) | No | Air | X-axial; Z-radial |
| 75 | 2,5 | 1200 | 5 | New (1) | No | Air | X-axial; Z-radial |
| 76 | 2,5 | 1200 | 5 | New (1) | No | Air | X-axial; Z-radial |
| 77 | 2,5 | 1200 | 5 | New (1) | No | Air | X-axial; Z-radial |
| 78 | 2,5 | 1200 | 5 | New (1) | No | Air | X-axial; Z-radial |
| 79 | 2,5 | 600 | 5 | New (2) | Yes | Air | X-axial; Z-radial |
| 80 | 2,5 | 600 | 5 | New (2) | No | Air | X-axial; Z-radial |
| 81 | 2,5 | 600 | 5 | New (2) | No | Air | X-axial; Z-radial |
| 82 | 2,5 | 600 | 5 | New (2) | No | Air | X-axial; Z-radial |
| 83 | 2,5 | 1200 | 5 | New (2) | No | Air | X-axial; Z-radial |
| 84 | 2,5 | 1200 | 5 | New (2) | No | Air | X-axial; Z-radial |
| 85 | 2,5 | 1200 | 5 | New (2) | No | Air | X-axial; Z-radial |
| 86 | 2,5 | 1200 | 5 | New (2) | No | Air | X-axial; Z-radial |
| 87 | 2,5 | 600 | 5 | New (3) | Yes | Air | X-axial; Z-radial |
| 88 | 2,5 | 600 | 5 | New (3) | No | Air | X-axial; Z-radial |
| 89 | 2,5 | 600 | 5 | New (3) | No | Air | X-axial; Z-radial |
| 90 | 2,5 | 600 | 5 | New (3) | No | Air | X-axial; Z-radial |
| 91 | 2,5 | 1200 | 5 | New (3) | No | Air | X-axial; Z-radial |
| 92 | 2,5 | 1200 | 5 | New (3) | No | Air | X-axial; Z-radial |
| 93 | 2,5 | 1200 | 5 | New (3) | No | Air | X-axial; Z-radial |
| 94 | 2,5 | 1200 | 5 | New (3) | No | Air | X-axial; Z-radial |

### 6.4.6 Results analysis

In these last trials, the testbench was creating more irregular vibrations which is visible in the results. In these tests we can see that it is no longer so linear which of the liquids works best, thus proving that these results are not reproducible or that the irregular vibrations on the testbench did not allow to get constant results.

On the test bench, the vibration differences can be seen depending on the mounting method, but on these new trials it is not so clear to evaluate which one works better. In the previous trials oil best transmitted the vibrations to the sensor. Also because of these inconstant vibrations coming from the testbench it was not possible to see if the difference in which of the liquids was applied first has an impact on the results or not.

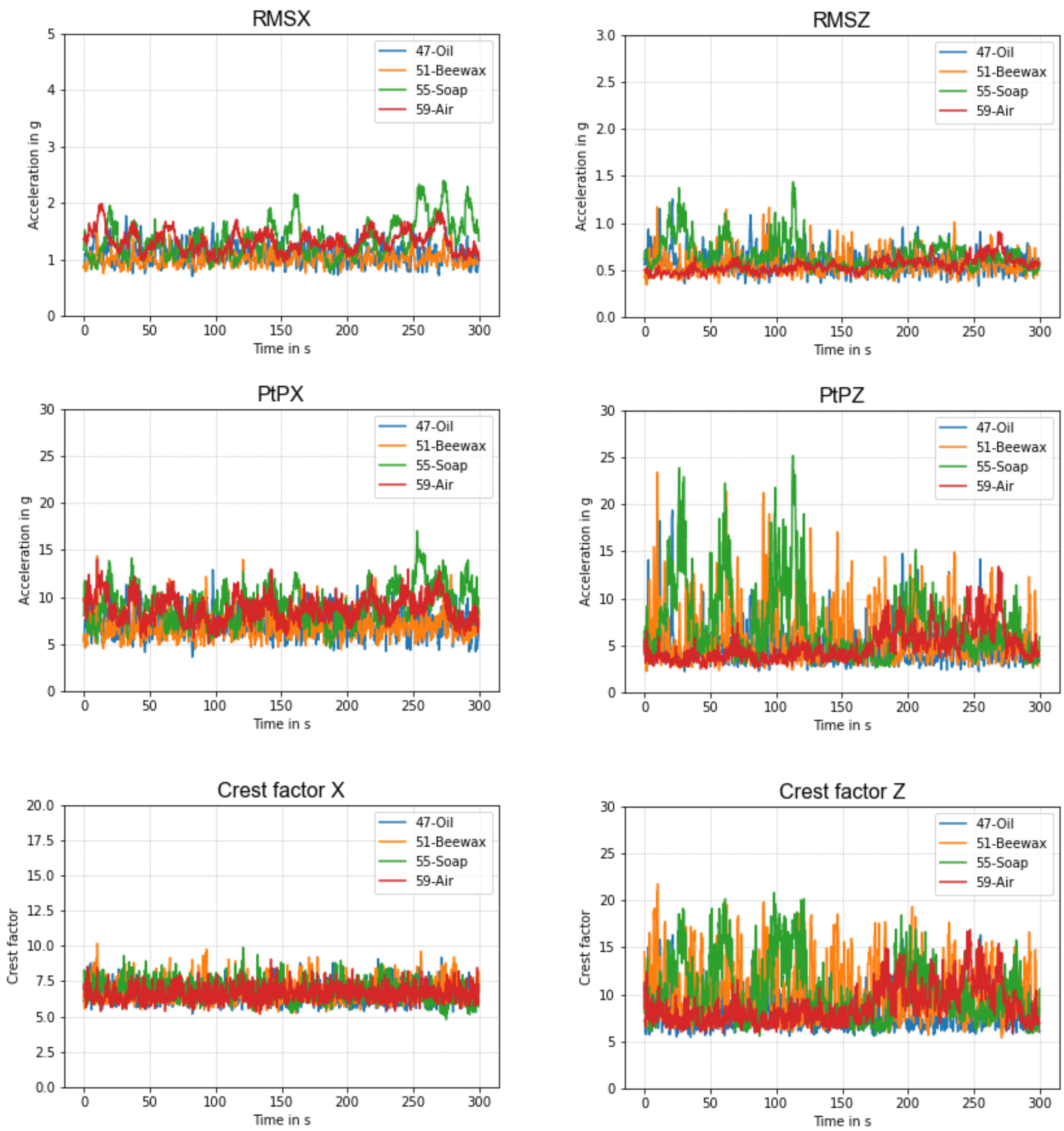


*Figure 29 -Results from the second trials with oil, beeswax, soap and air*

In the graphics, figure 30, it can be seen the results of comparing some of the tests at 600 rpm. The goal with these tests was to see if in fact the bearing with 50 hours worked better than new bearings. After observing these graphics, it was possible to see that the 50 hours bearing has almost the same behavior as the new bearings.

In the trials with the new bearings with 0 hours running and 50 hours bearing it was possible to see a small difference. So the new bearing with 0 hours shows less vibration then the run-in new bearing with 50 hours. A normal bearing should last more time than 50 hours but if it is possible to see already by a 50 hour a change on the bearing on the test bench, that would be great. That means that it is possible to see the bearing condition in more detail then initial foreseen, leading to a more precise condition monitoring of this component.

The trials in the testbench with a new bearing (0h) and a new bearing (50h) proved that the new bearing (0h) should shows less vibrations then the 50h bearing.

This leads to conclude that in the previous trials in the polishing head, the polishing head was maybe wrongly assembled which caused more vibrations in the trials with the new bearing then in the ones with the 50 hours bearing.

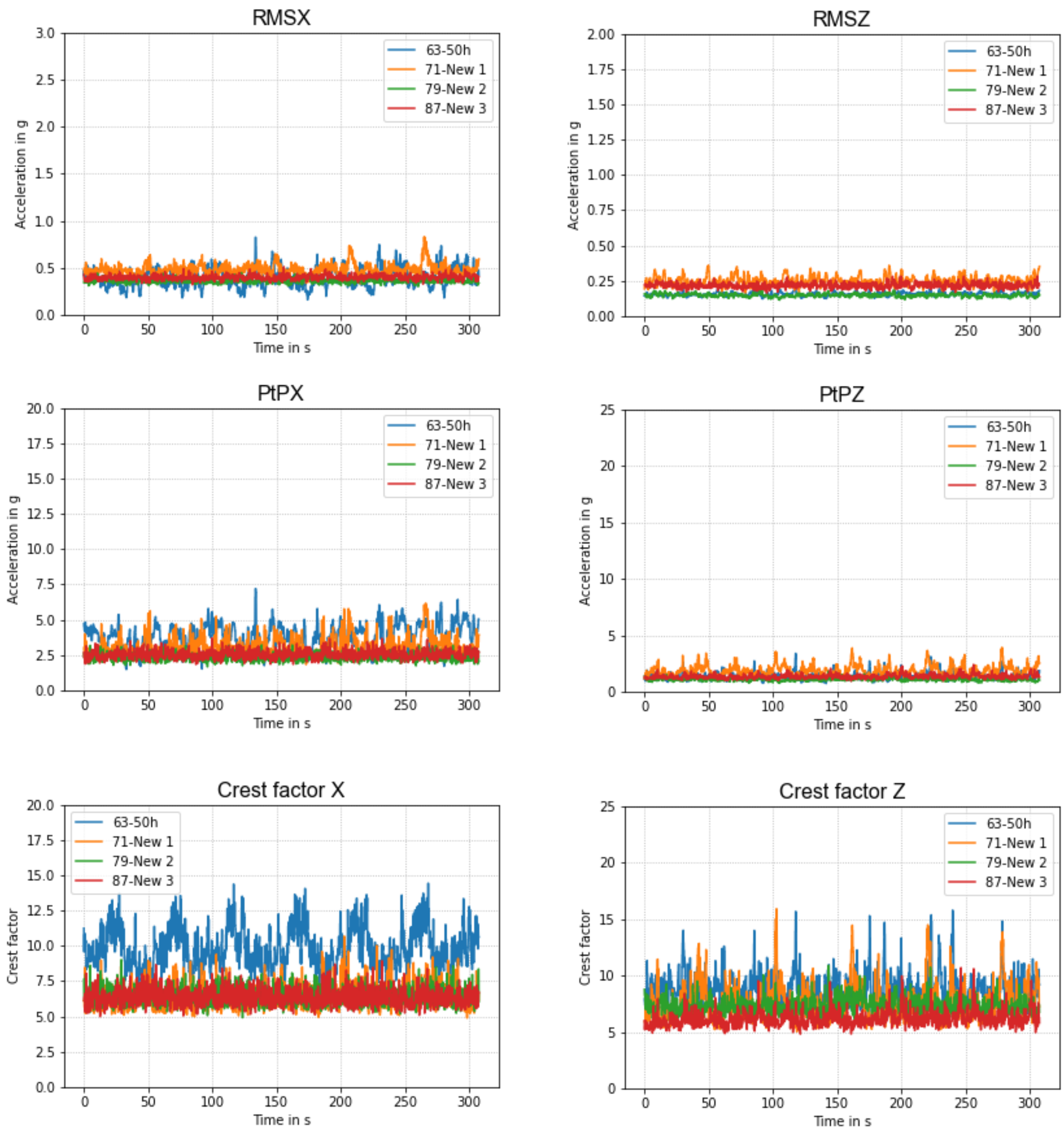


*Figure 30 – Results from the trials with 50h and new bearings with 600rpm*

From this BALLUFF sensor the RMS stays the same and the Peak to Peak just increases. In the begging the values are the same when the bearing is in good condition, so the values are constant (green arrows in figure 31. Then it will come to a point where the RMS will continue being good and constant but somewhere while this is still constant it will come to a point where that value, the peak starts increasing as seen in figure 31.

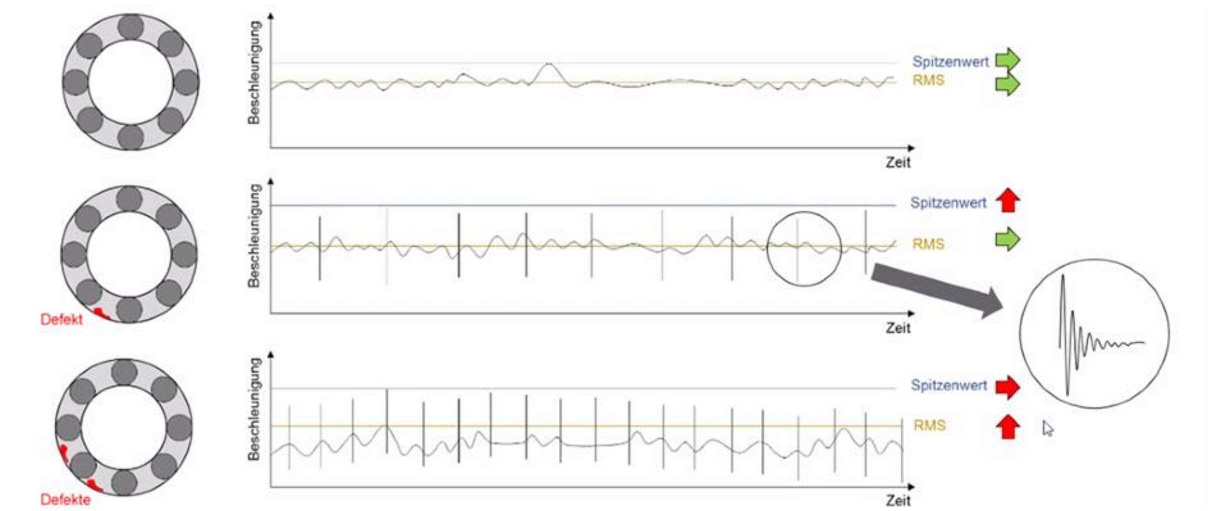


*Figure 31 -RMS and Peak to Peak behavior in the different bearings*

So as it can be seen in figure 32, there is a ratio of crest factor of 3 to 1 when there is no error and then a defect starts to show up and this is why the peak is increasing and while it increases the RMS stays constant, before the RMS starts increasing again. Then there is a ratio from 10 to 1 or 15 to 1. A bigger one than at the beginning. And then when there is more defects on the bearing the peak to peak keeps being constant and the RMS keeps increasing at the end until it reaches the same ratio that there was in the beginning, but there is at the end a higher value of vibrations so this means the bearing should be replaced.

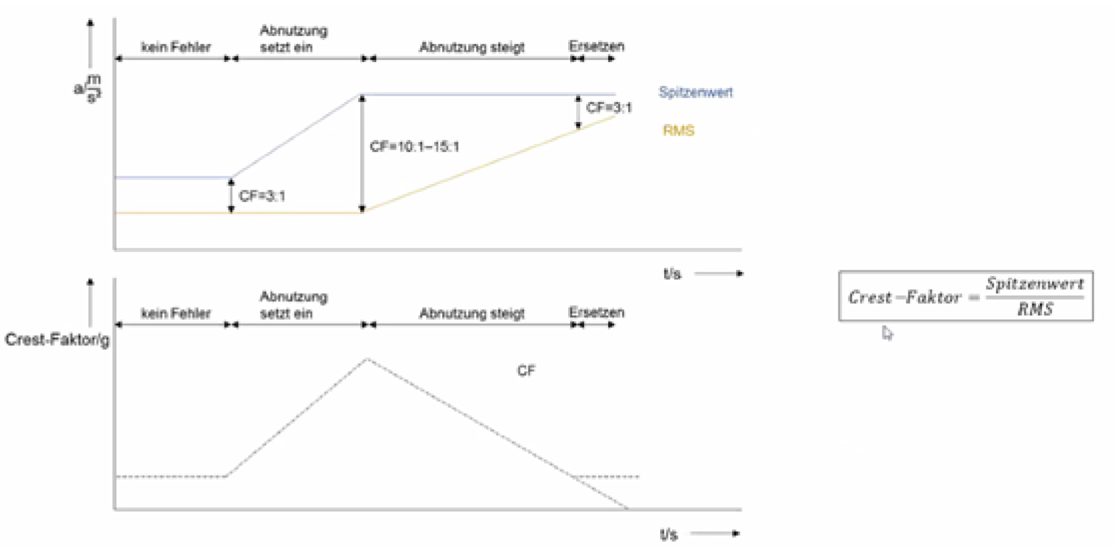


*Figure 32 – Crest factor diagram*

In the graphics in figure 33 it can be seen the results of the tests with 1200 rpm, with new bearings and a 50h bearing. After observing these graphics, it was possible to see that the 50 hours bearing has almost the same behavior as the new bearings just like the trials with 600 rpm. With these trials it can be seen that with a higher number of revolutions per minute the range of values is higher, thus containing higher peaks.

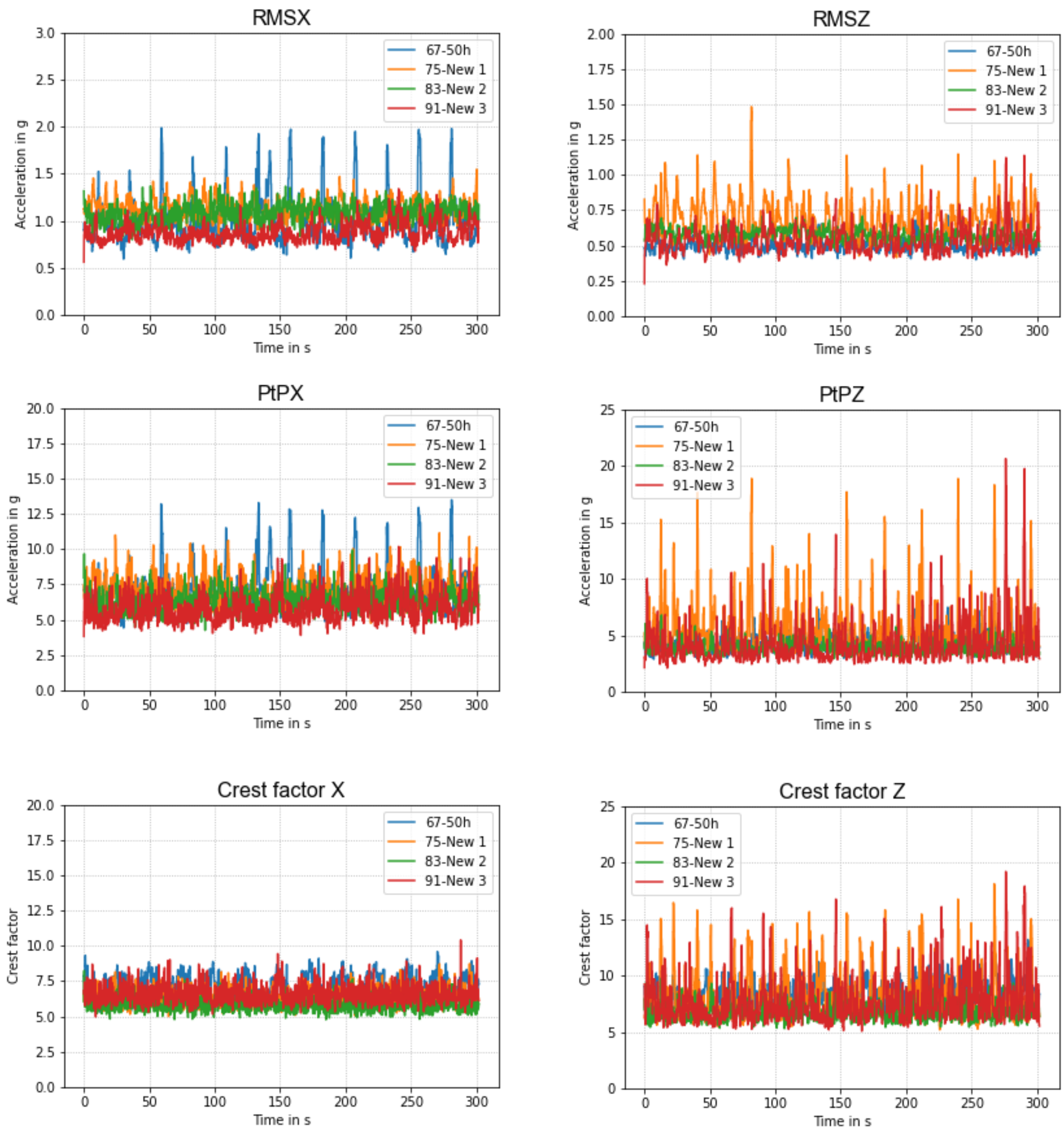


*Figure 33 -Results from the trials with 50h and new bearings with 1200rpm*

## 6.5 Trials with the ASC-325 sensor

To perform the trials with the sensor from the company ASC, the sensor was fitted via 4 M3 socket head cap screws to the component that fits on top of the bearing. For the trials with this sensor the new component that fits directly to the testbench was already used. This new adapter already has the correct tolerances and fitted perfectly onto the testbench. With this new adapter it was already possible to obtain more accurate results with no need to find an error-solution to solve the problem.

Then the bearing to be tested was placed and secured with two washers and a socket head cap screw, just as in the previous tests. Next, the cable ties and the carabiner were placed in order to apply the desired force. Finally, the sensor was checked to see if it is leveled using a leveling ruler. If it isn't leveled, the cable ties are adjusted until it is leveled. After this, the trials can be started.

### 6.5.1 Trials (DOE)

For the first tests with this sensor the same DOE, table 9, was used as with the other sensor, with the difference that all three axes were measured.

*Table 9 – First trials with the ASC-325 sensor*

| Run | Weight (Kg) | RPM (rpm) | Time (min) | Bearing type | New mounted ? | Mounting | Measured axis |
|---|---|---|---|---|---|---|---|
| 8 | 1 | 1200 | 10 | New | Yes | Air | X-axial; Y-radial; Z-radial |
| 11 | 0,5 | 600 | 10 | New | No | Air | X-axial; Y-radial; Z-radial |
| 12 | 1 | 600 | 5 | New | No | Air | X-axial; Y-radial; Z-radial |
| 14 | 2,5 | 1200 | 10 | New | No | Air | X-axial; Y-radial; Z-radial |
| 16 | 1 | 600 | 5 | New | No | Air | X-axial; Y-radial; Z-radial |
| 18 | 0,5 | 1200 | 5 | New | No | Air | X-axial; Y-radial; Z-radial |
| 20 | 2,5 | 1200 | 5 | New | No | Air | X-axial; Y-radial; Z-radial |
| 23 | 2,5 | 600 | 10 | New | No | Air | X-axial; Y-radial; Z-radial |
| 1 | 0,5 | 1200 | 10 | Corrosion | Yes | Air | X-axial; Y-radial; Z-radial |
| 5 | 2,5 | 600 | 5 | Corrosion | No | Air | X-axial; Y-radial; Z-radial |
| 6 | 2,5 | 1200 | 5 | Corrosion | No | Air | X-axial; Y-radial; Z-radial |
| 7 | 2,5 | 1200 | 10 | Corrosion | No | Air | X-axial; Y-radial; Z-radial |
| 9 | 0,5 | 1200 | 5 | Corrosion | No | Air | X-axial; Y-radial; Z-radial |
| 15 | 0,5 | 600 | 10 | Corrosion | No | Air | X-axial; Y-radial; Z-radial |
| 21 | 1 | 600 | 5 | Corrosion | No | Air | X-axial; Y-radial; Z-radial |
| 24 | 2,5 | 1200 | 10 | Corrosion | No | Air | X-axial; Y-radial; Z-radial |
| 2 | 0,5 | 600 | 5 | Milled | Yes | Air | X-axial; Y-radial; Z-radial |
| 3 | 2,5 | 600 | 10 | Milled | No | Air | X-axial; Y-radial; Z-radial |
| 4 | 2,5 | 600 | 5 | Milled | No | Air | X-axial; Y-radial; Z-radial |
| 10 | 2,5 | 1200 | 10 | Milled | No | Air | X-axial; Y-radial; Z-radial |
| 13 | 0,5 | 600 | 10 | Milled | No | Air | X-axial; Y-radial; Z-radial |
| 17 | 2,5 | 1200 | 10 | Milled | No | Air | X-axial; Y-radial; Z-radial |
| 19 | 0,5 | 1200 | 5 | Milled | No | Air | X-axial; Y-radial; Z-radial |
| 22 | 0,5 | 1200 | 5 | Milled | No | Air | X-axial; Y-radial; Z-radial |
| 25 | 0,5 | 600 | 10 | Milled | No | Air | X-axial; Y-radial; Z-radial |

### 6.5.2 Results analysis

As shown in figure 36, the data obtained with this sensor is different. This sensor provides raw data, in the different axes. In order to analyze this data obtained graphics were made in Fourier transform format. What the Fourier transform does is basically transform a signal from time domain into frequency domain through a mathematical function. In the results obtained it can be observed that there are extra frequencies. These small frequencies might be due to the fact that there are other bearings in the test bench where the sensor is probably also measuring them.

To better understand the results obtained with these trials with the OS 325MF-PG-002 sensor it is important to understand the composition of a bearing. A bearing is composed by different elements such as the outer ring, the inner ring, the rolling elements, the cage and the seals, as showed in figure 34.

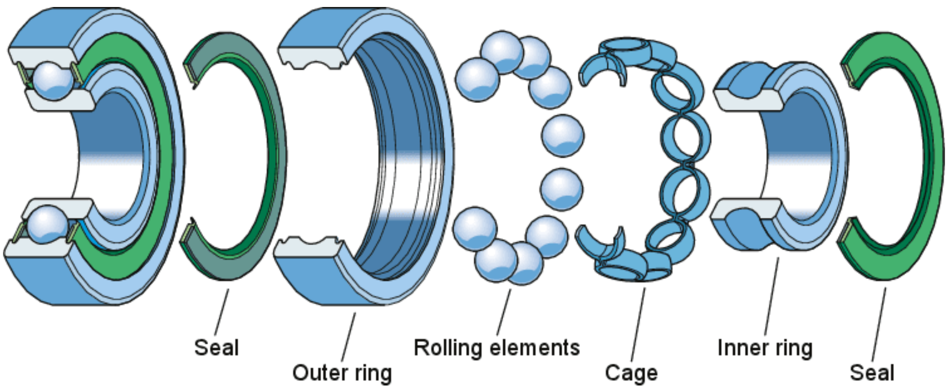


*Figure 34 – Elements of the bearing*
*Source: https://skyhighelearn.com/how-to-select-right-bearing-for-your-application-bearing-selection-guide/*

With these trials good results were achieved because for example in corrosive bearing and in the milled bearing it can be detected the damage. On the milled bearing it is possible to recognize the damage in the outer ring and on the corrosive bearing it is possible to spot the damage in all of the parts. This can be seen in all single parts of the bearing, such as the damage in the outer ring, the damage on the inner ring and on the cage of the bearing.

$$\text{Rotational Speed} = \frac{600\ rpm}{60} = 10/\text{s}$$

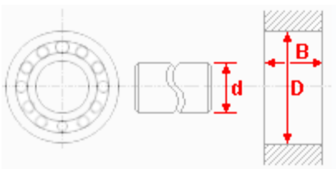


| | 6001 |
|---|---|
| d | 12 mm |
| D | 28 mm |
| B | 8 mm |

| | | 6001 | |
|---|---|---|---|
| | | frequency Related to 1/s | frequency Related to 10/s |
| Overrolling frequency factor on outer ring | BPFFO | 3,0476 | 30,476 |
| Overrolling frequency factor on inner ring | BPFFI | 4,9524 | 49,524 |
| Overrolling frequency factor on rolling element | BSFF | 1,9809 | 19,809 |
| Ring pass frequency factor on rolling element | RPFFB | 3,9618 | 39,618 |
| Speed factor of rolling element set for rotating inner ring | FTFF_i | 0,3810 | 3,810 |
| Speed of rolling element set for rotating outer ring | FTFF_o | 0,6190 | 6,190 |

*Figure 35 - FAG Media Bearing Frequency Theoretical Values 600rpm*

In the milled one it can be seen by checking the table in figure 35 that there is an overroling frequency factor on the outer ring of 30, 476 Hz. And it can be checked that on the diagram in figure 36 of the milled bearing, that there is at 30 Hz a peak because there is a damage on the outer ring and then at 60 Hz and then at 90 Hz because of the oscillation from it, and this peak happens because this bearing was milled in the outer ring. In the case of the new bearing there are no peaks because since this is a new bearing it doesn't have damage and therefore no peaks can be measured. For the corrosive bearing it is possible to see all the damages this bearing has. Around 3Hz it can be seen a defect on the speed factor of rolling element set for rotating inner ring, then at around 6Hz it can be observed a defect on the speed of rolling element set for rotating outer ring, then around 20Hz it can be seen a defect on the overrolling frequency factor on rolling element. Around 30Hz it can be detect another defect, this time on the overrolling frequency factor on the outer ring and then again at 60Hz. And it can also be detected a defect on the ring pass frequency factor on rolling element, around 40Hz.

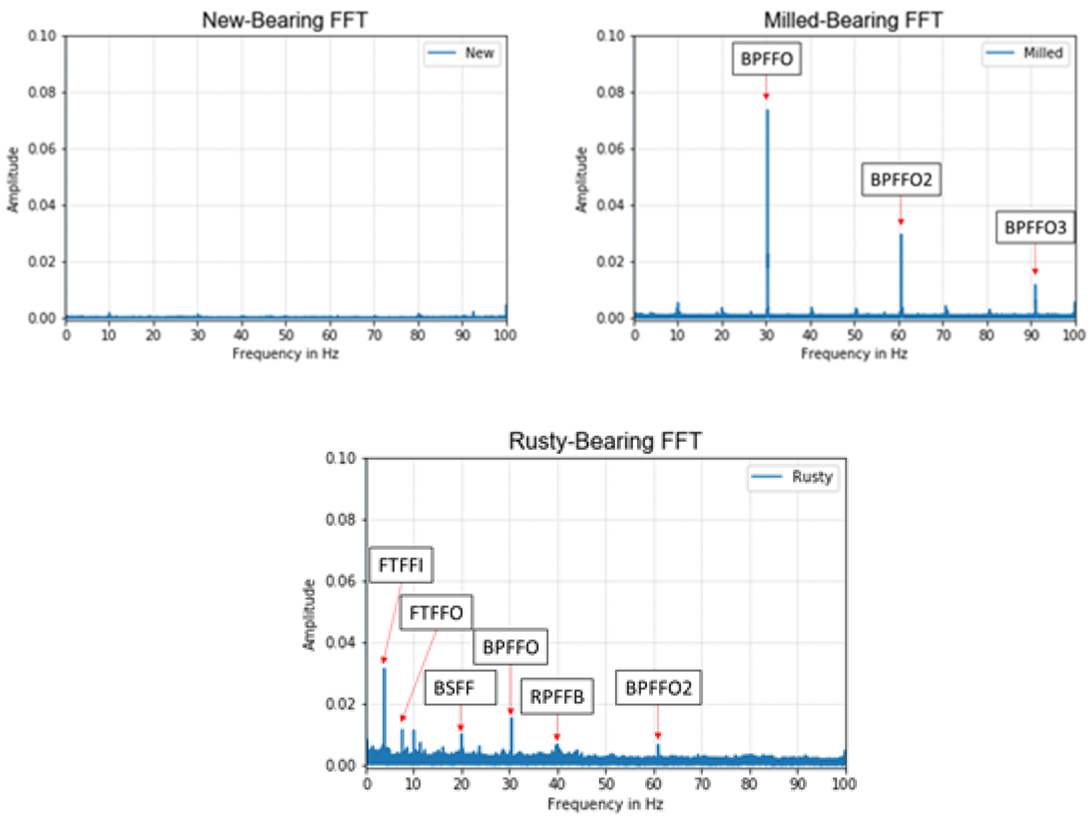


*Figure 36 - Results from the first trials with the ASC-325 sensor*

### 6.5.3 Second Trials (DOE)

For these second trials a new DOE was performed, in which the bearing with 50 hours and three new bearings were compared. This DOE came about after the first trials performed on the polishing head robot. Because after these trials it was found that there was a better performance with the 50 hours bearing than the new bearing, or the bearings were incorrectly assembled which led to the 50 hours bearing having a better performance than the new bearing. For more details about the first tests performed on the robot see chapter 8, subchapter 8.1. In order to find out whether in fact the bearings were mounted incorrectly or whether in fact a bearing with a few hours of running time gives better results, this DOE was created. The purpose of this DOE is to verify the behavior of these different bearings, which one performs best, and to understand what happened in the robot trials.

*Table 10 - Second trials in the testbench with ASC-325 sensor*

| Run | Weight(Kg) | RPM (rpm) | Time (min) | Bearing type | New mounted ? | Mounting | Measured axis |
|---|---|---|---|---|---|---|---|
| 26 | 2,5 | 600 | 5 | 50h | Yes | Air | X-axial; Y-radial; Z-radial |
| 27 | 2,5 | 600 | 5 | 50h | No | Air | X-axial; Y-radial; Z-radial |
| 28 | 2,5 | 600 | 5 | 50h | No | Air | X-axial; Y-radial; Z-radial |
| 29 | 2,5 | 600 | 5 | 50h | No | Air | X-axial; Y-radial; Z-radial |
| 30 | 2,5 | 1200 | 5 | 50h | No | Air | X-axial; Y-radial; Z-radial |
| 31 | 2,5 | 1200 | 5 | 50h | No | Air | X-axial; Y-radial; Z-radial |
| 32 | 2,5 | 1200 | 5 | 50h | No | Air | X-axial; Y-radial; Z-radial |
| 33 | 2,5 | 1200 | 5 | 50h | No | Air | X-axial; Y-radial; Z-radial |
| 34 | 2,5 | 600 | 5 | New (1) | Yes | Air | X-axial; Y-radial; Z-radial |
| 35 | 2,5 | 600 | 5 | New (1) | No | Air | X-axial; Y-radial; Z-radial |
| 36 | 2,5 | 600 | 5 | New (1) | No | Air | X-axial; Y-radial; Z-radial |
| 37 | 2,5 | 600 | 5 | New (1) | No | Air | X-axial; Y-radial; Z-radial |
| 38 | 2,5 | 1200 | 5 | New (1) | No | Air | X-axial; Y-radial; Z-radial |
| 39 | 2,5 | 1200 | 5 | New (1) | No | Air | X-axial; Y-radial; Z-radial |
| 40 | 2,5 | 1200 | 5 | New (1) | No | Air | X-axial; Y-radial; Z-radial |
| 41 | 2,5 | 1200 | 5 | New (1) | No | Air | X-axial; Y-radial; Z-radial |
| 42 | 2,5 | 600 | 5 | New (2) | Yes | Air | X-axial; Y-radial; Z-radial |
| 43 | 2,5 | 600 | 5 | New (2) | No | Air | X-axial; Y-radial; Z-radial |
| 44 | 2,5 | 600 | 5 | New (2) | No | Air | X-axial; Y-radial; Z-radial |
| 45 | 2,5 | 600 | 5 | New (2) | No | Air | X-axial; Y-radial; Z-radial |
| 46 | 2,5 | 1200 | 5 | New (2) | No | Air | X-axial; Y-radial; Z-radial |
| 47 | 2,5 | 1200 | 5 | New (2) | No | Air | X-axial; Y-radial; Z-radial |
| 48 | 2,5 | 1200 | 5 | New (2) | No | Air | X-axial; Y-radial; Z-radial |
| 49 | 2,5 | 1200 | 5 | New (2) | No | Air | X-axial; Y-radial; Z-radial |
| 50 | 2,5 | 600 | 5 | New (3) | Yes | Air | X-axial; Y-radial; Z-radial |
| 51 | 2,5 | 600 | 5 | New (3) | No | Air | X-axial; Y-radial; Z-radial |
| 52 | 2,5 | 600 | 5 | New (3) | No | Air | X-axial; Y-radial; Z-radial |
| 53 | 2,5 | 600 | 5 | New (3) | No | Air | X-axial; Y-radial; Z-radial |
| 54 | 2,5 | 1200 | 5 | New (3) | No | Air | X-axial; Y-radial; Z-radial |
| 55 | 2,5 | 1200 | 5 | New (3) | No | Air | X-axial; Y-radial; Z-radial |
| 56 | 2,5 | 1200 | 5 | New (3) | No | Air | X-axial; Y-radial; Z-radial |
| 57 | 2,5 | 1200 | 5 | New (3) | No | Air | X-axial; Y-radial; Z-radial |

### 6.5.4 Second trials results analysis

As mentioned earlier, to analyze the results obtained with this sensor, Fourier transforms were performed for the various axes. In these graphics it can be seen that there is a peak at 10 Hz. This is because the rotational speed is equal to 600 rotations per minute divided by 60 seconds, which results in the 10 Hz,

In these graphics in figure 37 it can be noticed also notice that the values in the Z-axis start at around 1 g and not in 0 like the other graphics. This happens due to gravitational forces, because on Earth all components have a weight or a downward force of gravity.

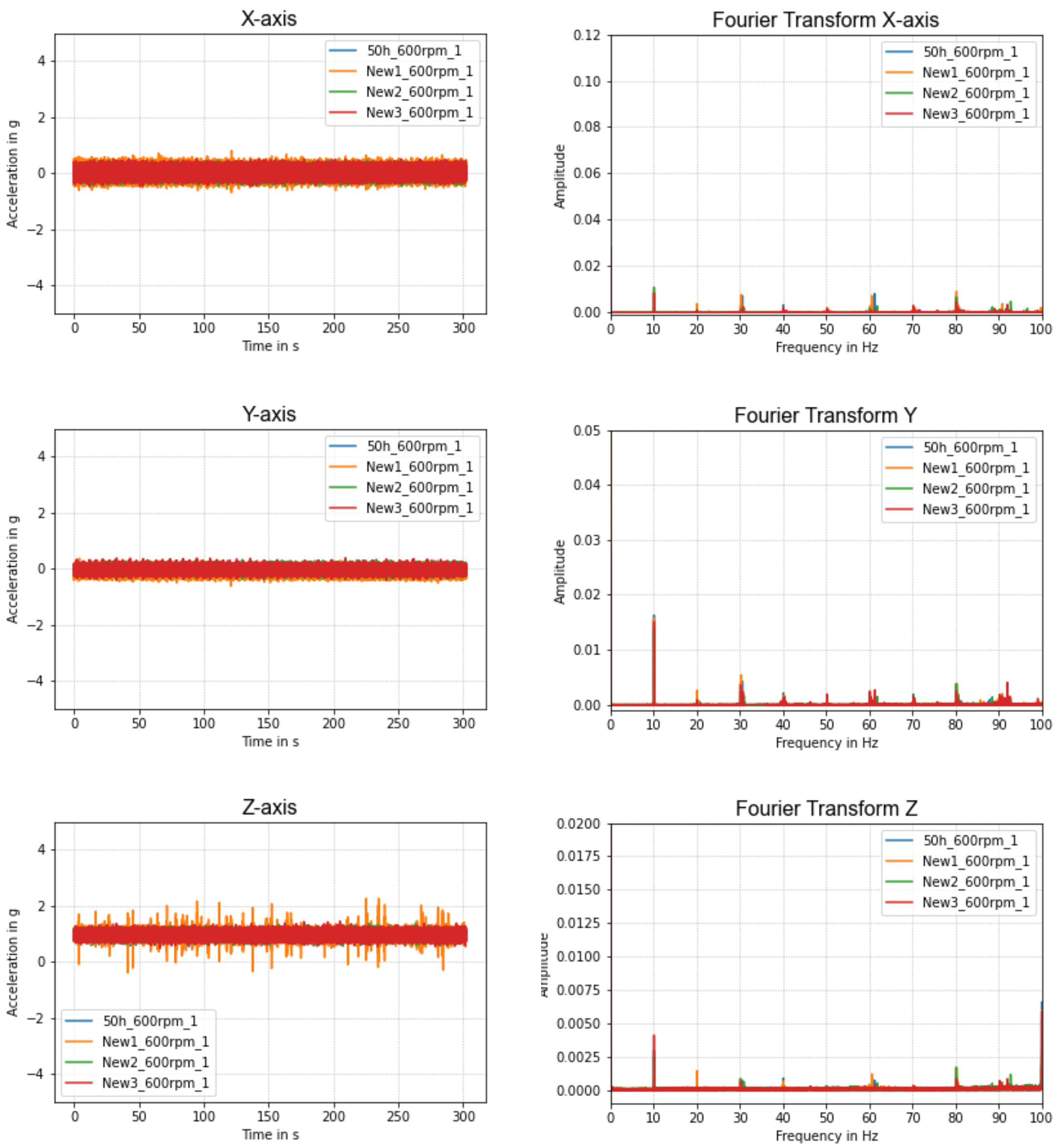


*Figure 37 – Results of the second trials with the ASC-325 sensor with new and 50h bearings with 600rpm*

In the tests at 1200 rpm the rotational speed is equal to 1200 rotations per minute divided by 60 seconds, which gives a result of 20 seconds. That is, in every 20 hertz, because it is in frequency domain, there is a peak that can be seen in figure 39. And also with the following table on figure 38, it is possible to understand what each peak corresponds to in order to be able to analyze the results in more detail, in order to know where the vibrations are coming from. For example, the peak in 40 Hz corresponds to the overrolling frequency factor on a rolling element. Or for example, the peak in 80 Hz corresponds to the roverrolling frequency factor on the outer ring.

$$\text{Rotational speed} = \frac{1200\ rpm}{60} = 20/s$$


| | 6001 |
|---|---|
| d | 12 mm |
| D | 28 mm |
| B | 8 mm |

| | | 6001 | |
|---|---|---|---|
| | | frequency Related to 1/s | frequency Related to 20/s |
| Overrolling frequency factor on outer ring | BPFFO | 3,0476 | 60,952 |
| Overrolling frequency factor on inner ring | BPFFI | 4,9524 | 99,048 |
| Overrolling frequency factor on rolling element | BSFF | 1,9809 | 39,618 |
| Ring pass frequency factor on rolling element | RPFFB | 3,9618 | 79,236 |
| Speed factor of rolling element set for rotating inner ring | FTFF_i | 0,3810 | 7,62 |
| Speed of rolling element set for rotating outer ring | FTFF_o | 0,6190 | 12,38 |

*Figure 38 - FAG Media Bearing Frequency Theoretical Values 1200rpm*

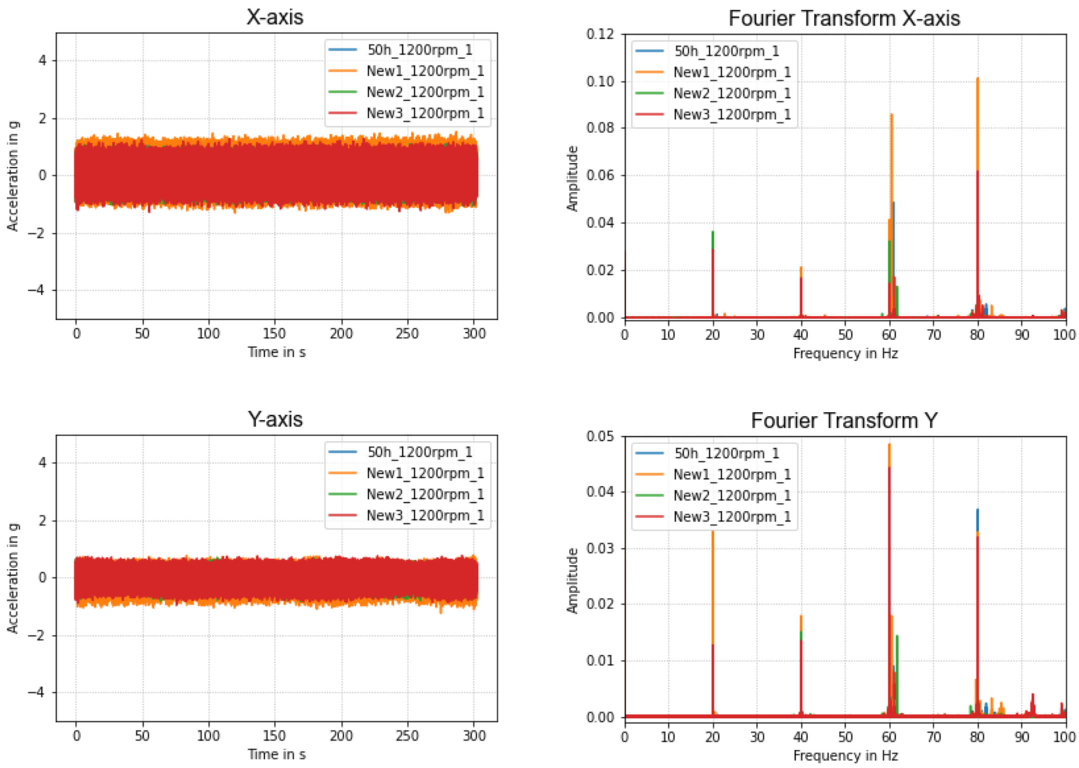

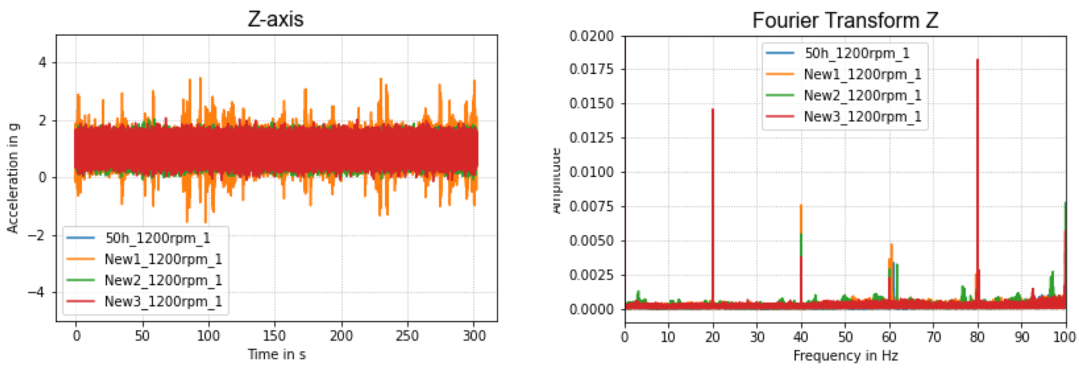


*Figure 39 - Results of the second trials with the ASC-325 sensor with new and 50h bearings with 1200rpm*

## 6.6 Conclusions on the trials in the testbench

After these trials in the testbench it was possible to withdraw very good conclusions such as the fact that the vibration differences can be seen depending on the mounting method, but on these second trials with the different liquids it was not so clear to see which one was more suitable. In the first trials with the liquids, oil provided best results in the transmission of vibrations to the sensor. This possibly happened because in the first trials the testbench was working properly, meanwhile in the second trials the vibrations on the testbench were not constant, which may had affected the results obtained, thus not being so clear in the second trials to see which one worked best.

With these trials in the testbench it was also possible to conclude that a new bearing with 0 hours running shows better results than a run-in bearing with 50 hours. This means that in the first trials in the polishing head, the bearings were incorrectly mounted, or something in the polishing head was wrongly assembled.

From the trials with new, milled and corrosive bearings it was possible to get good results where it can be seen the damage on the respective bearings throughout the vibrations. Specially with the ASC-325 sensor, where it was possible to identify the damage on different elements throughout the vibrations, providing feedback of the condition of the bearing and where that damage is located.

In conclusion, the sensors are suitable for condition monitoring. The bearings condition can be measured in situ on the testbench.

# 7. Implementation of the sensors in the polishing head machine

## 7.1 Where and how the sensor was implemented

To implement the sensors in the polishing head machine it was developed a component that has two docking zones, with a variation of sensor arrangement to later see if the difference in sensor location affects the results.

To implement the sensor into the polishing head machine the metal part/component made out of aluminum was developed that is fitted into the polishing head machine, figure 40. This component contains an area to fit the vibration sensors. The location of the sensor implementation is due to the fact that one of the main bearings of the machine is located in this area, and also for logical reasons, since it is much easier to attach or detach this end rather than to disassemble the whole robot and reassemble it.

*Figure 40 - Sensors mounted in the adapter that is mounted in the polishing head robot*

### 7.1.1 Sensors holder

This component has been produced in aluminum. This component consists of an M20 thread in the inner area and that area is the one that fits directly into the end of the polishing head. At the end of the component a magnet has been placed. This magnet is for the polishing tools to fit into the part, since these tools also contain a magnet inside. This component also has 14 M3 holes, 8 to fit the ASC-325 sensor, 4 on each side of the adapter, 4 to fit the BALLUFF sensor, 2 on each side, and 2 holes to fit the chain. In figure 41 it can be seen the different sensor arrangements, the yellow square corresponds to the ASC-325 sensor and the blue rectangle corresponds to the BALLUFF sensor.

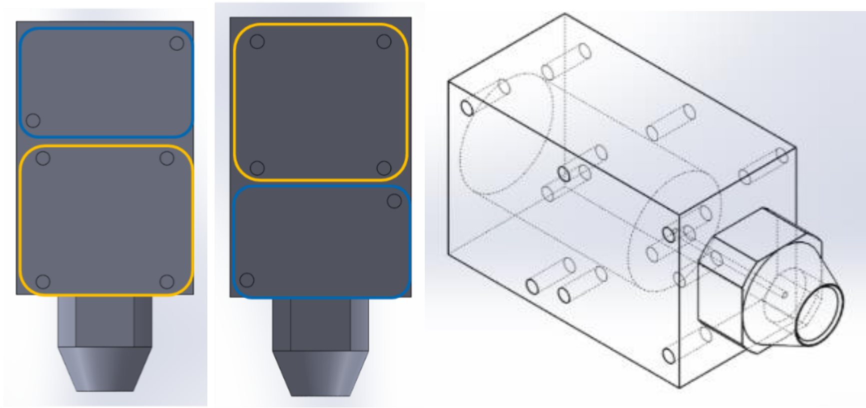

*Figure 41 – CAD model of the sensors adapter*

## 7.1.2 Energy chain

Since the selected sensors require a cable to connect to, it was necessary to think of a solution that would protect the cables from wear and tear or a solution that would soften or slow down the wear and tear on the cables. Several solutions were analyzed, such as arranging supports for the cables so that they would not get loose or sealing the cables with foam so that this coating layer would protect the cable, thus wearing off the coating and not the cable. After this research it was possible to realize that energy chains would be the most viable solution for this case. This was followed by further research into different energy chain types, how the cables are placed within the energy chain and their different sizes and lengths. To select the chain the measurements of the sensor cables were taken into consideration. After seeing that the cable for sensor BALLUFF has at the end in the IO-Link connection part a diameter of approximately 14,5 mm, a chain with an inner height of 14,9mm was selected. An open chain was selected because the closed chains would open during use due to the vibration, causing the locking to get loose and this would not be ideal because it could cause unnecessary additional vibrations. The selected chain was the model E2C.15 of the company IGUS, figure 42.

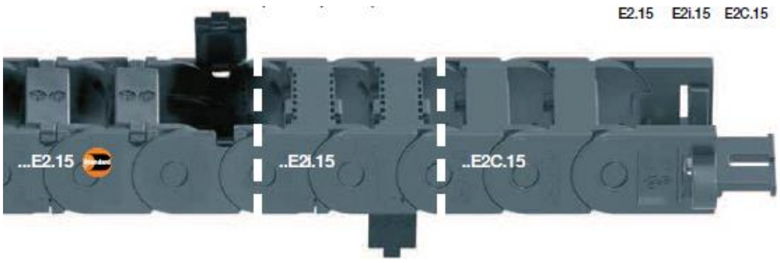


*Figure 42 – Energy chain model E2C.15 from IGUS*

To solve the problem with cables, a energy chain was used in order to prevent the cables from suffering damage. This was one of the main problems of the project since the machine is always rotating and moving it causes a lot of vibration in the cable and eventually the cable would break, so to avoid the cable to break it was used a energy chain. An energy chain is a chain made with plastics links connected to each other, where the cables go inside. This chain prevents the cables from getting damaged by protecting them and reducing the cable vibration because the cable is trapped inside the chain and there is not much space left for it to move. This chain was then attached to the adapter and another side component added to a polishing head cage post.

This is just a solution in order to protect the cables, but after some tests it was possible to realize that this would not be the best solution for this project, because the more revolutions per minute that were applied the more extra vibration is created by the chain, thus affecting the results. This solution only works at lower rotating angular frequency's.

*Figure 43 – Energy chain assembled into the polishing head robot*

In order to prevent the energy chain causing additional vibrations, some of the links were mounted on the opposite order which makes the links block. This means that the links don't have any angle to move making that part of the chain stiff. Then in order not to have too many extra vibrations the chain was blocked in some parts, so that it wouldn't be so loose and wouldn't echo/reverberate small vibrations turning them into big vibrations.

### 7.1.3 Cables connection

To connect the cables these were attached inside the chain, then the BALLUFF sensor cable was connected to the IO-Link USB Master and this device was placed on one of the legs of the polishing stand, then the device was connected to the computer thus activating the sensor. The ASC-325 sensor was connected to the power supply and the NI USB 6001, and then connected to the computer.

# 8. Trials with the sensors in the polishing head machine

## 8.1 First Trials

Since there are different possible combinations of parameters of the robot polishing process, it then becomes complicated to figure out which factors have the greatest impact in the machine performance. For this it was necessary to develop a series of trials with different combinations in order to understand and gain a deeper understanding of the operation and polishing process of this machine. In figure 44 it can be seen the polishing head robot trials set-up with the energy-chain and polishing track.

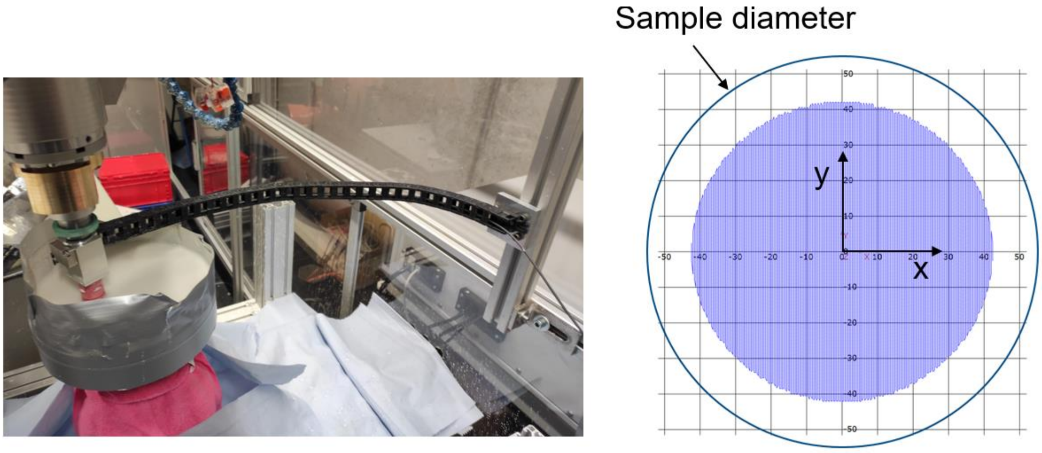


*Figure 44 – Robot trials set-up; Polishing track (units in mm)*

### 8.1.1 DOE (BALLUFF)

*Table 11 – DOE of the first trials with the BALLUFF sensor on the robot*

| Run | Weight(Kg) | RPM (rpm) | Time (min) | Vorschub (mm/s) | Bearing | New mounted? | Monting | Workpiece | Polishing track | Eccentric (mm) | Tool size (mm) | Tool coating | Point distance (mm) | Oscillation | Polishing agent | Measured axis |
|---|---|---|---|---|---|---|---|---|---|---|---|---|---|---|---|---|
| 1 | 2,5 | 600 | 10 | 23,5 | ~ 50h | Yes | Air | Plan | Y-Mäander | 7 | 15 | Suba500 | 0,4 x 0,4 | 1 | Opaline | X-axial; Z-radial |
| 2 | 2,5 | 1200 | 10 | 23,5 | ~ 50h | No | Air | Plan | Y-Mäander | 7 | 15 | Suba500 | 0,4 x 0,4 | 1 | Opaline | X-axial; Z-radial |
| 3 | 2,5 | 600 | 10 | 23,5 | Corrosion | Yes | Air | Plan | Y-Mäander | 7 | 15 | Suba500 | 0,4 x 0,4 | 1 | Opaline | X-axial; Z-radial |
| 4 | 2,5 | 1200 | 10 | 23,5 | Corrosion | No | Air | Plan | Y-Mäander | 7 | 15 | Suba500 | 0,4 x 0,4 | 1 | Opaline | X-axial; Z-radial |
| 5 | 2,5 | 600 | 10 | 23,5 | Milled | Yes | Air | Plan | Y-Mäander | 7 | 15 | Suba500 | 0,4 x 0,4 | 1 | Opaline | X-axial; Z-radial |
| 6 | 2,5 | 1200 | 10 | 23,5 | Milled | No | Air | Plan | Y-Mäander | 7 | 15 | Suba500 | 0,4 x 0,4 | 1 | Opaline | X-axial; Z-radial |
| 7 | 2,5 | 600 | 10 | 23,5 | New 0h | Yes | Air | Plan | Y-Mäander | 7 | 15 | Suba500 | 0,4 x 0,4 | 1 | Opaline | X-axial; Z-radial |
| 8 | 2,5 | 1200 | 10 | 23,5 | New 0h | No | Air | Plan | Y-Mäander | 7 | 15 | Suba500 | 0,4 x 0,4 | 1 | Opaline | X-axial; Z-radial |

To start the first trials on the polishing machine a DOE was created. In the table 11 it can be seen some of the set-up defined on the robot. As polishing agent Opaline was used. This agent was changed after every hour, since this agent tends to become lumpy when left for some time at rest. For this reason, it was changed to ensure that it did not become gritty, so as not to alter the results obtained.

## 8.1.2 Results

After these first tests, results in figure 45, it was noticed that the bearing with 50h running showed less vibrations than the new bearing with zero hours. After these tests it was concluded that this could have been due to incorrect mounting of the bearings in the polishing machine, which would lead to more abnormal vibrations in their operation, or because in fact a bearing with some running-in performs better than a brand new bearing because it has already had some use.

It can also be seen that as expected, the corrosive and milled bearings have higher vibrations, between 10g and 20g in the case of the peak to peak in the X-axis, when compared to the new bearing and the bearing with fifty hours, that have values between 1g to 4g. Also it is possible to observe in the crest factor in the X-axis that the values of the corrosive and milled bearing have an interval of around 10g and the new and 50 hour bearing only have an interval of less then 5g. So it was possible to get good results with the BCM0001 sensor, where it can be seen the difference between the different bearings. This was good because it was not known if it was in fact possible to also analyze it in the polishing head robot the different bearings.

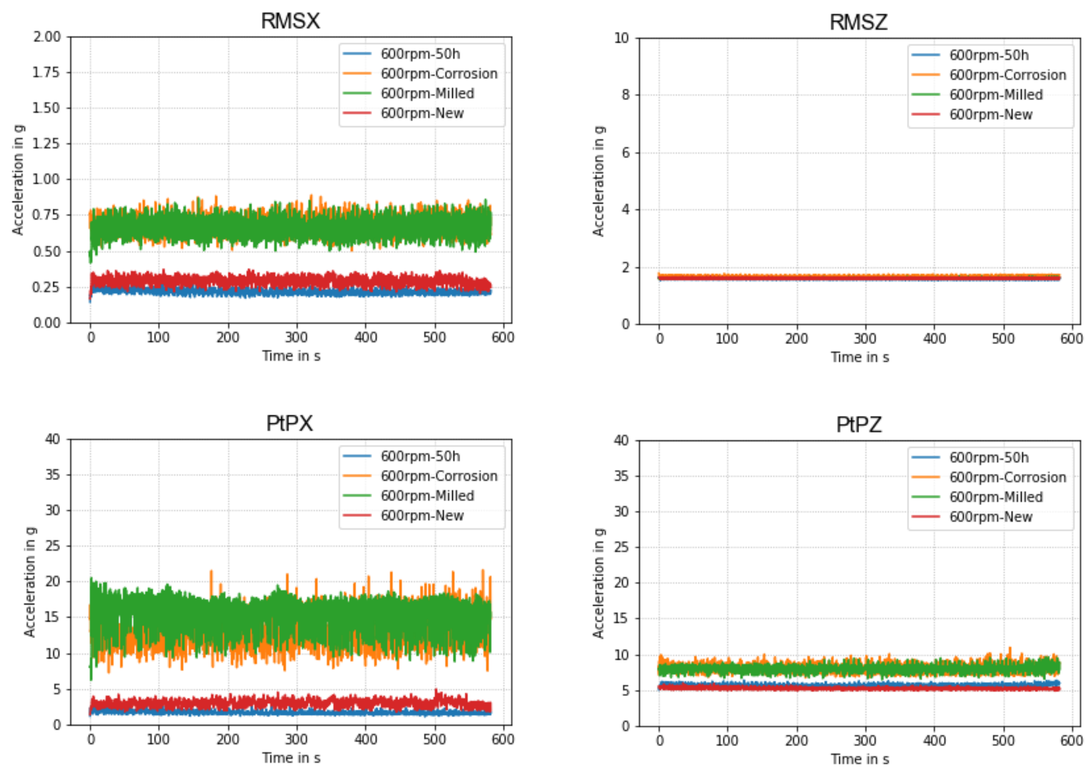

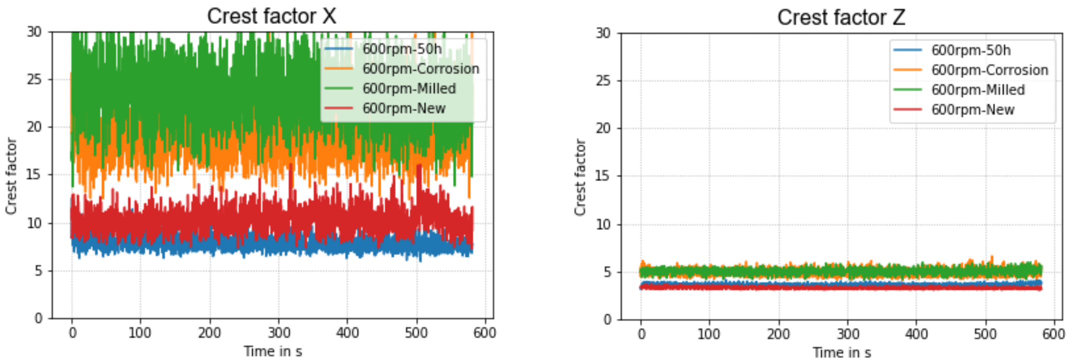


*Figure 45 – Results from the first trials on the robot with 600rpm*

In the tests with 1200rpm it can be observed in the comparison graphs between the different bearing types that the results are saturated at 32g, has it can be seen in the peak-to-peak diagrams on figure 46, since this is the sensor limit. In these tests with more rotations, it is also possible to verify that again the bearing with 50 hours presents a better performance than the bearing with 0 hours, noticing now in a more visible and clear way the disparity of values between them.

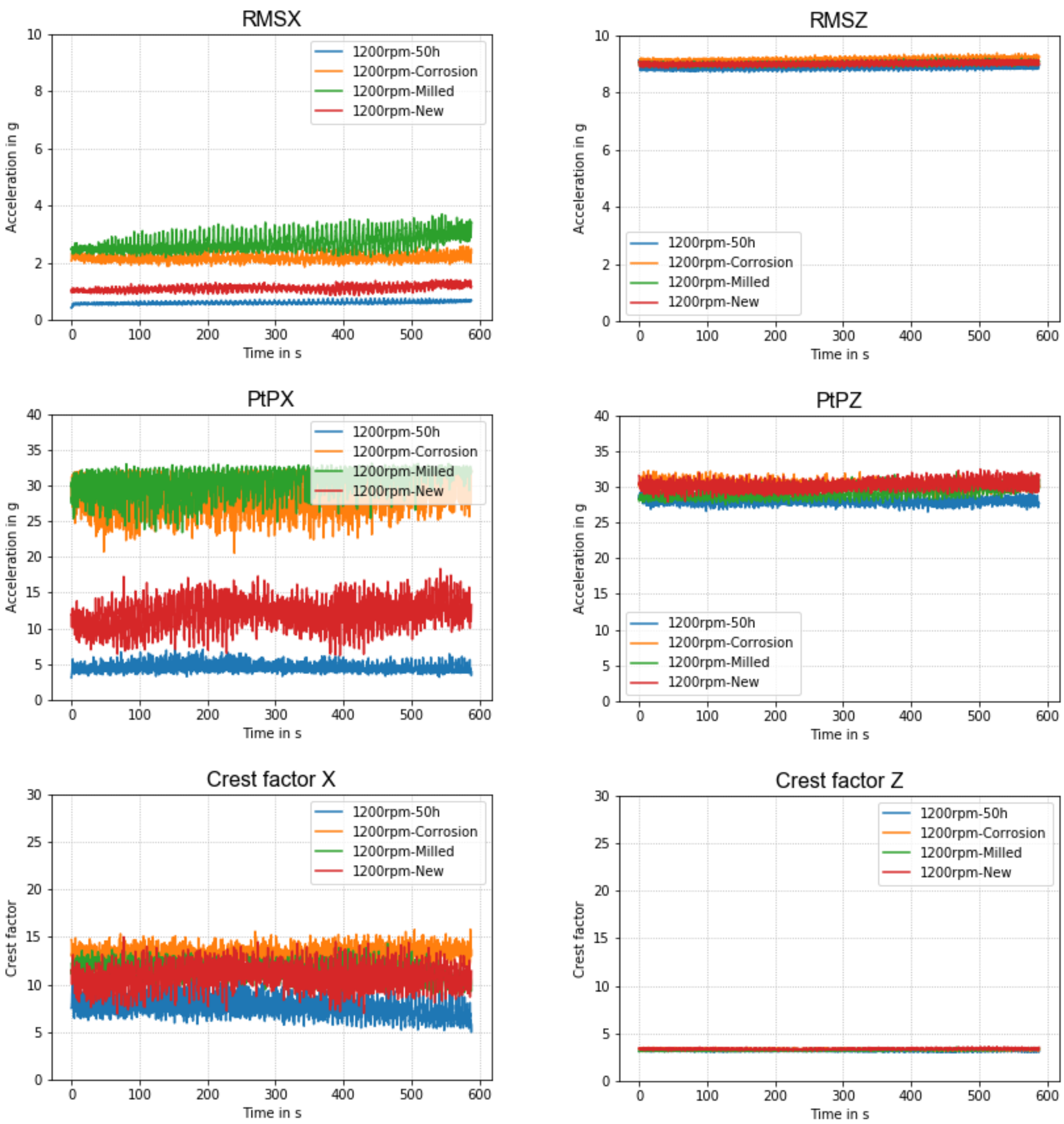


*Figure 46 – Results from the first trials on the robot with 1200rpm*

## 8.2 Second Trials

In these second trials, the same mounting set-up was used. A lot of things may have an impact on the results and in order to obtain the most similar results or in order to reproduce them, the exact same set-up that it was used in the first trials it was used throughout these trials. So basically, none of the element's change, it was used the same number of links in the energy-chain, the same angle of the adapter, and the same mounting of different elements. The only variable that changed in these trials was that a foam in form of a tube was inserted inside the energy chain so that the cables wouldn't move in the interior of the chain in order not to send additional vibrations to the sensor.

## 8.2.1 DOE (BALLUFF)

For this second trials, a DOE was made for the BALLUFF sensor where all different bearings were tested in the polishing head, by the order seen in Table 12. In the polishing head robot trials, it was always used the same program, the only difference between them was the rotations per minute.

*Table 12 – DOE of the second trials on the robot with the BALLUFF sensor*

| Run | Weight(Kg) | RPM (rpm) | Time (min) | Vorschub (mm/s) | Bearing | New mounted? | Monting | Workpiece | Polishing track | Eccentric (mm) | Tool size (mm) | Tool coating | Point distance (mm) | Oscillation | Polishing agent | Measured axis |
|---|---|---|---|---|---|---|---|---|---|---|---|---|---|---|---|---|
| 1 | 2,5 | 600 | 10 | 23,5 | ~ 50h | Yes | Air | Plan | Y-Mäander | 7 | 15 | Suba500 | 0,4 x 0,4 | 1 | Opaline | X-axial; Z-radial |
| 2 | 2,5 | 600 | 10 | 23,5 | ~ 50h | No | Air | Plan | Y-Mäander | 7 | 15 | Suba500 | 0,4 x 0,4 | 1 | Opaline | X-axial; Z-radial |
| 3 | 2,5 | 600 | 10 | 23,5 | ~ 50h | No | Air | Plan | Y-Mäander | 7 | 15 | Suba500 | 0,4 x 0,4 | 1 | Opaline | X-axial; Z-radial |
| 4 | 2,5 | 600 | 10 | 23,5 | Corrosion | Yes | Air | Plan | Y-Mäander | 7 | 15 | Suba500 | 0,4 x 0,4 | 1 | Opaline | X-axial; Z-radial |
| 5 | 2,5 | 600 | 10 | 23,5 | Corrosion | No | Air | Plan | Y-Mäander | 7 | 15 | Suba500 | 0,4 x 0,4 | 1 | Opaline | X-axial; Z-radial |
| 6 | 2,5 | 600 | 10 | 23,5 | Corrosion | No | Air | Plan | Y-Mäander | 7 | 15 | Suba500 | 0,4 x 0,4 | 1 | Opaline | X-axial; Z-radial |
| 7 | 2,5 | 600 | 10 | 23,5 | Milled | Yes | Air | Plan | Y-Mäander | 7 | 15 | Suba500 | 0,4 x 0,4 | 1 | Opaline | X-axial; Z-radial |
| 8 | 2,5 | 600 | 10 | 23,5 | Milled | No | Air | Plan | Y-Mäander | 7 | 15 | Suba500 | 0,4 x 0,4 | 1 | Opaline | X-axial; Z-radial |
| 9 | 2,5 | 600 | 10 | 23,5 | Milled | No | Air | Plan | Y-Mäander | 7 | 15 | Suba500 | 0,4 x 0,4 | 1 | Opaline | X-axial; Z-radial |
| 10 | 2,5 | 600 | 10 | 23,5 | New 1 | Yes | Air | Plan | Y-Mäander | 7 | 15 | Suba500 | 0,4 x 0,4 | 1 | Opaline | X-axial; Z-radial |
| 11 | 2,5 | 600 | 10 | 23,5 | New 1 | No | Air | Plan | Y-Mäander | 7 | 15 | Suba500 | 0,4 x 0,4 | 1 | Opaline | X-axial; Z-radial |
| 12 | 2,5 | 600 | 10 | 23,5 | New 1 | No | Air | Plan | Y-Mäander | 7 | 15 | Suba500 | 0,4 x 0,4 | 1 | Opaline | X-axial; Z-radial |
| 13 | 2,5 | 600 | 10 | 23,5 | New 2 | Yes | Air | Plan | Y-Mäander | 7 | 15 | Suba500 | 0,4 x 0,4 | 1 | Opaline | X-axial; Z-radial |
| 14 | 2,5 | 600 | 10 | 23,5 | New 2 | No | Air | Plan | Y-Mäander | 7 | 15 | Suba500 | 0,4 x 0,4 | 1 | Opaline | X-axial; Z-radial |
| 15 | 2,5 | 600 | 10 | 23,5 | New 2 | No | Air | Plan | Y-Mäander | 7 | 15 | Suba500 | 0,4 x 0,4 | 1 | Opaline | X-axial; Z-radial |
| 16 | 2,5 | 600 | 10 | 23,5 | New 3 | Yes | Air | Plan | Y-Mäander | 7 | 15 | Suba500 | 0,4 x 0,4 | 1 | Opaline | X-axial; Z-radial |
| 17 | 2,5 | 600 | 10 | 23,5 | New 3 | No | Air | Plan | Y-Mäander | 7 | 15 | Suba500 | 0,4 x 0,4 | 1 | Opaline | X-axial; Z-radial |
| 18 | 2,5 | 600 | 10 | 23,5 | New 3 | No | Air | Plan | Y-Mäander | 7 | 15 | Suba500 | 0,4 x 0,4 | 1 | Opaline | X-axial; Z-radial |

## 8.2.2 Results (BALLUFF)

With these results in figure 47 it was possible to observe that both the bearing at 50 hours and the new bearings at 0 hours that there is not much variation between the vibration range.

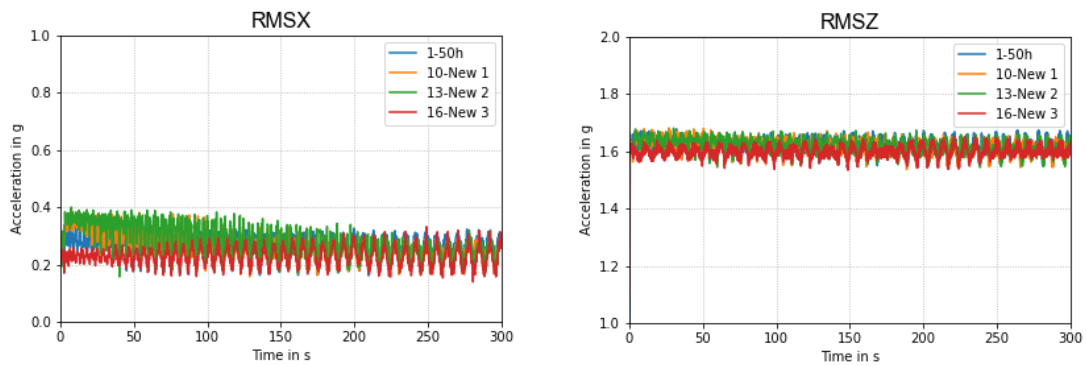

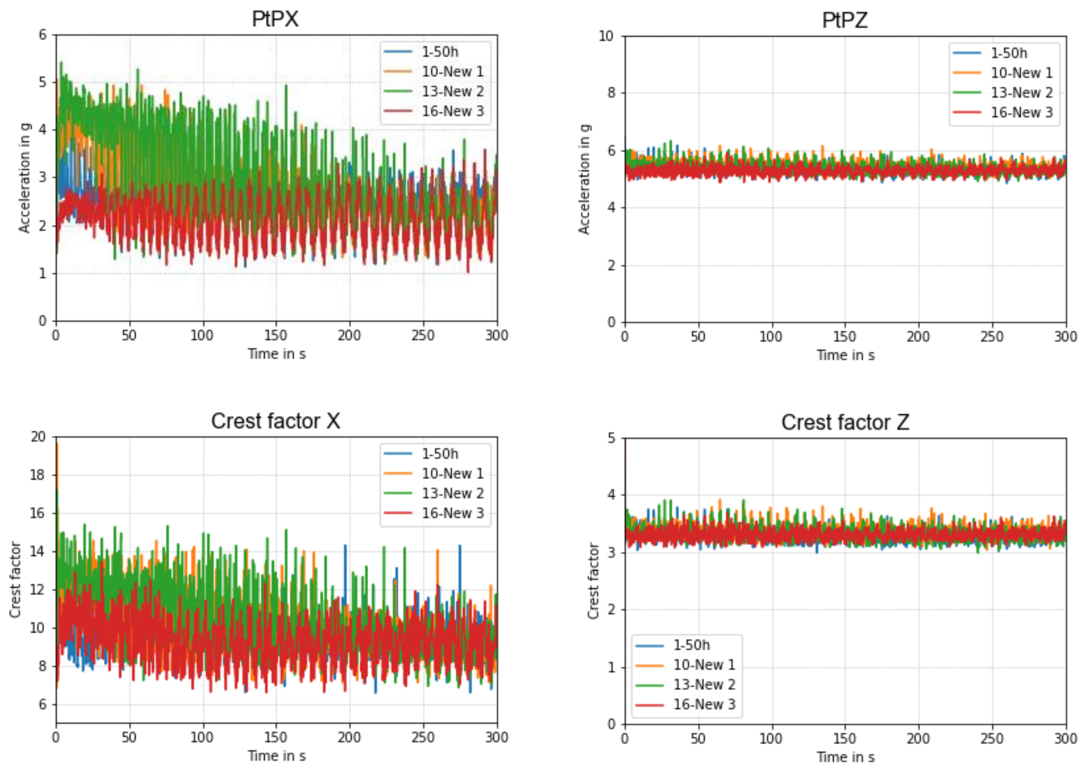


*Figure 47 – Results of the second trials on the robot with the BALLUFF sensor with 50h and new bearings with 600rpm*

After these tests in figure 48, it was possible to see that the results of the first tests were not reproducible, since the discrepancy in values between the new and 50h bearings between the corrosive and milled bearings can no longer be seen.

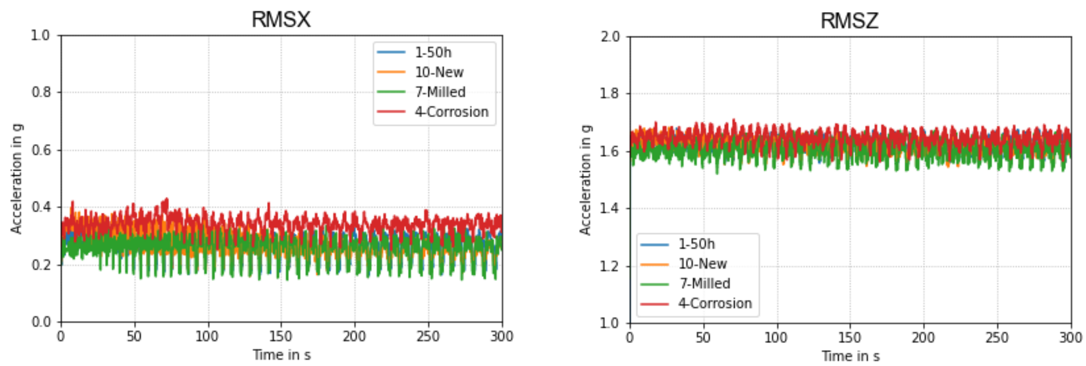

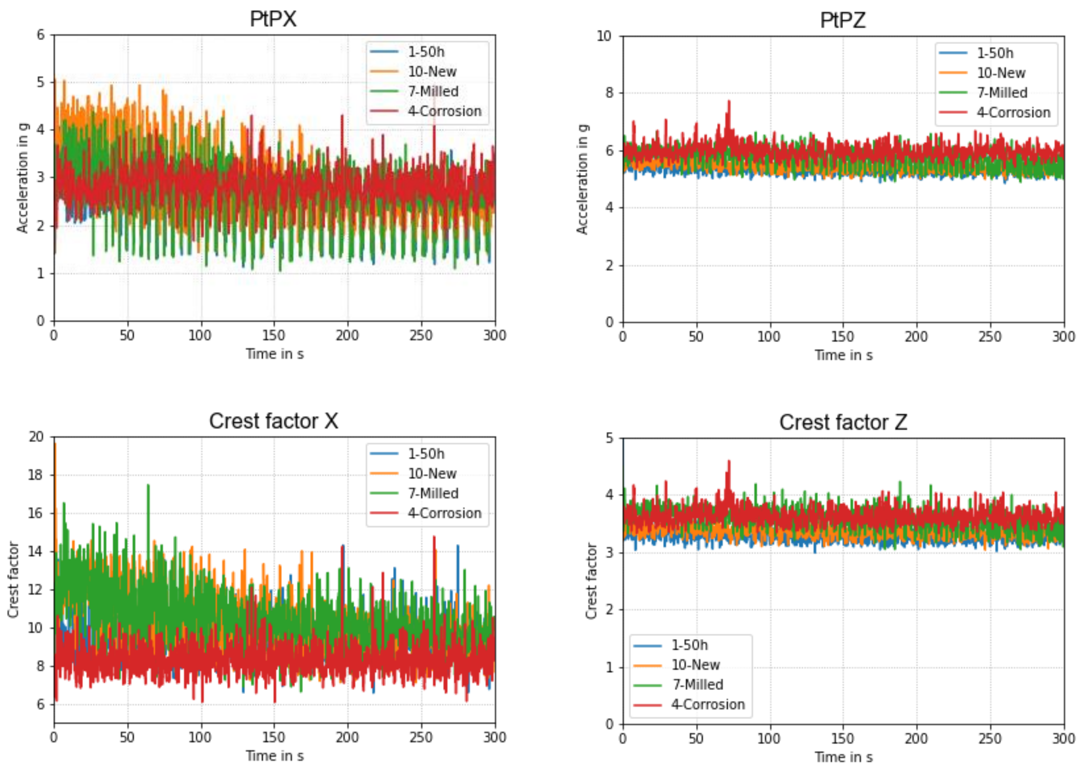


*Figure 48 - Results of the second trials on the robot with the BALLUFF sensor with corrosive, milled, 50h and new bearings with 600rpm*

### 8.2.3 DOE (ASC-325)

For the DOE for the ASC-325 sensor the same bearings were used, only the order that they were tested changed. For this DOE the same 600 revolutions per minute program was used with a runtime of ten minutes.

*Table 13 – DOE of the second trials on the robot with the ASC-325 sensor*

| Run | Weight(Kg) | RPM (rpm) | Time (min) | Bearing type | New mounted ? | Mounting | Measured axis |
|---|---|---|---|---|---|---|---|
| 1 | 2,5 | 600 | 10 | 50h | Yes | Air | X-axial;Y-radial;Z-radial |
| 2 | 2,5 | 600 | 10 | 50h | No | Air | X-axial;Y-radial;Z-radial |
| 3 | 2,5 | 600 | 10 | 50h | No | Air | X-axial;Y-radial;Z-radial |
| 4 | 2,5 | 600 | 10 | New (1) | Yes | Air | X-axial;Y-radial;Z-radial |
| 5 | 2,5 | 600 | 10 | New (1) | No | Air | X-axial;Y-radial;Z-radial |
| 6 | 2,5 | 600 | 10 | New (1) | No | Air | X-axial;Y-radial;Z-radial |
| 7 | 2,5 | 600 | 10 | New (2) | Yes | Air | X-axial;Y-radial;Z-radial |
| 8 | 2,5 | 600 | 10 | New (2) | No | Air | X-axial;Y-radial;Z-radial |
| 9 | 2,5 | 600 | 10 | New (2) | No | Air | X-axial;Y-radial;Z-radial |
| 10 | 2,5 | 600 | 10 | New (3) | Yes | Air | X-axial;Y-radial;Z-radial |
| 11 | 2,5 | 600 | 10 | New (3) | No | Air | X-axial;Y-radial;Z-radial |
| 12 | 2,5 | 600 | 10 | New (3) | No | Air | X-axial;Y-radial;Z-radial |
| 13 | 2,5 | 600 | 10 | Corrosion | Yes | Air | X-axial;Y-radial;Z-radial |
| 14 | 2,5 | 600 | 10 | Corrosion | No | Air | X-axial;Y-radial;Z-radial |
| 15 | 2,5 | 600 | 10 | Corrosion | No | Air | X-axial;Y-radial;Z-radial |
| 16 | 2,5 | 600 | 10 | Milled | Yes | Air | X-axial;Y-radial;Z-radial |
| 17 | 2,5 | 600 | 10 | Milled | No | Air | X-axial;Y-radial;Z-radial |
| 18 | 2,5 | 600 | 10 | Milled | No | Air | X-axial;Y-radial;Z-radial |

### 8.2.4 Results (ASC-325)

As can be seen from the graphics in figure 49, in the trials at 600 rotations per minute with the ASC-325 sensor the results are saturated, making it hard to draw conclusions. In order to prevent this from happening again, lower rotations per minute were used in the following tests.

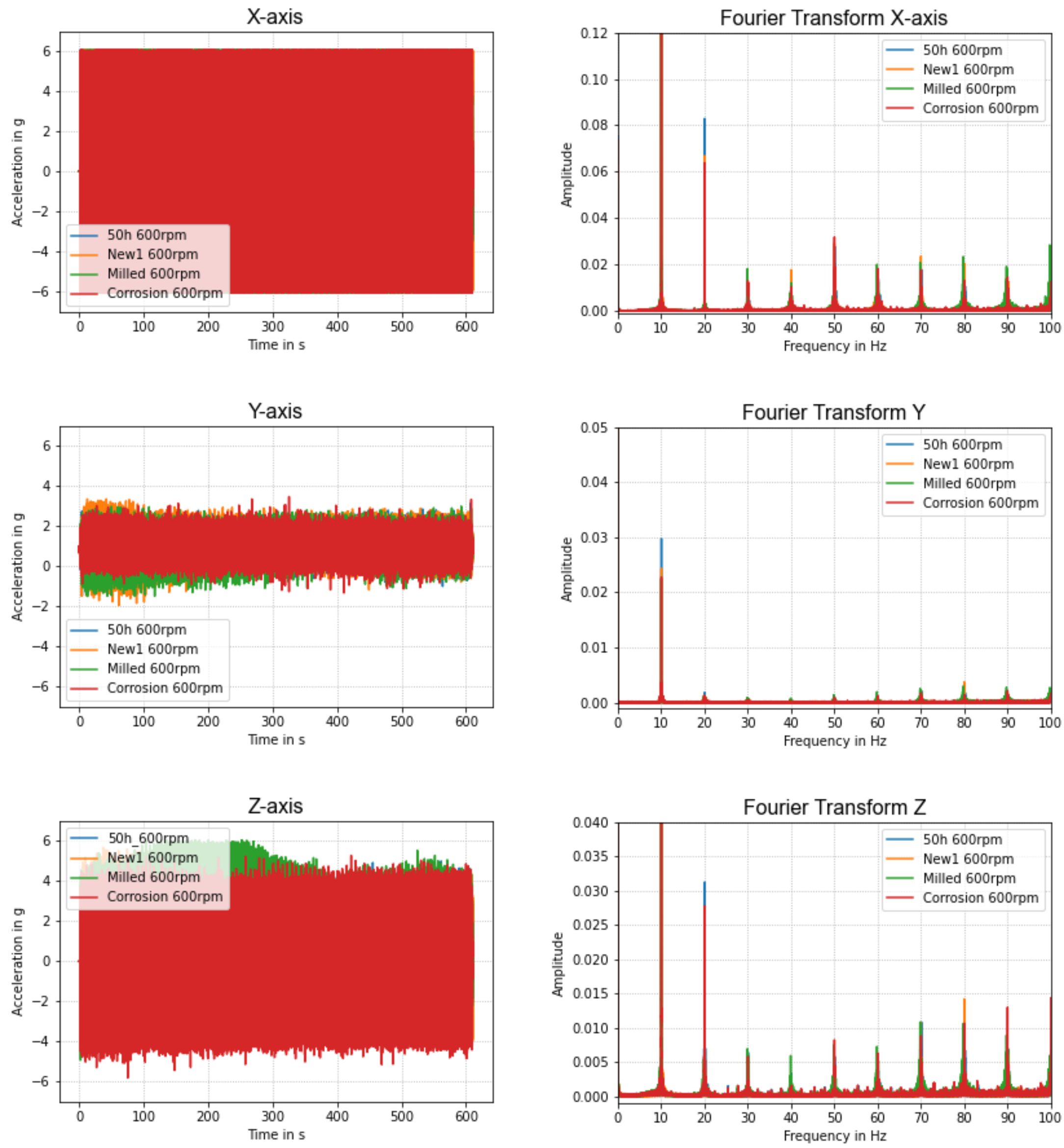


*Figure 49 – Results of the second trials on the robot with 50h, new, milled and corrosive bearings with 600rpm*

In these trials, figure 50, it can be observed that there are extra frequencies, and this might be because of the other bearings in the polishing head robot. In the graphics in the middle of figure 49 it can be seen the theory of the peaks the bearing 6001 should have. With these graphics it is possible to observe that the other bearings of the polishing head robot are also being measured, has it can be seen in the diagrams the theory values of the other bearings match some of the peaks obtained in the results of this trial. The reason the peaks of the bearing 6001 are higher than the other bearings on the test bench is because that is the bearing being tested, where the sensor is measuring, so it will have higher values than the other bearings.

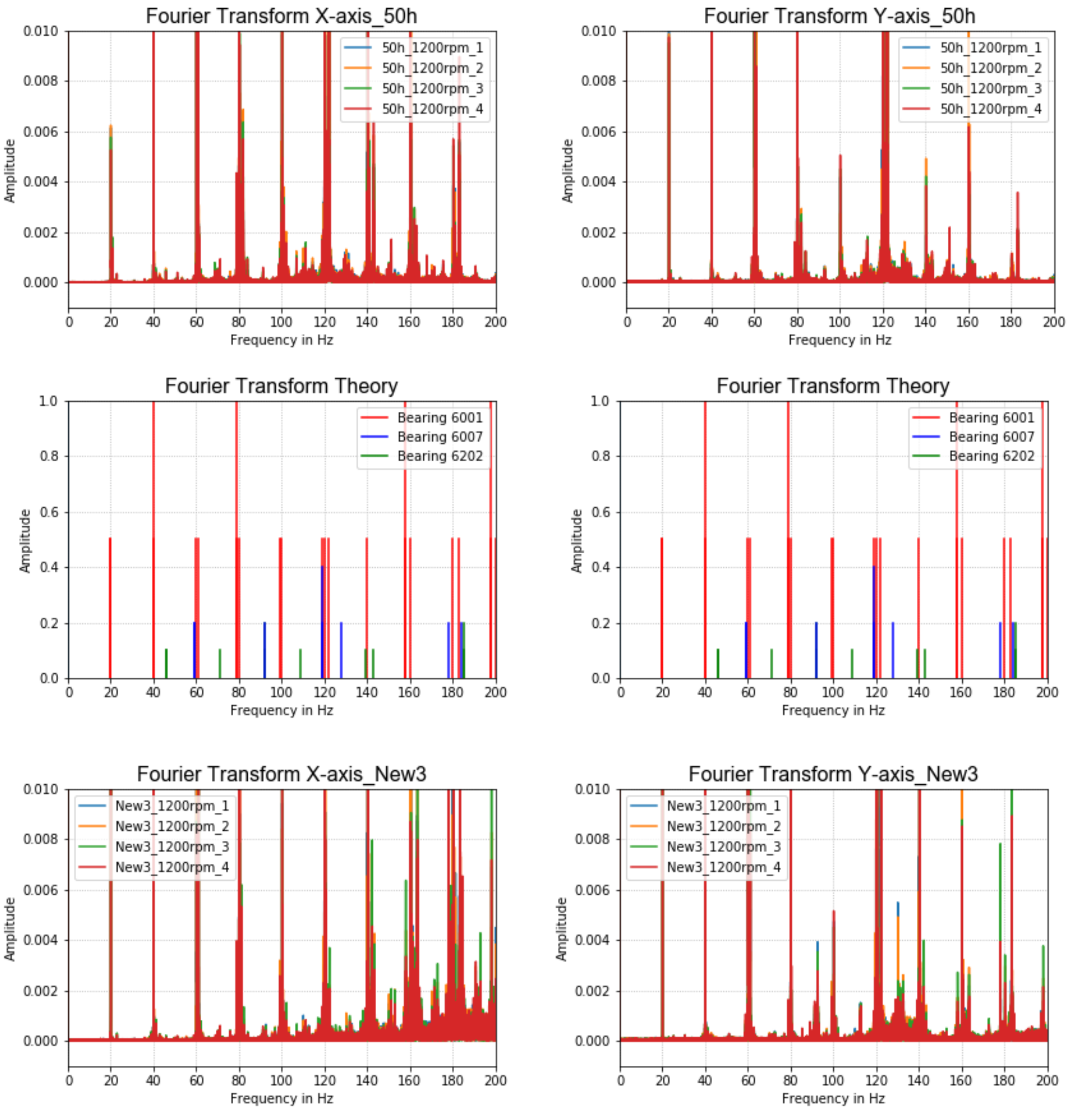


*Figure 50 - Results of the second trials on the robot with 50h, new, milled and corrosive bearings with 600rpm and Fourier Transform Theory*

## 8.3 Last Trials

For the last tests on the robot the foam that was inside the energy chain was removed to see if the first tests on the robot were reproducible, which turned out to still not be, so the chain was also removed and in order not to damage the cables only lower rotations per minute were used. After several attempts, the follow trials were the final results of the last trials performed on the robot.

### 8.3.1 DOE (BALLUFF)

In order to reproduce the results obtained in the first test, for this DOE, table 14, the various types of bearings were used, but this time only programs with low rotations per minute were used so as not to damage the cables. The fact of using low rotations per minute is also a plus, because in the ASC-325 sensor the values are no longer saturated. For these trials both sensors were used at the same time. One of the possibilities for not having such repeatability of results could be that the same bearings were always used, causing them to start working better with use. To verify that this was not the case, another bearing with corrosion and another milled bearing were used.

*Table 14 – DOE of the last trials on the robot with the BALLUFF sensor and with the ASC-325 sensor*

| Run | Weight(Kg) | RPM (rpm) | Time (min) | Vorschub (mm/s) | Bearing | New mounted? | Monting | Workpiece | Polishing track | Eccentric (mm) | Tool size (mm) | Tool coating | Point distance (mm) | Oscillation | Polishing agent | Measured axis | Measured axis |
|---|---|---|---|---|---|---|---|---|---|---|---|---|---|---|---|---|---|
| 1 | 2,5 | 300 | 10 | 23,5 | ~ 50h | Yes | Air | Plan | Y-Mäander | 7 | 15 | Suba500 | 0,4 x 0,4 | 1 | Opaline | X-axial; Z-radial | X-axial;Y-radial; Z-radial |
| 2 | 2,5 | 300 | 10 | 23,5 | ~ 50h | No | Air | Plan | Y-Mäander | 7 | 15 | Suba500 | 0,4 x 0,4 | 1 | Opaline | X-axial; Z-radial | X-axial;Y-radial; Z-radial |
| 3 | 2,5 | 600 | 10 | 23,5 | ~ 50h | No | Air | Plan | Y-Mäander | 7 | 15 | Suba500 | 0,4 x 0,4 | 1 | Opaline | X-axial; Z-radial | X-axial;Y-radial; Z-radial |
| 4 | 2,5 | 600 | 10 | 23,5 | ~ 50h | Yes | Air | Plan | Y-Mäander | 7 | 15 | Suba500 | 0,4 x 0,4 | 1 | Opaline | X-axial; Z-radial | X-axial;Y-radial; Z-radial |
| 5 | 2,5 | 300 | 10 | 23,5 | Corrosion | No | Air | Plan | Y-Mäander | 7 | 15 | Suba500 | 0,4 x 0,4 | 1 | Opaline | X-axial; Z-radial | X-axial;Y-radial; Z-radial |
| 6 | 2,5 | 300 | 10 | 23,5 | Corrosion | No | Air | Plan | Y-Mäander | 7 | 15 | Suba500 | 0,4 x 0,4 | 1 | Opaline | X-axial; Z-radial | X-axial;Y-radial; Z-radial |
| 7 | 2,5 | 600 | 10 | 23,5 | Corrosion | Yes | Air | Plan | Y-Mäander | 7 | 15 | Suba500 | 0,4 x 0,4 | 1 | Opaline | X-axial; Z-radial | X-axial;Y-radial; Z-radial |
| 8 | 2,5 | 600 | 10 | 23,5 | Corrosion | No | Air | Plan | Y-Mäander | 7 | 15 | Suba500 | 0,4 x 0,4 | 1 | Opaline | X-axial; Z-radial | X-axial;Y-radial; Z-radial |
| 9 | 2,5 | 300 | 10 | 23,5 | Milled | No | Air | Plan | Y-Mäander | 7 | 15 | Suba500 | 0,4 x 0,4 | 1 | Opaline | X-axial; Z-radial | X-axial;Y-radial; Z-radial |
| 10 | 2,5 | 300 | 10 | 23,5 | Milled | Yes | Air | Plan | Y-Mäander | 7 | 15 | Suba500 | 0,4 x 0,4 | 1 | Opaline | X-axial; Z-radial | X-axial;Y-radial; Z-radial |
| 11 | 2,5 | 600 | 10 | 23,5 | Milled | No | Air | Plan | Y-Mäander | 7 | 15 | Suba500 | 0,4 x 0,4 | 1 | Opaline | X-axial; Z-radial | X-axial;Y-radial; Z-radial |
| 12 | 2,5 | 600 | 10 | 23,5 | Milled | No | Air | Plan | Y-Mäander | 7 | 15 | Suba500 | 0,4 x 0,4 | 1 | Opaline | X-axial; Z-radial | X-axial;Y-radial; Z-radial |
| 13 | 2,5 | 300 | 10 | 23,5 | New | Yes | Air | Plan | Y-Mäander | 7 | 15 | Suba500 | 0,4 x 0,4 | 1 | Opaline | X-axial; Z-radial | X-axial;Y-radial; Z-radial |
| 14 | 2,5 | 300 | 10 | 23,5 | New | No | Air | Plan | Y-Mäander | 7 | 15 | Suba500 | 0,4 x 0,4 | 1 | Opaline | X-axial; Z-radial | X-axial;Y-radial; Z-radial |
| 15 | 2,5 | 600 | 10 | 23,5 | New | No | Air | Plan | Y-Mäander | 7 | 15 | Suba500 | 0,4 x 0,4 | 1 | Opaline | X-axial; Z-radial | X-axial;Y-radial; Z-radial |
| 16 | 2,5 | 600 | 10 | 23,5 | New | Yes | Air | Plan | Y-Mäander | 7 | 15 | Suba500 | 0,4 x 0,4 | 1 | Opaline | X-axial; Z-radial | X-axial;Y-radial; Z-radial |

### 8.3.2 Results (BALLUFF)

In these 300 rpm results with the BALLUFF sensor, it is a little difficult to draw conclusions, because the results with this sensor are more noticeable at higher rpm. However, as small as the difference may be, the bearing with the most vibrations are the corrosive one, as expected, and then the milled one. However, there is not much difference between the different bearings, they all have values around 0,10g and 0,30g, and because of this low interval of values it is hard to draw conclusions.

With these trials, figure 51, the goal was to try to reproduce again the same results to verify if it was in fact possible to always see the different behavior of the bearings. It was not known if it was possible to see the damages of the bearing on the robot but after the first trials it was possible to conclude that in fact it was possible but then the same results were not reproducible in these trials.

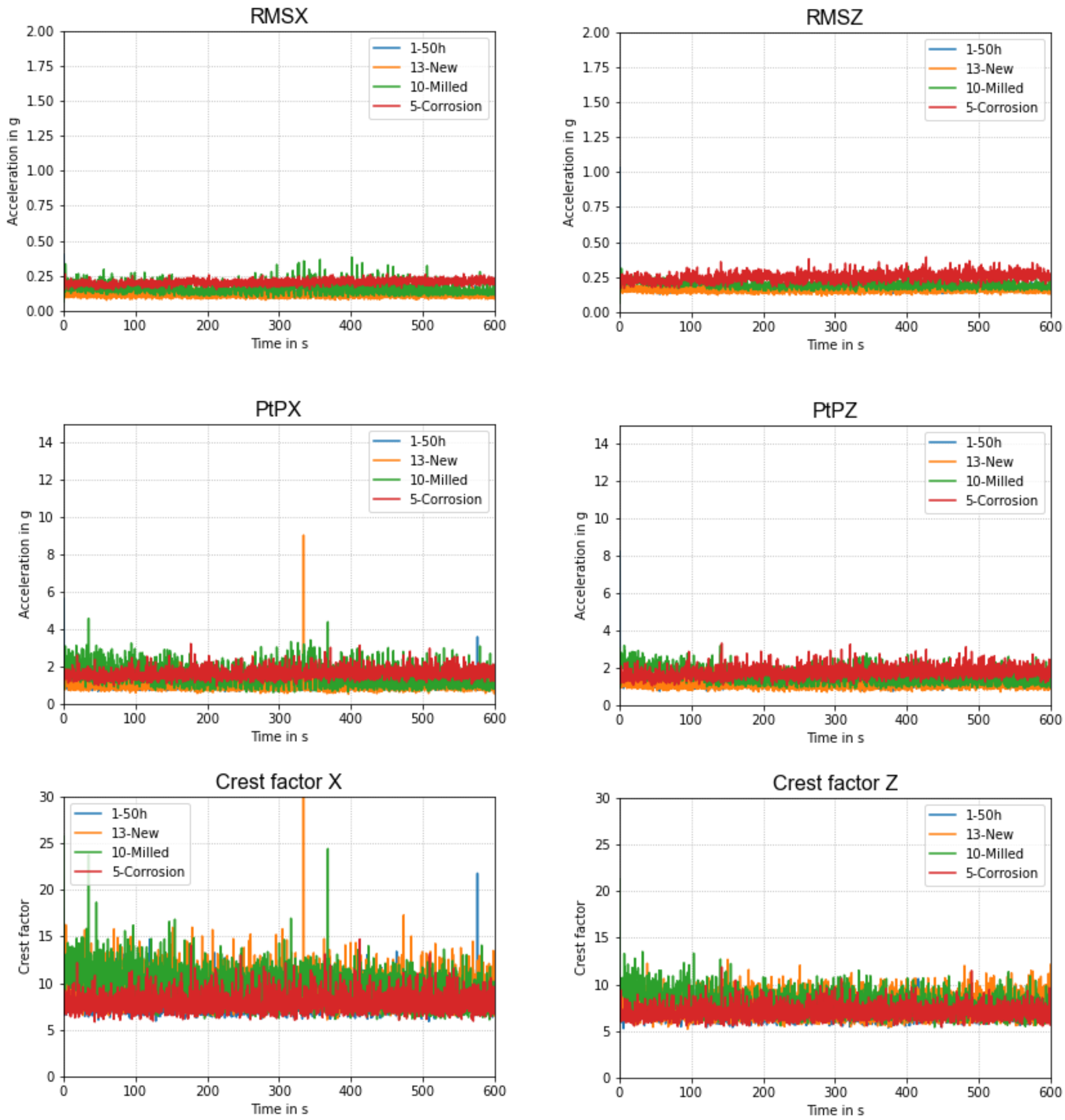


*Figure 51 – Results of the last trials on the robot with the BALLUFF with 300rpm*

In these results, figure 52, it can be observed that after a certain moment the amplitude of the vibrations decreased considerably. This may be due to the bearing breaking in, settling down, that is, after a certain moment it begins to show less vibration because it has already settled down. In these tests it can be observed that the bearing with corrosion already demonstrates more vibrations in relation to the other bearings, but the disparity of values between them is short, compared with the first tests performed on the robot. And that the milled bearing shows almost the same values as the new and the 50-hour bearing.

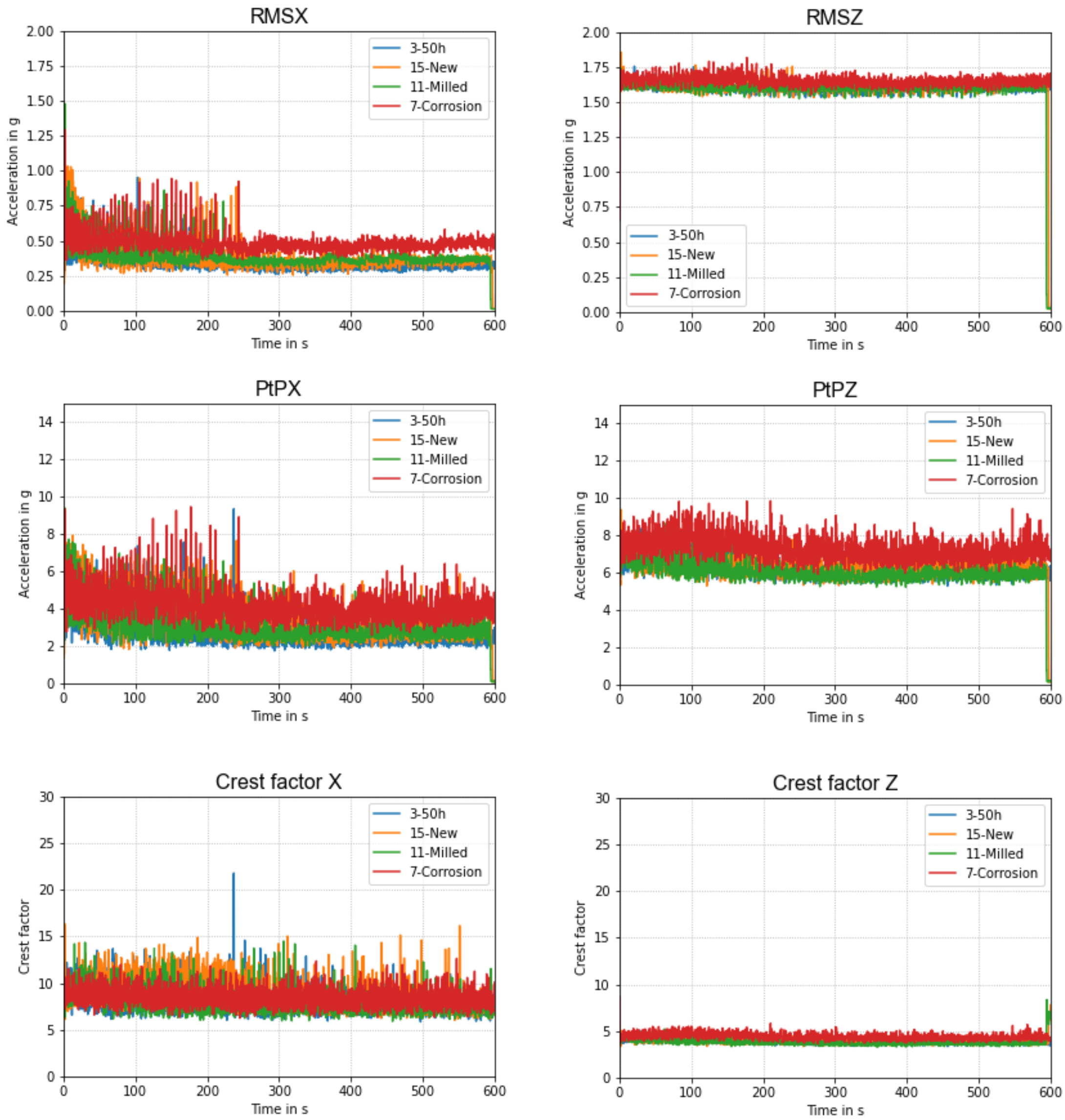


*Figure 52 – Results of the last trials with the BALLUFF sensor with 600rpm*

### 8.3.3 Results (ASC-325)

The same happened with the results of the sensor ASC-325, and it is not possible to observe through the vibrations which type of bearing is in the robot, not being possible to analyze the state of the robot. Through these trials it is not possible to verify the behavior of the polishing machine since the values between the vibration amplitude are similar in these trials with 300 rpm. In the trials with 600 rpm it is even more complicated to draw conclusions since the results were saturated. These trials were performed with 300 rpm to prevent saturated data and also because there was no energy chain this time, so with less vibration the lower is the chance of cable damaging. In these trials, figure 53, comparing the 50 hour bearing with a corrosive bearing it can be seen a difference between the values. The corrosive bearing has more vibrations than the 50 hours bearing.

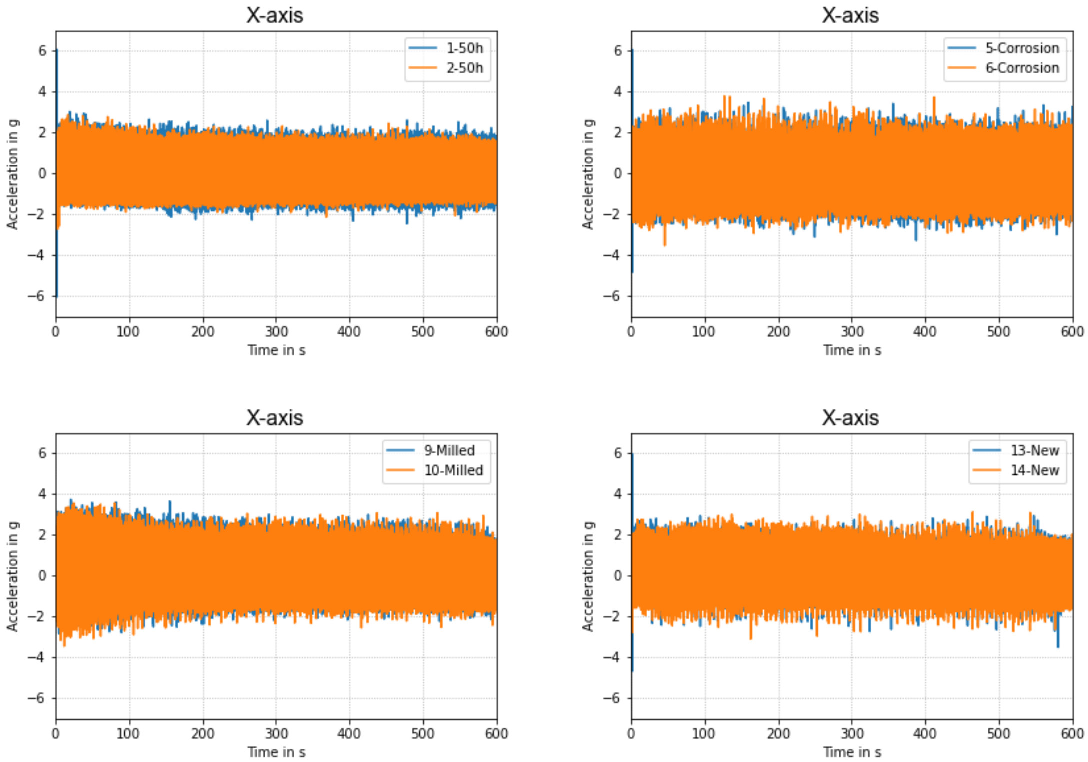


*Figure 53 – Results of the last trials with 300rpm*

In these trials it was once again tried to reproduce the results from the first trials in the polishing head, but once again it was not possible. This trials were also made with new bearings with new damages because it was noticed that the damge on the previous bearings were just gone and for some reason the results were still not reproducible.

In order to get more information from these trials, figure 54, fourier transform format graphics were performed again to observe the peaks and compare them with the theory. In these graphics it is possible to observe that after a higher peak it always comes smaller peaks until there is again a high peak. This happens because the vibrations resonate.

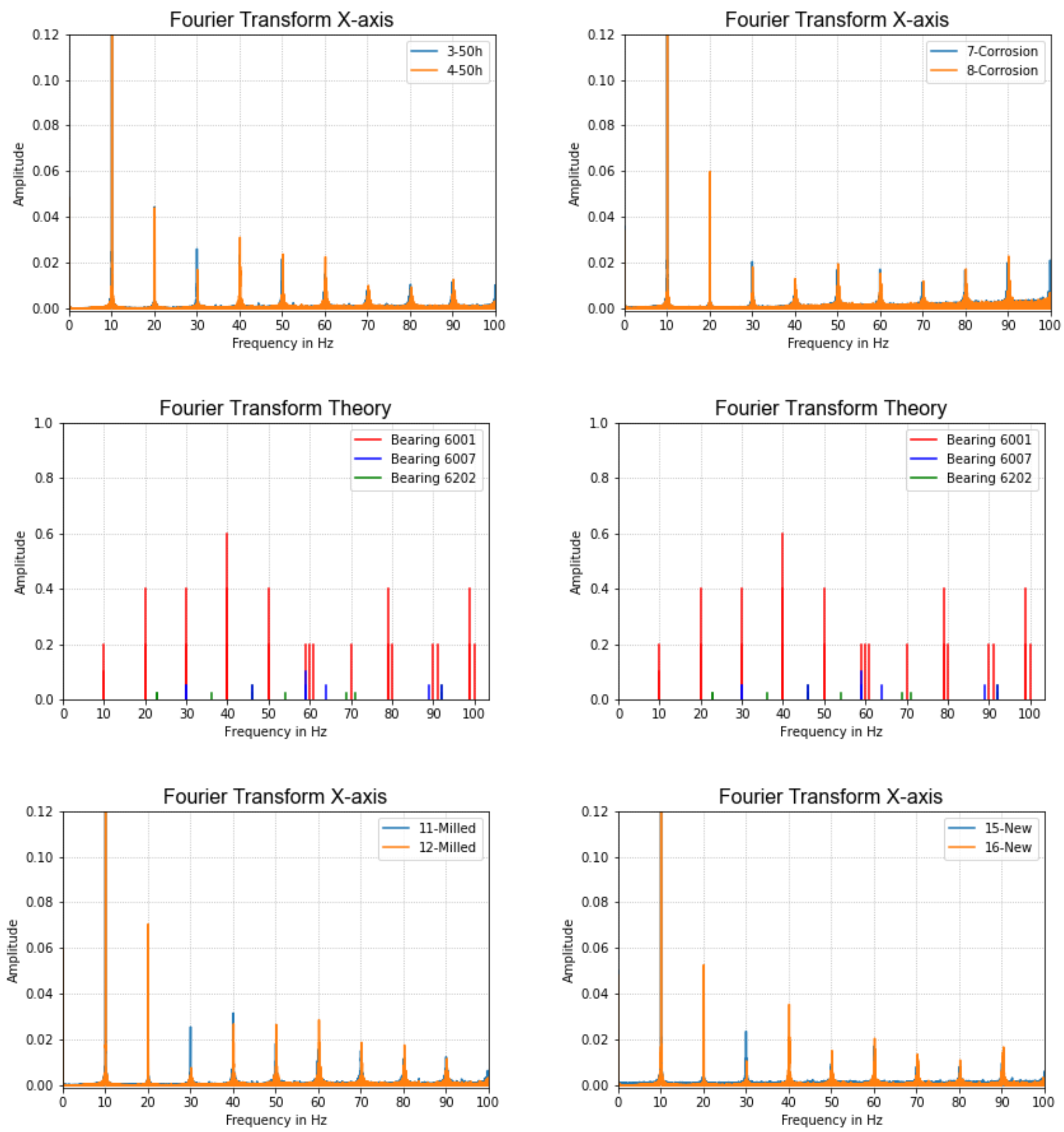


*Figure 54 - Results of the last trials with 600rpm and theory of the bearing 6001*

## 8.4 Analysis and conclusion of the results

In contrast to the trials on the test bench, in the case of the new bearings and the 50-hour bearings, it is not so easy to see on the robot which one works better since the results are very similar. However, when comparing new, milled, and corrosion bearings, it is already possible to see a difference between these bearings, however small it may be in some cases, like for example in the last trials with the BALLUFF sensor and also with the ASC-325 sensor.

After the tests performed on the robot it was possible that the first results were not repeatable, this can be due to several factors. Even after keeping the same set up the results were not similar. Even after using other bearings, the results were still not reproducible.

However, the first results obtained in the robot were positive. One factor that may have influenced the not reproducible results may have been that during the assembly and disassembly of the robot some of the components were not well assembled, which led to no constant or reproducible results. Even in the results with the 50 hours old bearings and the new ones, it was not possible to verify a difference between them.

For these tests on the robot the ASC-325 sensor worked better at lower rpm, in the sense that more information can be gleaned from the results. The BALLUFF sensor works best for a faster analysis of the results obtained.

In the last trials it was used less rotations per minute because of the fact that the energy chain wasn't being used and specially because the ASC-325 sensor. Because of this sensor lower rotations per minute had to be used otherwise the results would be saturated. After these trials it was possible to conclude that the ASC-325 wasn't the best sensor option for this project and that another sensor with bigger range would be more suitable.

Even though the ASC-325 sensor range wasn't the best, this sensor allowed to get more detailed information, when performed trials with lower rotations per minute, and through the analysis of the peaks in the Fourier Transform it was possible to see which part of the bearing was causing the peak.

# 9. Conclusions and future work

In this final chapter and after this work it was possible to take some conclusions and to foresee some of the future work that can be done in this project.

## 9.1 Conclusions

After this project it was possible to draw several conclusions. First, the chain did a good job protecting the cables, as they were not damaged after the various tests they were subjected to, but it was proven that this is not the best solution at all, since at high rotations per minute it creates more vibrations. With the rotational movement of the machine the chain creates small repercussions through the chain thus creating large vibrations, having a whiplash effect. But at low rotations per minute this solution is perfect, as it no longer creates excessive vibrations, since the movements are small. This solution has yet another disadvantage, that it can only be used when polishing flat surfaces, because this energy chain only moves in two axes. To improve this aspect, research on energy chains that move in all three axes would be a possible solution to this problem, since they would have more freedom of movement.

Second, the trials performed in the test bench it was possible to withdraw very good conclusions on the state of the bearing, because with the results achieved it was possible to see the damages of the bearings throughout the vibrations. In the trials on the test bench it was also observed that the mounting method doesn't have that much influence in the results.

The components designed for this project worked correctly, such as the adapter for the vibration sensors, but this can still be improved, since after trying to place the ASC-325 sensor on the opposite side it did not fit because with the energy chain assembled there was no room to place it since the adapter had to be mounted with a small inclination in order to give the energy chain freedom to bend. Another aspect that could be improved in this adapter is the fact that when it is screwed it is never in the same position, to solve this problem and so that it would always stay in the same position a metallic ring was used that when tightened with the adapter, it would get stuck. However, this was only a temporary solution. If a new adapter is created in the future, it would be good to come up with a method that makes this adapter always stays in the same position when it is mounted.

After testing with the sensors on both the testbench and the polishing head robot, it was possible to conclude that it is possible to monitor the behavior of the bearings. There are several factors that cause vibrations in the machine, and with this project it was possible to conclude that the machine's bearings and their condition have an impact on the polishing head robot's performance. Many of the results obtained through the tests were positive, in the sense that they helped to understand the behavior of the bearings and to see and prove theories. And with some of the trials performed it was possible to obtain very good results, where for example in the milled bearing or even in the corrosive bearing it was possible to see the damages on the different elements of the bearings. In the case of the milled bearing, it was possible to see the damage on the outer ring and in the corrosive bearing it was possible to see the damage in all of the different parts, the damage in the outer ring, in the inner ring, in the cage of the bearing and on the spheres of the bearing.

After all these trials it was possible to conclude that the ASC-325 sensor wasn't the best option in the way that if this sensor had a bigger range, it would be possible to do trials with more rotations per minute that would have shown higher peaks, and that would have helped to read more clearly the results.

However, in the last trials the results obtained fell short, since it was not possible to reproduce the same results. This may be due to the fact that minor changes were made in the set-up of the trials, or something may have changed in the robot between trials which led to non-repeatability of the results. With this work a lot of knowledge was gained and there was a big learning curve, not only in vibration sensors, or condition monitoring but also regarding the polishing processes and the various factors that can influence the performance of this machine.

## 9.2 Future work

As future work, it will be necessary to come up with a more viable solution for the protection of the cables, since the solution arranged for this project is a bit limiting. Not only in terms of movement, but also in terms of having vibration repercussions, which is a negative factor because it influences the results that are obtained. For this it would be suggested getting a solution that not only works at high rotations per minute, but also for polishing on curved surfaces.

Another factor that would be advised to improve would be the sensor adapter, since whenever it is attached it is never mounted in the same position. To solve this, it would be good to develop an adapter that has a mechanism that makes it so that when it is mounted on the polishing head it is always in the same position.

It would also be advisable to find a sensor that can give raw data with a higher range, in order to be able to do trials with higher rotations per minute.

More trials should be done with robot. It was possible to obtain good results on the test bench and the next goal would be to obtain the same results with the polishing head robot, and for that more analysis needs to be done on the robot. In order to do that it would be good to do more trials on the robot to see if it is possible or not to check the damage on the bearings in the polishing head or not.

In addition, it would be a plus if the trials with the sensors on the different sides of the adapter were performed since, due to time limits, it was not possible to perform these tests. With these tests it will be possible to see later on if the location of the sensors has an impact on the results or not. And if it does have an impact, it will be possible to understand where the sensors are best placed in order to get the best possible results.

# 10. References


[1] ABB, [Online]. Available: https://global.abb/group/en [Accessed October 2020]

[2] Steve Hanly, "Vibration Sensor Types and Where to Buy Them" [Online]. Available: https://blog.endaq.com/vibration-sensor-types-and-where-to-buy-them [Accessed October 2020]

[3] The Editors of Encyclopaedia Britannica, "Vibration" [Online]. Available: https://www.britannica.com/science/vibration [Accessed October 2020]

[4] Elprocus, "Vibration Sensor Working and Applications" [Online]. Available: https://www.elprocus.com/vibration-sensor-working-and-applications/ [Accessed October 2020]

[5] Realpars, "What is a vibration sensor?" [Online]. Available: https://realpars.com/vibration-sensor/ [Accessed October 2020]

[6] MATLAB, [Online]. Available: https://de.mathworks.com/products/matlab.html?requestedDomain= [Accessed October 2020]

[7] Anaconda, [Online]. Available: https://www.anaconda.com/products/individual [Accessed November 2020]

[8] Vibcloud,, "Vibration monitoring made easy" [Online]. Available: https://www.vib.cloud/index.html [Accessed November 2020]

[9] IO-Link, "What is IO-Link" [Online]. Available: https://io-link.com/en/Technology/what_is_IO-Link.php?thisID=73 [Accessed November 2020]

[10] IFM, "Acceleration sensor VSM101" [Online]. Available: https://www.ifm.com/de/en/product/VSM101 [Accessed November 2020]

[11] SKF, "SKF Vibration Sensors Catalog" [Online]. Available: https://www.skf.com/binaries/pub12/Images/0901d196804926fe-11604_16-EN-Vibration-Sensor-Catalogue--OK_tcm_12-267858.pdf [Accessed November 2020]

[12] ASC, "ASC OS-325MF-PG Accelerometer" [Online]. Available: https://www.asc-sensors.de/en/sensoren/asc-os-325mf-pg-en/ [Accessed November 2020]

[13] Fluke, "3561 FC Vibration Sensors" [Online]. Available: https://www.fluke.com/en/product/condition-monitoring/vibration/3561-vibration-sensor [Accessed December 2020]

[14] Althen, "Wireless IoT Vibration Measurement Solution" [Online]. Available: https://www.althensensors.com/measurement-systems/turn-key-measurement-systems/earthquake-vibration-measurement-systems/14461/wireless-iot-vibration-measurement-solution/ [Accessed December 2020]

[15] PCE, [Online]. Available: https://www.pce-instruments.com/english/measuring-instruments/test-meters/vibration-meter-pce-instruments-vibration-meter-sensor-pce-vms-501-det_5889780.htm [Accessed December 2020]

[16] PCB Piezotroncis, "670A01 | ECHO® WIRELESS VIBRATION SENSOR" [Online]. Available: https://www.pcb.com/products?m=670A01 [Accessed December 2020]

[17] Yokogawa, "Sushi sensor" [Online]. Available: https://www.yokogawa.com/de/solutions/products-platforms/oprex/oprex-transformation/oprex-asset-management-and-integrity/sushi-sensor/ [Accessed December 2020]

[18] iQunet, "Wireless Battery-Powered Vibration Sensor" [Online]. Available: https://iqunet.com/wp-content/uploads/2017/10/161010-Wireless-Battery-Powered-Vibration-Sensor-IVIB161010-ACC3-016-Datasheet-D1019-en-CUST-200817.pdf [Accessed December 2020]

[19] Cole-Parmer, "Vibration Sensor Selection Guide" [Online]. Available: https://www.coleparmer.com/tech-article/sensor-selection-guide [Accessed November 2020]

[20] Balluff, "Condition Monitoring Sensor" [Online]. Available: https://www.balluff.com/en/de/products/product-news-overview/product-news/condition-monitoring-sensor/ [Accessed November 2020]

[21] Balluff, "BCM0001 Condition Monitoring sensors with multi-function" [Online]. Available: https://my.balluff.com/en-DE/products/PV9343665?ca=A0001&cg=G0119&product=F011901 [Accessed November 2020]

[22] Balluff, "BCM0002 Condition Monitoring sensors with multi-function" [Online]. Available: https://my.balluff.com/en-DE/products/BCM0002 [Accessed November 2020]

[23] Fluke, [Online]. Available: https://www.fluke.com/en-us/product/condition-monitoring/vibration/3561-vibration-sensor# [Accessed December 2020]

[24] Fluke, “Understanding the benefits of vibration monitoring and analysis” [Online]. Available: https://www.fluke.com/en-us/learn/blog/vibration/understanding-the-benefits-of-vibration-monitoring-and-analysis [Accessed December 2020]

[25] IFM, [Online]. Available: https://www.ifm.com/de/de/product/VTV122 [Accessed December 2020]

[26] Steve Hanly, “Top 9 Accurate Wireless Vibration Monitoring Systems” [Online]. Available: https://blog.endaq.com/top-accurate-wireless-vibration-monitoring-systems [Accessed December 2020]

[27] PCB Piezotronics, “Vibration monitoring for dangerous, remote, and hard-to-reach assets” [Online]. Available: https://www.pcb.com/industrial-sensors/accelerometers/wireless-vibration-monitoring-system [Accessed December 2020]

[28] ReliabilityWeb, “Why is Monitoring Vibration Important?” [Online]. Available: https://reliabilityweb.com/articles/entry/why_is_monitoring_vibration_important# [Accessed January 2021]

[29] Carolyn Mathas, “What You Need to Know About Vibration Sensors” [Online]. Available: https://www.digikey.com/en/articles/what-you-need-to-know-about-vibration-sensors [Accessed January 2021]

[30] MathWorks, “fft” [Online]. Available: https://www.mathworks.com/help/matlab/ref/fft.html [Accessed January 2021]

[31] Jonathan Trout, “Vibration Analysis Explained” [Online]. Available: https://www.reliableplant.com/vibration-analysis-31569 [Accessed February 2021]

[32] CCOHS, “Vibration – Introduction” [Online]. Available: https://www.ccohs.ca/oshanswers/phys_agents/vibration/vibration_intro.html [Accessed February 2021]

[33] Sparkfun, “Accelerometer Basics” [Online]. Available: https://learn.sparkfun.com/tutorials/accelerometer-basics/all [Accessed February 2021]

[34] Wiresmith, “What Is CompactDAQ?” [Online]. Available: https://www.wiresmithtech.com/articles/what-is-compactdaq/ [Accessed March 2021]

[35] Tony L. SchmitzK. Scott Smith, “Mechanical Vibrations” [Online]. Available: https://link.springer.com/book/10.1007%2F978-3-030-52344-2 [Accessed March 2021]

[36] MathWorks, “Getting Started with NI Devices” [Online]. Available: https://www.mathworks.com/help/daq/getting-started-with-session-based-interface-using-ni-devices.html [Accessed April 2021]

[37] MathWorks, “Create a Simple App Using GUIDE” [Online]. Available: https://www.mathworks.com/help/matlab/creating_guis/about-the-simple-guide-gui-example.html [Accessed April 2021]

[38] National Instruments, [Online]. Available: https://www.ni.com/de-de.html [Accessed April 2021]

[39] Stat ease, [Online]. Available: https://www.statease.com/ [Accessed March 2021]

## 11. Appendicies

Appendix A – BALLUFF BCM0001 sensor Data Sheet

Condition Monitoring Sensors

**BCM R15E-001-DI00-01,5-S4**
**Order Code: BCM0001**

BALLUFF

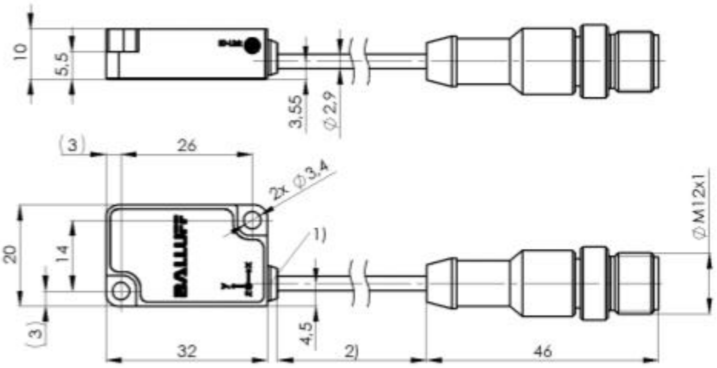


1) LED green, 2) Cable length

### Basic features

| | |
|---|---|
| **Approval/Conformity** | CE<br>cULus<br>EAC<br>WEEE |
| **Function** | Vibration Velocity<br>Vibration Acceleration<br>Vibration Severity Zone<br>Contact Temperature<br>Sensor Self-Awareness |
| **Principle of operation** | Condition Monitoring Sensors |
| **Series** | R15 |

### Display/Operation

| | |
|---|---|
| **Display** | Run - LED green<br>Communication - LED green, slow flashing (1 Hz)<br>Ping - LED green, asyncronous very fast flashing (4 Hz) and fast flashing (2 Hz) |

### Electrical connection

| | |
|---|---|
| **Bending radius min., fixed cable** | 3 x D |
| **Bending radius min., flexible cable** | 5 x D |
| **Cable diameter D** | 2.9 mm +0.1/-0.05 mm |
| **Conductor cross-section** | 0.14 mm² |
| **Connection** | Cable with connector, M12x1-Male, 3-pin, 1.5 m, PUR |
| **Number of conductors** | 3 |
| **Polarity reversal protected** | yes |
| **Protection against device mix-ups** | yes |
| **Short-circuit protection** | yes |

### Electrical data

| | |
|---|---|
| **Current draw max.** | 10 mA |
| **Operating voltage Ub** | 18...30 VDC |
| **Protection class** | III |
| **Rated operating voltage Ue DC** | 24 V |
| **Ready delay tv max.** | 1.5 s |

Internet www.balluff.com

Subject to change without notice: 279553

eCl@ss 9.1: 27-20-90-90
ETIM 6.0:
BCM0001_0.36_2021-06-14

1 / 3

Condition Monitoring Sensors
# BCM R15E-001-DI00-01,5-S4
# Order Code: BCM0001

BALLUFF

## Environmental conditions

| | |
|---|---|
| **Ambient temperature** | 0...70 °C |
| **EN 61000-4-2, ESD** | Severity Level 2 |
| **EN 61000-4-3, RFI** | Severity Level 3 |
| **EN 61000-4-4, Burst** | Severity Level 4 |
| **EN 61000-4-6, High-frequency fields** | Severity Level 3 |
| **IP rating** | IP67, IP68, IP69K |
| **Storage temperature** | -20...70 °C |

## Function module contact temperature

| | |
|---|---|
| **Contact temperature, measuring error** | ±2 % FS |
| **Contact temperature, measuring range** | 0...70 °C |
| **Contact temperature, non-linearity** | ±0.75 % FS |
| **Contact temperature, resolution** | 0.1 °C |
| **Contact temperature, settling time** | 5 min |

## Function module vibration

| | |
|---|---|
| **Vibration, frequency range** | 2...3200 Hz |
| **Vibration, measuring principle** | MEMS |
| **Vibration, number of measuring axes** | 3 |
| **Vibration, sampling rate** | 6400 Hz |

## Function module vibration acceleration

| | |
|---|---|
| **Vibration acceleration, measuring error RMS** | ±5 %FS @79.4 Hz |
| **Vibration acceleration, measuring range RMS** | 0...16 g |
| **Vibration acceleration, non-linearity RMS** | ±2 %FS @79.4 Hz |
| **Vibration acceleration, resolution RMS** | 0.006 g @79.4 Hz |
| **Vibration acceleration, statistical evaluation variables [for each measuring axis]** | RMS<br>Peak to Peak |

## Function module vibration velocity

| | |
|---|---|
| **Vibration velocity, evaluation variables [for each measuring axis]** | RMS<br>Peak to Peak<br>Mean<br>Standard Deviation<br>Crest Factor<br>Skew<br>Kurtosis |
| **Vibration velocity, measuring error RMS** | ±5 %FS @79.4 Hz |
| **Vibration velocity, measuring range RMS** | 0...220 mm/s @79.4 Hz |
| **Vibration velocity, non-linearity RMS** | ±2 %FS @79.4 Hz |
| **Vibration velocity, resolution RMS** | 0.42 mm/s @79.4 Hz |

## Material

| | |
|---|---|
| **Housing material** | Stainless steel (1.4404) |

## Mechanical data

| | |
|---|---|
| **Dimension** | 20 x 10 x 32 mm |
| **Mounting part** | Screw M3 (2x) |
| **Weight** | 30 g |

## Output/Interface

| | |
|---|---|
| **Baud rate** | COM3 (230,4 kBaud) |
| **Interface** | IO-Link 1.1 |
| **Interface setting option** | Flexible process data configuration<br>Vibration measurement based on ISO 10816-3<br>Data preprocessing (statistics)<br>Events (pre-alarms and main alarms)<br>Delay times for alarms<br>Search function with LED display (ping) |
| **Process data IN** | 20 bytes |
| **Process data OUT** | 0 bytes |
| **Process data cycle min.** | 10 ms |

## Remarks

For additional information, refer to user's guide.
Order accessories separately.
For more information about MTTF and B10d see MTTF / B10d Certificate

Indication of the MTTF- / B10d value does not represent a binding composition and/or life expectancy assurance; these are simply experiential values with no warranty implications. These declared values also do not extend the expiration period for defect claims or affect it in any way.

## Connector Drawings

## Wiring Diagrams

| Pin | Color | Signal |
|---|---|---|
| 1 | BN | +24V |
| 3 | BU | GND |
| 4 | BK | C/Q |

Appendix B – BALLUFF Condition monitoring sensor with integrated data preprocessing

BALLUFF

**Flexible, smart condition monitoring in the smallest possible space**

# CONDITION MONITORING SENSOR WITH INTEGRATED DATA PREPROCESSING

Unscheduled stops and faults in the production process can be avoided using our new multi-functional condition monitoring sensor. This intelligent sensor provides you with condition information which you can use for automating costintensive manual inspections.
This condition data is also an essential component for implementing smart and flexible manufacturing – a key to IIoT.

The Balluff condition monitoring sensor detects various physical variables such as vibration, temperature, relative humidity, and ambient pressure, processes them, and provides the desired data to a host system via IO-Link. In addition, the sensor can detect and communicate its condition, keeping you informed continuously of its temperature, number of operating hours, and start cycles.

The standardized IO-Link protocol means you can easily parameterize the sensor and match the processing in the sensor to your specific application. The process data structure permits five measured or preprocessed data types to be freely configured and cyclically transmitted. It is also possible to perform an acyclical request for additional statistical processing variables.

Additionally, you can use automated monitoring of measurement or processing variables to define limit values for pre- or main alarms. This generates warning messages, alerting you when problematic events occur.

The condition monitoring sensor from Balluff makes an essential contribution to the efficient and faultless operation of any equipment and significantly increases the efficiency of the overall system.

**Features**

- Multiple measurements in one device: vibration, temperature, relative humidity, ambient pressure
- Integrated processing circuitry with configurable data preprocessing
- Configurable events and status indicators
- Fast connection, and simple to incorporate using IO-Link
- Compact form factor for restricted spaces


CE c UL us LISTED

IO-Link

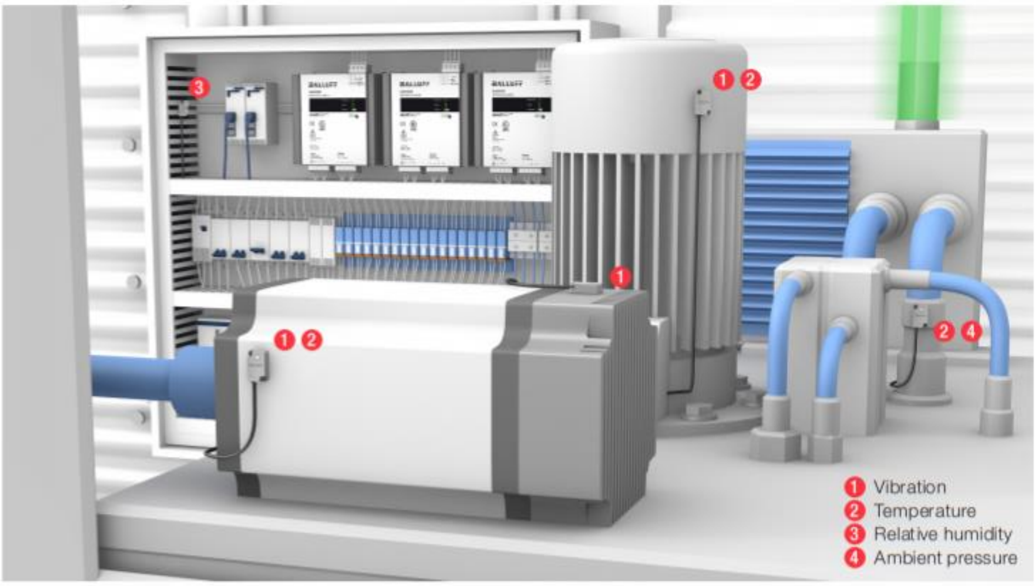

## CONDITION MONITORING SENSOR WITH MULTIFUNCTION

| | BCM0002 | BCM0001 |
|---|---|---|
| Function modules | ▪ Vibration (velocity/acceleration)<br>▪ Contact temperature<br>▪ Relative humidity<br>▪ Ambient pressure<br>▪ Sensor self-awareness | ▪ Vibration (velocity/acceleration)<br>▪ Contact temperature<br>▪ Sensor self-awareness |
| Vibration, frequency range | 2…3200 Hz | 2…3200 Hz |
| Vibration, measuring principle | MEMS | MEMS |
| Measuring range: Vibration, velocity RMS | 0…220 mm/s at 79.4 Hz (3 measuring axes) | 0…220 mm/s at 79.4 Hz (3 measuring axes) |
| Measuring range: Vibration, acceleration RMS | 0…16 g | 0…16 g |
| Measuring range: Contact temperature | 0…70 °C | 0…70 °C |
| Measuring range: Relative humidity | 5…95 %RH | |
| Measuring range: Ambient pressure | 300…1100 hPa | |
| Interface | IO-Link 1.1, COM3 (230.4 kBaud) | IO-Link 1.1, COM3 (230.4 kBaud) |
| Interface setting options | ▪ Flexible process data configuration<br>▪ Vibration measurement based on ISO 10816-3<br>▪ Data preprocessing (e.g. RMS, peak to peak, mean, standard deviation, min, max)<br>▪ Events (pre-alarms and main alarms)<br>▪ Delay times for alarms<br>▪ Search function with LED display (ping) | ▪ Flexible process data configuration<br>▪ Vibration measurement based on ISO 10816-3<br>▪ Data preprocessing (e.g. RMS, peak to peak, mean, standard deviation, min, max)<br>▪ Events (pre-alarms and main alarms)<br>▪ Delay times for alarms |
| IP rating | IP67 | IP67, IP68, IP69K |
| Housing material | Stainless steel 1.4404 | Stainless steel 1.4404 |
| Dimensions | 32 × 20 × 10 mm | 32 × 20 × 10 mm |
| Connection | 1.5 m PUR cable with M12 male, 3-pole | 1.5 m PUR cable with M12 male, 3-pole |

## ACCESSORIES

| | BAM03FA |
|---|---|
| Description | Magnetic holder, material aluminum, 32 × 20 × 12.5 mm, mounting with M3 screws |

## CONNECTIVITY

| | BCC0372 | BCC0374 |
|---|---|---|
| Cable | PUR black, 2 m, drag chain compatible | PUR black, 5 m, drag chain compatible |
| For connection 1 | M12 female, straight, 5-pole, A-coded | M12 female, straight, 5-pole, A-coded |
| For connection 2 | M12 male, straight, 3-pole, A-coded | M12 male, straight, 3-pole, A-coded |

www.balluff.com

Balluff GmbH · Schurwaldstrasse 9 · 73765 Neuhausen a. d.F. · Germany · Tel. +49 7158 173-0 · Fax +49 7158 5010 · balluff@balluff.de

Doc. no. 944906 · EN · H20 · Replaces D20 · Subject to change.

## BCM R15E-_ _ _-DI00-_ _,_-S4
## Condition Monitoring Sensor

CE The CE Mark verifies that our products meet the requirements of the current EMC Directive.

### Intended use

The Condition Monitoring Sensor (BCM) together with a machine controller (such as a PLC) or an Edge gateway together with an IO-Link master forms a condition monitoring system. It is intended for temporary or permanent use installed in a machine or system and used in the industrial sector. Flawless function in accordance with the specifications in the technical data is ensured only when using original Balluff accessories. Use of any other components will void the warranty.
Opening the BCM or non-approved use are not permitted and will result in the loss of warranty and liability claims against the manufacturer.

### General safety notes

**Installation** and **startup** may only be performed by qualified personnel with basic electrical knowledge.
The **operator** is responsible for ensuring that local safety regulations are observed.
In particular, the operator must take steps to ensure that a defect in the BCM will not result in hazards to persons or equipment.
If defects and unresolvable faults occur in the BCM, take it out of service and secure against unauthorized use.

### Downloading further instructions

A detailed user's guide can be downloaded from the Internet at **www.balluff.com** or requested via e-mail from **service@balluff.de**.

### Dimensions and function

The BCM is an intelligent condition monitoring sensor. It is used for acquiring condition information for a system or machine and for monitoring trends. It cannot replace a precision measurement system for determining condition.

| LED | | Operating state |
|---|---|---|
| **Color** | **State** | |
| Green | On | IO-Link communication inactive |
| | Inverse flashing (1 Hz), $t_{on}:t_{off}$ = 9:1 | IO-Link communication active |
| | Alternating flashing 4 Hz/2 Hz | PING function active |
| Orange[1] | Flashing (2 Hz, 10 s) | Event triggered |

The display duration for an event triggering is extended by 10 s if a further event is triggered during that time.

The Ping function makes it possible to identify the BCM via an optical signal after it is connected to an IO-Link master.

### Electrical connection

| Pin | Wire color | Signal |
|---|---|---|
| 1 | Brown | +24V (operating voltage UB+) |
| 3 | Blue | GND (operating voltage UB-; reference potential) |
| 4 | Black | C/Q (IO-Link) |

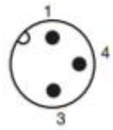


Pin assignments for connector (pin side view)

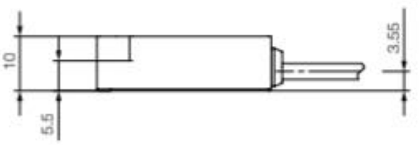


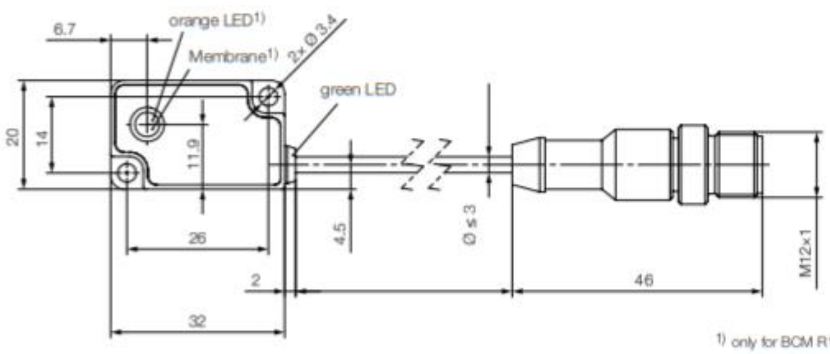


1) only for BCM R15E-**002**-...

## Installation

**Important installation notes**

The choice of a suitable installation location depends on various factors. Depending on the variables to be monitored, module-specific instructions must be followed.

If variables are being detected from different modules, the installation notes for all corresponding modules must be taken into consideration!

For secure and lasting installation of the BCM the sensor must be attached directly on the machine or relevant component to be monitored. To ensure the best possible signal quality, we recommend tightening the sensor using screws.

Alternately the sensor can be temporarily attached to the surface using a magnetic holder (Accessories BAM MB-CM-055-R15-4).

**Contact temperature measurement**

The contact temperature is measured at the underside of the BCM housing. The temperature represents the contact temperature for the mounting surface.

For optimal thermal coupling the BCM must lie flat on the mounting surface. To prevent small air gaps, a heat transfer medium should be used between the surfaces.

**Relative humidity and ambient pressure measurement**[1)]

The relative humidity and the ambient pressure are measured on the upper side of the BCM housing. The sensor elements are located below the membrane inside the housing.

During use ensure that the membrane is not covered up and that there is good air circulation.

**Vibration measurement**

Vibration is measured inside the BCM housing. Measurement is based on MEMS technology. The BCM detects acceleration in three axes.

To monitor linear motion, make sure one axis of the sensor is aligned to the direction of the main force.

In rotary systems, one of the axes must be aligned axially, tangentially and radially.

1) only for BCM R15E-**002**-...

## Cable routing

**Cable routing**

**NOTICE**

**Damage to the sensor**

Excessive strain on the cable can damage the sensor.

- ► The cable must be routed tension-free.
- ► Avoid tensile forces on the cable (observe a maximum tensile load of 20 N).

Do not route the cable between BCM and IO-Link master or between IO-Link master and controller/Edge gateway near high voltage cables (inductive interference can occur).

The cable must be routed such that it is free of tension (tensile force < 20 N).

## Cable routing (continued)

**Bending radius for fixed cable**

The bending radius for a fixed cable must be at least three times the cable diameter.

**Bending radius for flexible routing**

The bending radius for flexible cable routing must be at least five times the cable diameter.

**Cable length**

Cable length max. 20 m.

## Startup

**⚠ DANGER**

**Uncontrolled system movement**

When starting up, if the sensor is part of a closed loop system whose parameters have not yet been set, the system may perform uncontrolled movements. This could result in personal injury and equipment damage.

- ► Persons must keep away from the system's hazardous zones.
- ► Startup must be performed only by trained technical personnel.
- ► Observe the safety instructions of the equipment or system manufacturer.

1. Check connections for tightness and correct polarity. Replace damaged connections.
2. Check BCM for tight attachment.
3. Turn on the system.
4. Check measured values and adjustable parameters and readjust the BCM if necessary.

i Check for the correct values, especially after replacing the BCM or after repair by the manufacturer.

i The BCM must be individually configured in most cases. The description in this user's guide can be used to aid in configuration. Assigning of parameters requires a basic understanding of the variables to be measured.

A BCM can be replaced simply and without loss of the configuration parameters by using the IO-Link function Data Storage or the parameter server.

**Operating notes**

- Regularly check function of the BCM and all associated components.
- Take the BCM out of service whenever there is a malfunction.
- Secure the system against unauthorized use.
- Check fasteners and retighten if needed.
- When installing using a magnetic holder, bear in mind that vibration may affect proper fit. Regularly check for proper holding and correct alignment when using this installation method.

No. 945227 EN · C20; subject to modification. Replaces A20.

ASC – smart in motion

ASC GERMAN SENSOR ENGINEERING

## MEMS Capacitive Accelerometer

# ASC OS-325MF-PG

Triaxial
MEMS Capacitive
Measurement Range: ±2 to ±200 g
Noise Density: 10 to 680 µg/√Hz
Frequency Range (±5 %): DC to 2900 Hz
Stainless-Steel Housing (IP68)
Made in Germany

CE

### MEMS Capacitive Accelerometer

The key components in capacitive accelerometers are high-quality micro-electro-mechanical systems (MEMS) that feature excellent long-term stability and reliability. This technology enables the measurement of static (DC) and constant accelerations, which can be used to calculate the velocity and displacement of moving objects. Depending on the design of the spring-mass-damping system, however, it is also possible to detect dynamic (AC) accelerations with amplitudes up to ±200 g and within a frequency response range of up to 2.9 kHz (±5 %) or 7 kHz (±3 dB). Other advantages of capacitive accelerometers are their outstanding temperature stability, excellent response behavior and achievable resolution.

### Description

The accelerometers of type ASC OS-325MF-PG are based on proven MEMS technology and capacitive operating principle. The integrated electronic circuitry enables a differential analog voltage output (±2.7 V FSO) and flexible power supply voltage from 5 to 40 VDC. The MF (Medium Frequency) accelerometers from ASC provide a wide frequency response range from 0 Hz to 7 kHz (±3 dB) and an extremely robust design with shock resistance up to 6,000 g.

The sensors feature a robust, reliable stainless-steel housing with protection class IP68 and an integrated cable with configurable length and connectors.

The hermetically sealed housing of the accelerometers is ideal for very harsh environmental conditions, e.g. bogie stability tests and monitoring applications in rail transport or condition monitoring of vehicles and their components in the construction sector.

### Features

- Low Noise Differential Voltage Output
- DC Response, Gas damped
- Very High Shock Resistance
- Excellent Offset and Scale Factor Stability

### Options

- Customized Cable Length
- Customized Connector
- TEDS Module
- V4A Stainless-Steel Housing

### Applications

- Railway Engineering
- Condition Monitoring
- Structural Health Monitoring

More applications in several markets are figured out on our web page www.asc-sensors.de

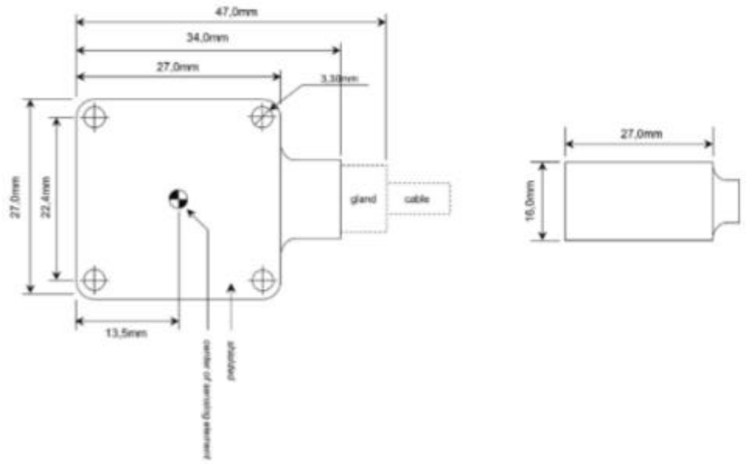

## ASC OS-325MF-PG

## MEMS Capacitive Accelerometer

### Typical Specification

#### Dynamic

| | | | | | | | | |
|---|---|---|---|---|---|---|---|---|
| Measurement Range | g | ±2 | ±5 | ±10 | ±30 | ±50 | ±100 | ±200 |
| Scale Factor (sensitivity) | mV/g | 1350 | 540 | 270 | 90 | 54 | 27 | 13.5 |
| Noise Density | µg/√Hz | 10 | 20 | 35 | 100 | 170 | 340 | 680 |
| Specified Frequency Response Range (±5 %) | Hz | 0 to 700 | 0 to 1150 | 0 to 2000 | 0 to 2300 | 0 to 2700 | 0 to 2900 | 0 to 2500 |
| Frequency Response Range (±3 dB) | Hz | 0 to 1150 | 0 to 1900 | 0 to 3200 | 0 to 4000 | 0 to 4500 | 0 to 5000 | 0 to 7000 |
| Amplitude Non-Linearity | % FSO | <0.1 (typ) \| <0.3 (max) | | | | | | |
| Transverse Sensitivity | % | <1 | | | | | | |

#### Electrical

| | | | | | | | | |
|---|---|---|---|---|---|---|---|---|
| Power Supply Voltage | V | 5 to 40 | | | | | | |
| Operating Current Consumption | mA | <10 | | | | | | |
| Offset (bias) | mV | ±10 | | | | | | |
| Broadband Noise (over specified frequency range ±5 %) | µV | 250 | 310 | 410 | 440 | 475 | 490 | 460 |
| Resistive Load | kΩ | 1000 | | | | | | |
| Isolation | | Case Isolated | | | | | | |

#### Environmental

| | | | | | | | | |
|---|---|---|---|---|---|---|---|---|
| Temperature Coefficient of the Scale Factor | ppm/K | 120 (typ) \| 20 to 220 (max) | | | | | | |
| Temperature Coefficient of the Offset (max) | mg/K | ±0.2 | ±0.5 | ±1 | ±3 | ±5 | ±10 | ±20 |
| Operating Temperature Range | °C | Standard with Cable K3: -15 to +70<br>Optional with Cable K4: -20 to +100 | | | | | | |
| Storage Temperature Range | °C | -55 to +125 | | | | | | |
| Shock Limit (0.1 ms, half-sine) | g | 6000 | | | | | | |
| Protection Class | | IP68<br>Please note: the housing is hermetically sealed and therefore not repairable. | | | | | | |

#### Physical

| | | |
|---|---|---|
| Sensing Element | | MEMS Capacitive |
| Case Material | | Stainless-Steel |
| Connector at Cable End | | Optional |
| Mounting | | Adhesive \| Screw Holes |
| Weight (without cable) | gram | 68 |
| Cable K3 (standard) | | 22 gram per meter \| AWG 30 \| Polyurethane (PUR) \| Diameter 3.75 mm \| waterproof |
| Cable K4 (optional) | | 29 gram per meter \| AWG 30 \| Fluorethylenpropylen (FEP) \| Diameter 3.75 mm \| waterproof |

## ASC OS-325MF-PG

## MEMS Capacitive Accelerometer

### Sensor Calibration

**Factory Calibration (supplied with the sensor)**

| Part Number | | | | | | | | |
|---|---|---|---|---|---|---|---|---|
| Measurement Range (sensor) | g | ±2 | ±5 | ±10 | ±30 | ±50 | ±100 | ±200 |
| Applied Frequency (min) | Hz | 1 | 10 | 10 | 10 | 10 | 10 | 10 |
| Applied Frequency (max) | Hz | 100 | 1150 | 2000 | 2300 | 2700 | 2900 | 2500 |
| Input Amplitude | $m/s^2$ | 5 | 5 | 50 | 100 | 200 | 200 | 200 |
| Reference Frequency for Determination of Scale Factor | Hz | 16 | 80 | 80 | 80 | 80 | 80 | 80 |

**Calibration according DIN ISO 17025 (order separately)**

| Part Number | | | | | | | | |
|---|---|---|---|---|---|---|---|---|
| Measurement Range (sensor) | g | ±2 | ±5 | ±10 | ±30 | ±50 | ±100 | ±200 |
| Applied Frequency (min) | Hz | 0.5 | 10 | 10 | 10 | 10 | 10 | 10 |
| Applied Frequency (max) | Hz | 150 | 1900 | 3200 | 4000 | 4500 | 5000 | 7000 |
| Input Amplitude | $m/s^2$ | 5 | 5 | 50 | 100 | 200 | 200 | 200 |
| Reference Frequency for Determination of Scale Factor | Hz | 16 | 80 | 80 | 80 | 80 | 80 | 80 |

Remarks:

- The conversion factor 1 g corresponds to 9.80665 $m/s^2$.
- If any other calibration procedure is required, don't hesitate to contact us. Our services include both factory calibration and calibration in accordance with DAkkS guidelines.
- Furthermore, sensors have to be calibrated regularly to ensure accurate and precise results. On request we will be glad to remind you of the next scheduled calibration of your sensors.

### Cable Code / Pin Configuration (8 Wire System)

| | Pin | Color Code Cable Type K3 | Color Code Cable Type K4 | Description | |
|---|---|---|---|---|---|
| 1 | Supply + | Blue | Red | Power: | supply voltage +5 to +40 VDC |
| 2 | Supply - | Brown | Black | Power: | GND |
| 3 | Signal + | White | Green/Purple | X-Axis: | positive, analog output voltage signal for differential mode |
| 4 | Signal - | Grey | White/Purple | X-Axis: | negative, analog output voltage signal for differential mode |
| 5 | Signal + | Yellow | Green/Grey | Y-Axis: | positive, analog output voltage signal for differential mode |
| 6 | Signal - | Pink | White/Grey | Y-Axis: | negative, analog output voltage signal for differential mode |
| 7 | Signal + | Green | Green | Z-Axis: | positive, analog output voltage signal for differential mode |
| 8 | Signal - | Blue | White | Z-Axis: | negative, analog output voltage signal for differential mode |

# ASC OS-325MF-PG

## MEMS Capacitive Accelerometer

### Cable Configuration

**8 Wire System - 8L**
Common power supply for all axes, no cable switch

**8 Wire System - 8L3**
Common power supply for all axes, including cable switch

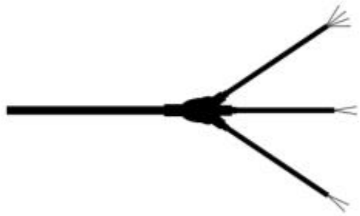

### Ordering Information

| Series | Model | - | Range [g] | - | Cable | - | Cable Length [m] | Connector & Pinout | - | Cable Configuration |
|---|---|---|---|---|---|---|---|---|---|---|
| ASC OS | -325MF-PG | | 002 | | K3 | | 1 | A | | 8L |
| | | | 005 | | K4 | | | | | 8L3 |
| | | | 010 | | | | | | | |
| | | | 030 | | | | | | | |
| | | | 050 | | | | | | | |
| | | | 100 | | | | | | | |
| | | | 200 | | | | | | | |

*Example:*
**ASC OS-325MF-PG-002-K3-1A-8L**

Ordering information are based on standard configurations. All customized versions regarding connector and/or pinout will lead to a corresponding product match code:

- Standard length of the integrated cable is 1 meter. However, different customized cable lengths are possible on request.
- Standard version has no connector at the cable end which is identified by "A" in the product match code. However, it is possible to assemble almost all connector types during production.

## Safety Precaution for Installing and Operating

This data sheet is a part of the product. Read the data sheet carefully before using the product and keep it available for future operation. Handling, electrical connections, mounting or any other work performed at the sensor must be carried out by authorized experts only. Appropriate safety precautions must be taken to exclude any risk of personal injury and damage to operating equipment as a result of a sensor malfunction.

### Handling

The sensor is packaged in a reliable housing to protect the sensing elements and integrated electronic components from the ambient environment. However, poor handling of the product can lead to damages that may not be visible and cause electrical failure or reliability issues. Handle the component with caution:

- Avoid shocks and impacts on the housing, such as dropping the sensor on hard surface
- Never move the sensor by pulling the cable
- Make sure that the sensor is used within the specified environmental conditions
- Transport and store the sensor in its original or similar packaging
- The sensor should be mounted on a stable flat surface with all screws tightened or other mounting options
- Avoid any deformation during mounting the sensor
- Mounting tolerances may have an influence on the measured result

### Electrical

ASC's inertial sensors are working with many established data acquisition systems. However, make sure that a proper DAQ is used, for the corresponding operation principle of the sensor. Furthermore, suitable precautions shall be employed during all phases of shipment, handling and operating:

- Active sensor pins are susceptible to damage due to electrostatic discharge (ESD)
- Make sure that the sensor is used within the specified electrical conditions
- Check all electrical connections prior to initial setup of the sensor
- Completely shield the sensor and connecting cable
- Do not perform any electrical modifications at the sensor
- Do not perform any adaptions on the wiring or connectors while the device under power
- Never plug or unplug the electrical connection while the sensor is under power
- When a certain pin is not used during operation, make sure that the pin is insulated

## Quality

- We have a quality management system according to ISO 9001:2015.
- The Deutsche Akkreditierungsstelle GmbH (DAkkS) has awarded to our calibration laboratory the DIN EN ISO/IEC 17025:2018 accreditation for calibrations and has confirmed our competence to perform calibrations in the field of mechanical acceleration measurements. The pictured DAkkS-ILAC logo refers exclusively to the accredited service.
- All ASC products are CE-compliant.



ASC GmbH | Ledererstraße 10 | 85276 Pfaffenhofen | Germany | Phone: +49 8441 786547-0 | E-mail: office@asc-sensors.de | www.asc-sensors.de

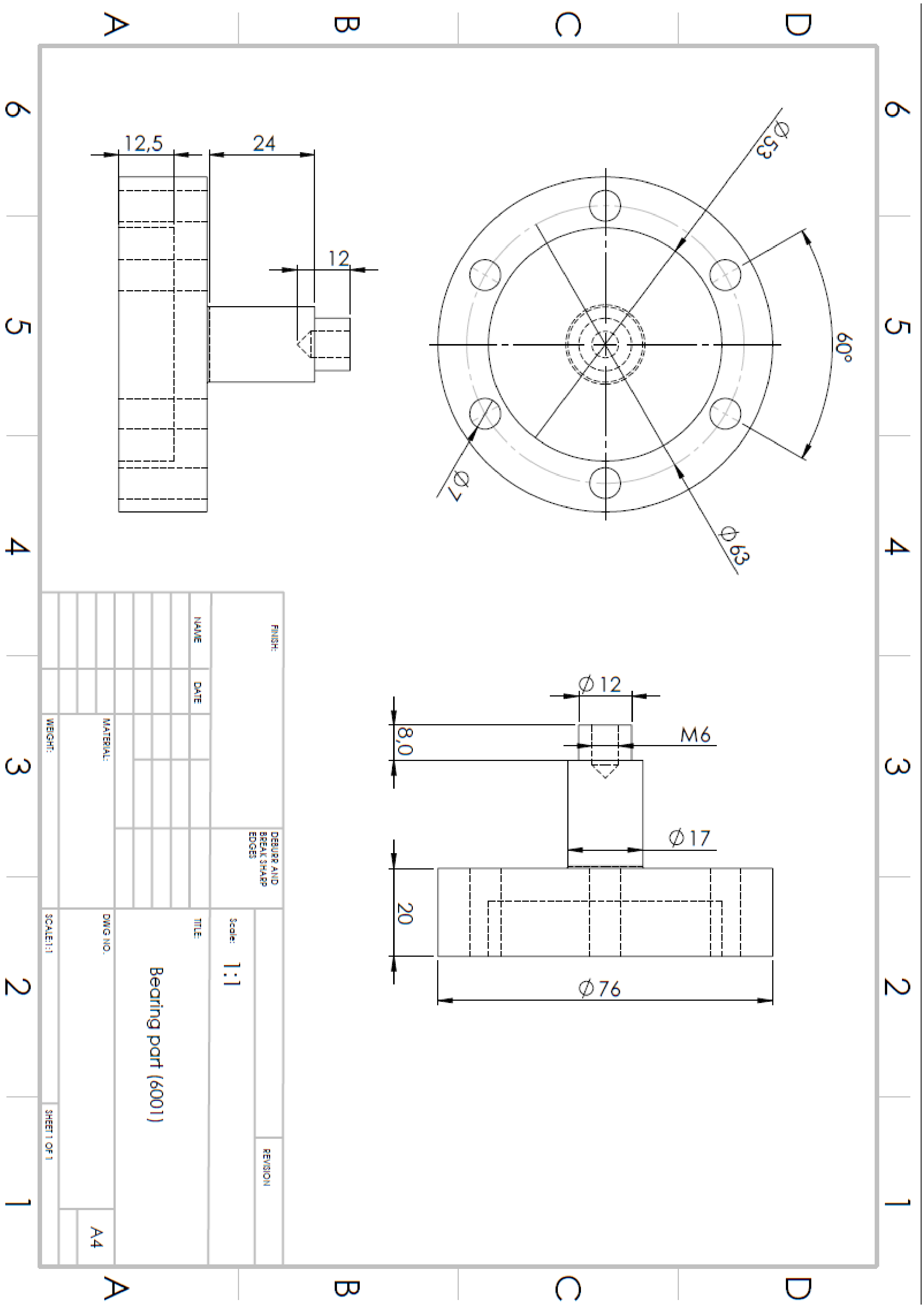
12,5
24
12
Ø53
60°
Ø7
Ø63
Ø12
M6
8,0
Ø17
20
Ø76
FINISH:
DEBURR AND BREAK SHARP EDGES
NAME
DATE
MATERIAL:
WEIGHT:
TITLE:
Bearing part (6001)
Scale: 1:1
DWG NO.
SCALE:1:1
SHEET 1 OF 1
REVISION
A4

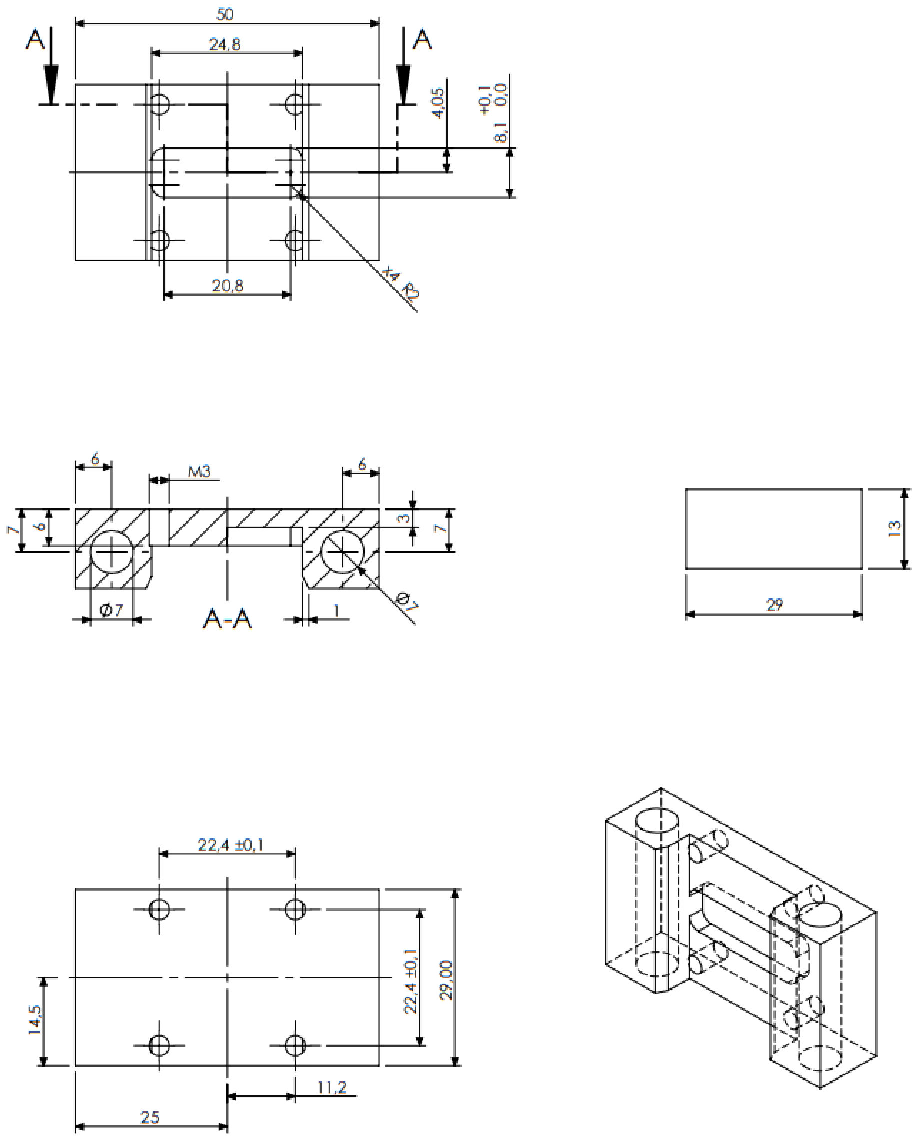


| | | |
|---|---|---|
| UNLESS OTHERWISE SPECIFIED: DIMENSIONS ARE IN MILLIMETERS SURFACE FINISH: TOLERANCES: LINEAR: ANGULAR: | FINISH: | DEBURR AND BREAK SHARP EDGES |

DO NOT SCALE DRAWING

REVISION

| | NAME | SIGNATURE | DATE |
|---|---|---|---|
| DRAWN | | | |
| CHK'D | | | |
| APPV'D | | | |
| MFG | | | |
| Q.A | | | |

TITLE: Sensor ASC Bearing test

MATERIAL: VA-Stahl

WEIGHT:

DWG NO.

A4

SCALE:1:1

SHEET 1 OF 1

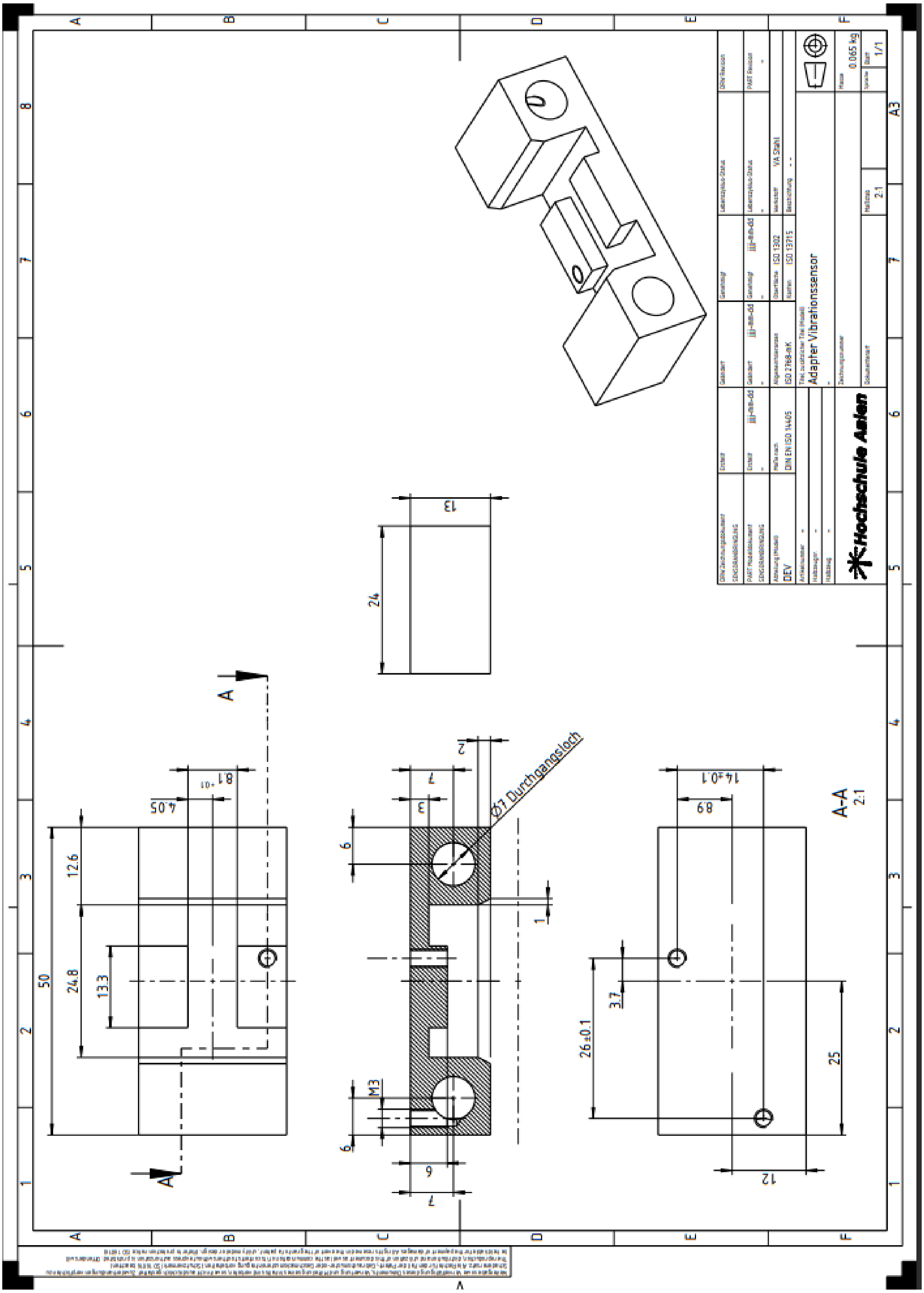
Adapter Vibrationssensor
Hochschule Aalen
Ø7 Durchgangsloch
A-A
2:1
M3
VA Stahl
ISO 2768-mK
DIN EN ISO 14405
0.065 kg
A3

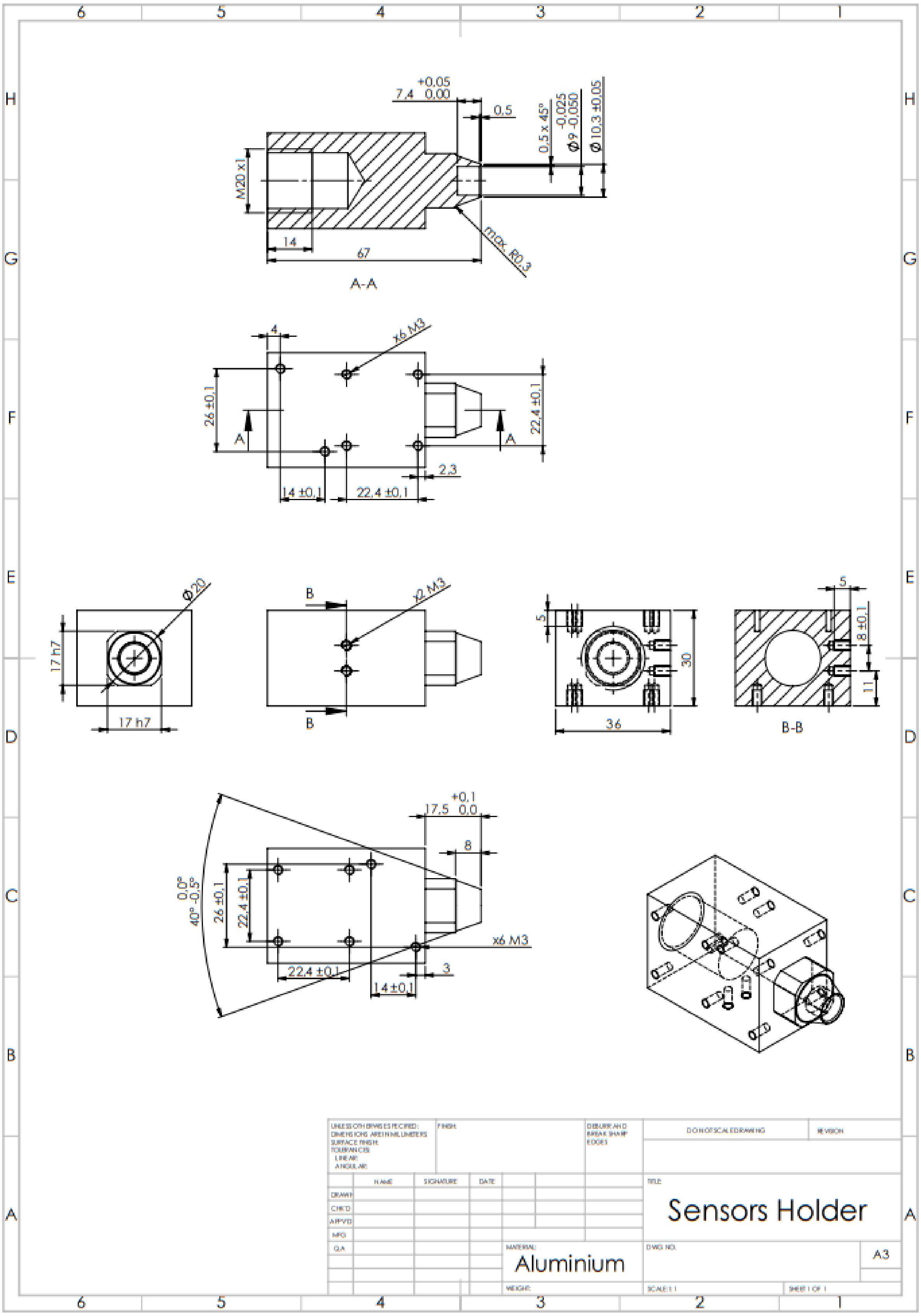
A-A
M20 x1
14
67
7,4 +0,05 0,00
0,5
0,5 x 45°
Ø 9 -0,025 -0,050
Ø 10,3 ±0,05
max. R0,3
x6 M3
4
26 ±0,1
22,4 ±0,1
2,3
14 ±0,1
A
Ø 20
17 h7
x2 M3
B
5
30
36
8 ±0,1
11
B-B
+0,1
17,5 0,0
8
40° 0,0° -0,5°
3
14±0,1
UNLESS OTHERWISE SPECIFIED: DIMENSIONS ARE IN MILLIMETERS SURFACE FINISH: TOLERANCES: LINEAR: ANGULAR:
FINISH:
DEBURR AND BREAK SHARP EDGES
DO NOT SCALE DRAWING
REVISION
NAME
SIGNATURE
DATE
DRAWN
CHK'D
APPV'D
MFG
Q.A
TITLE:
Sensors Holder
MATERIAL:
Aluminium
DWG NO.
A3
WEIGHT:
SCALE:1:1
SHEET 1 OF 1

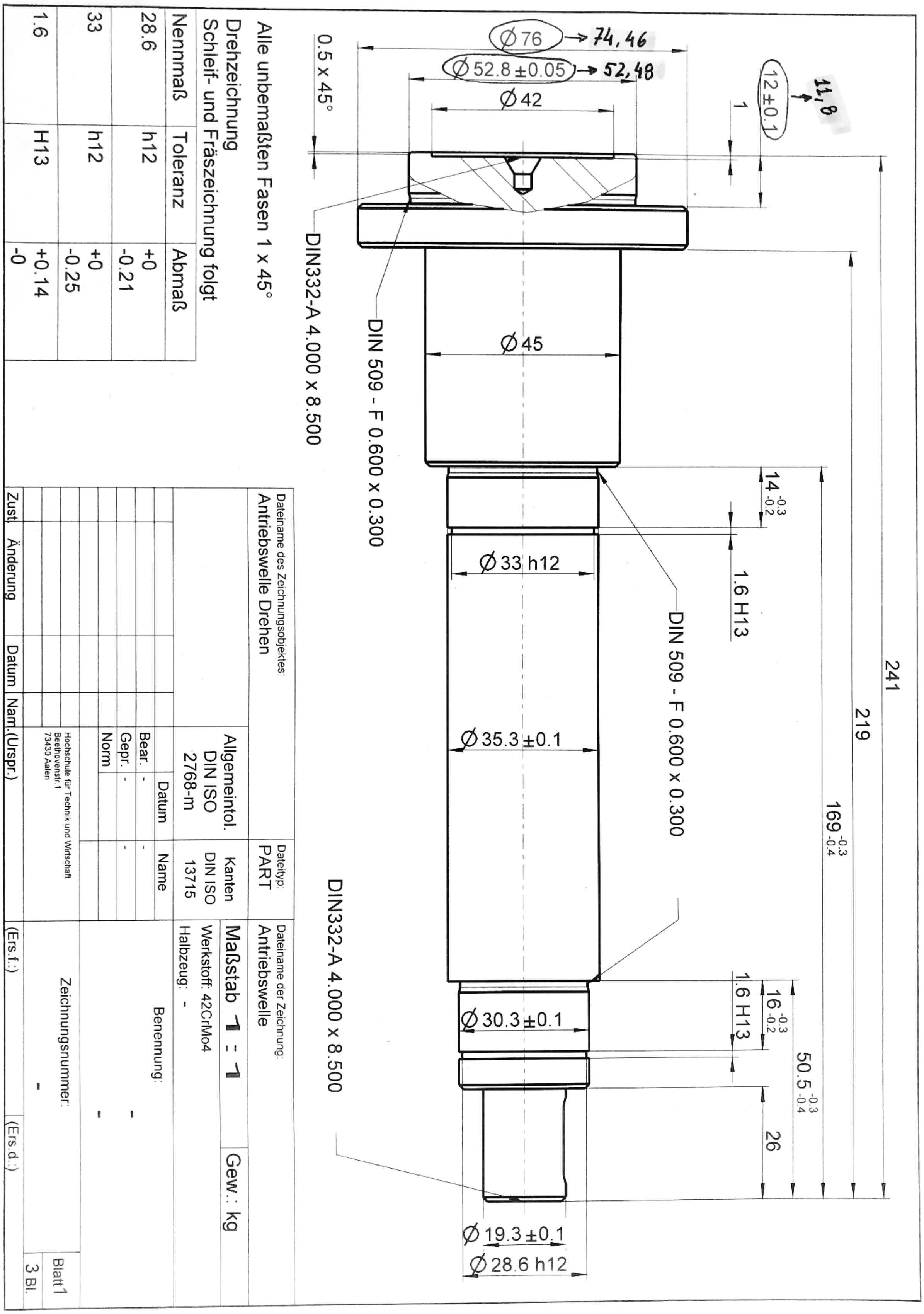
Ø76 → 74,46
Ø52.8 ±0.05 → 52,48
Ø42
12 ±0.1 → 11,8
1
0.5 x 45°
Alle unbemaßten Fasen 1 x 45°
Drehzeichnung
Schleif- und Fräszeichnung folgt
Nennmaß Toleranz Abmaß
28.6 h12 +0 -0.21
33 h12 +0 -0.25
1.6 H13 +0.14 -0
DIN332-A 4.000 x 8.500
DIN 509 - F 0.600 x 0.300
Ø45
14 -0.3 -0.2
1.6 H13
Ø33 h12
DIN 509 - F 0.600 x 0.300
Ø35.3 ±0.1
241
219
169 -0.3 -0.4
DIN332-A 4.000 x 8.500
1.6 H13
16 -0.3 -0.2
Ø30.3 ±0.1
50.5 -0.3 -0.4
26
Ø19.3 ±0.1
Ø28.6 h12
Dateiname des Zeichnungsobjektes:
Antriebswelle Drehen
Dateityp:
PART
Allgemeintol.
DIN ISO
2768-m
Kanten
DIN ISO
13715
Datum
Name
Bear. -
Gepr. -
Norm
Hochschule für Technik und Wirtschaft
Beethovenstr. 1
73430 Aalen
Dateiname der Zeichnung:
Antriebswelle
Maßstab 1 : 1
Gew.: kg
Werkstoff: 42CrMo4
Halbzeug: -
Benennung:
Zeichnungsnummer:
Blatt 1
3 Bl.
Zust.
Änderung
Datum
Nam.(Urspr.)
(Ers.f.:)
(Ers.d.:)

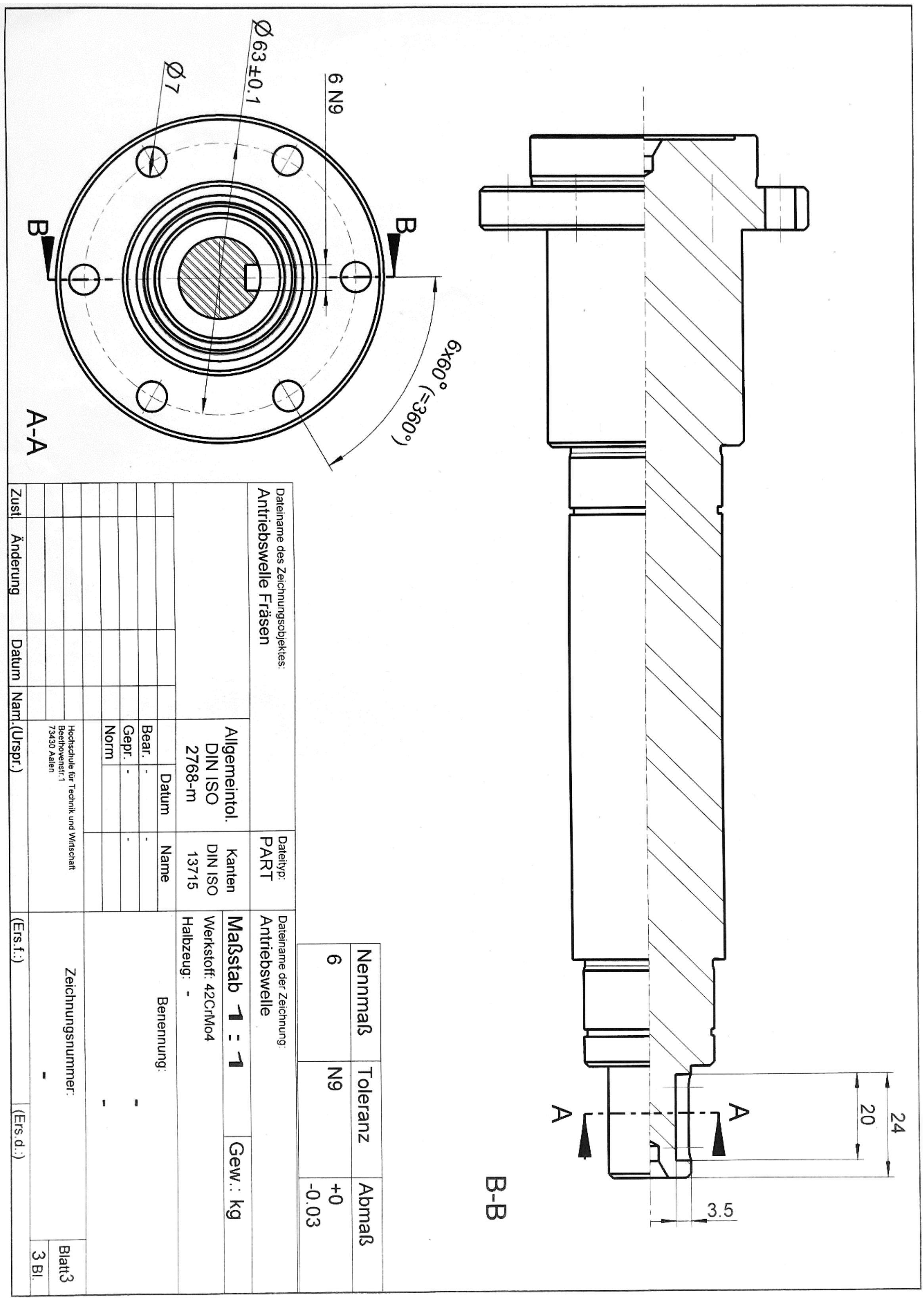
A-A
Ø63 ±0.1
Ø7
6 N9
B
B
6x60° (=360°)
B-B
A
A
24
20
3.5
Nennmaß
Toleranz
Abmaß
6
N9
+0
-0.03
Dateiname des Zeichnungsobjektes:
Antriebswelle Fräsen
Dateityp:
PART
Dateiname der Zeichnung:
Antriebswelle
Allgemeintol.
DIN ISO
2768-m
Kanten
DIN ISO
13715
Maßstab 1 : 1
Gew.: kg
Werkstoff: 42CrMo4
Halbzeug: -
Datum
Name
Bear. -
Gepr. -
Norm
Benennung:
Hochschule für Technik und Wirtschaft
Beethovenstr. 1
73430 Aalen
Zeichnungsnummer:
Blatt3
3 Bl.
Zust.
Änderung
Datum
Nam.(Urspr.)
(Ers.f.:)
(Ers.d.:)

Appendix F – ASC OS 325MF-PG-002 Calibration

ASC GmbH, Ledererstraße 10, 85276 Pfaffenhofen, Germany
www.asc-sensors.de

Kalibrierlaboratorium
*Calibration laboratory*

| 35588 X |
|---|
| ASC GmbH |
| 2021-02 |

# Werkskalibrierschein

*Factory Calibration Certificate*

| | |
|---|---|
| Gegenstand<br>*Object* | **Accelerometer** |
| Hersteller<br>*Manufacturer* | **ASC GmbH** |
| Typ<br>*Type* | **ASC OS-325MF-PG-005** |
| Fabrikat/Serien-Nr.<br>*Serial number* | **21-41733 X** |
| Auftraggeber<br>*Customer* | **HS-Aalen, ZOT**<br>**Anton-Huber-Straße 21**<br>**DE -73430 Aalen** |
| Auftragsnummer<br>*Order No.* | **AB21-0007** |
| Anzahl der Seiten des Kalibrierscheines<br>*Number of pages of the certificate* | **4** |
| Datum der Kalibrierung<br>*Date of calibration* | **18.02.2021** |

Dieser Kalibrierschein dokumentiert die Rückführung auf nationale Normale zur Darstellung der Einheiten in Übereinstimmung mit dem Internationalen Einheitensystem (SI).

Für die Einhaltung einer angemessenen Frist zur Wiederholung der Kalibrierung ist der Benutzer verantwortlich.

*This calibration certificate documents the traceability to national standards, which realize the units of measurement according to the international Systems of Units (SI).*

*The user is obliged to have the object recalibrated at appropriate intervals.*

Dieser Kalibrierschein darf nur vollständig und unverändert weiterverbreitet werden. Auszüge oder Änderungen bedürfen der Genehmigung des ausstellenden Kalibrierlaboratoriums. Kalibrierscheine ohne Unterschrift und Stempel haben keine Gültigkeit.

*This calibration certificate may not be reproduced other than completely except with permission of the issuing company. Calibration certificates without signature and seal are not valid.*

| Stempel<br>*Seal* | Datum<br>*Date* | geprüft durch<br>*reviewed by* | Bearbeiter<br>*Person in charge* |
|---|---|---|---|
| | 18.02.2021 | Dr. Robert Diemer | Julia Maas |

ASC GmbH, Ledererstraße 10, 85276 Pfaffenhofen, Germany
www.asc-sensors.de

## 1. Object of Calibration

| | |
|---|---|
| Object: | **Accelerometer** |
| Manufacturer: | **ASC GmbH** |
| Type: | **ASC OS-325MF-PG-005** |
| Serial number: | **21-41733 X** |

## 2. Calibration Method

Calibration was performed using the method of comparison according to Directive "DKD-R 3-1 Blatt 3 Stand 2010". The transducer was exposed to sinusoidal acceleration which was applied by means of an electrody-namic vibration exciter. The transducer was calibrated by comparing the output of the transducer under test with that of a reference acceleration transducer.

## 3. Environmental Conditions

| | |
|---|---|
| Environmental temperature of the test object: | **(21,0 ± 1) °C** |
| Relative humidity: | **(39 ± 5) %** |

## 4. Test Conditions

| | |
|---|---|
| Position of exciting axis (axes) relative to the earth gravity: | **horizontal** |
| Temperature of test object: | **(21,0 ± 2) °C** |
| Attachment of test object to vibration exciter: | **glued** |
| Tightening torque: | **-** |

Technical data of the connecting cable (cable of the laboratory)

| | |
|---|---|
| Manufacturer: | **Kabeltronik** |
| Type: | **Sensocord-M/D** |
| Length: | **2,5 m** |

Transducer:

**Manufacturer: ASC GmbH** **Type: ASC OS-325MF-PG-005** **S/N: 21-41733 X**

## 5. Measurement Uncertainty

These are the total relative measurement uncertainties at selected values:

- for determination of the transfer coefficient at 8 or 16 Hz 1,0%/1,1°
- for determination of the amplitude-frequency response in the frequency range

| | | |
|---|---|---|
| 0,4 Hz bis | <1 Hz | 1,5% / 1,5° |
| 1 Hz bis | 63 Hz | 1,25%/ 1,25° |
| >63 Hz bis | 160 Hz | 1,25% / 1,5° |

The specified values are the extended measurement uncertainties obtained by multiplying the standard measurement uncertainties by extension factor k = 2. They were ascertained in line with DKD-3. The values of the measuring quantity fall into the assigned intervals with a probability of 95 %.

## 6. Components of the Reference Measuring Equipment

| | Manufacturer | Type | Serial number |
|---|---|---|---|
| Vibration exciter | APS Dynamics Inc. | 113AB | 2150 |
| Ref. standard transducer | Honeywell | QA1400 | 1618 |
| Calibration system | SPEKTRA GmbH Dresden | SRS 35 | 200712 |

Calibration system DKD-K-08665 2020-08 and Ref. Standard transducer DKD-K-06671-2019-09
The listed components are traced back to national standards.

## 7. Results

### 7.1 Determination of the Transfer Coefficient

| | | |
|---|---|---|
| Frequency: | **16 Hz** | |
| Acceleration (peak): | **5 m/s²** | |
| Offset: | **3 mV** | |
| Standard deviation: | **0,0016 mV/(m/s²)** | **0 %** |
| Mean value: | **55,364 mV/(m/s²)** | **542,94 mV/g** |
| Supply voltage: | **10 VDC** | |

(acceleration due to gravity $g_n$ = 9,80665 m/s²)

Transducer:

**Manufacturer: ASC GmbH** **Type: ASC OS-325MF-PG-005** **S/N: 21-41733 X**

## 7.2 Amplitude-Frequency Response (relative to 16 Hz)

| Frequency Hz | Acceleration m/s² pk | Transfer coefficient mV/(m/s²) | Deviation % | Phase shift degree |
|---|---|---|---|---|
| 1 | 1,39 | 55,402 | 0,07 | -0,07 |
| 1,6 | 3,6 | 55,366 | 0 | -0,1 |
| 2 | 5,08 | 55,37 | 0,01 | -0,12 |
| 2,5 | 5,07 | 55,367 | 0 | -0,15 |
| 4 | 5,08 | 55,37 | 0,01 | -0,24 |
| 6,3 | 5,08 | 55,411 | 0,08 | -0,37 |
| 8 | 5,08 | 55,395 | 0,06 | -0,47 |
| 10 | 5,06 | 55,384 | 0,04 | -0,6 |
| 12,5 | 5,05 | 55,37 | 0,01 | -0,75 |
| 20 | 5 | 55,38 | 0,03 | -1,18 |
| 31,5 | 5 | 55,375 | 0,02 | -1,86 |
| 45 | 5 | 55,375 | 0,02 | -2,61 |
| 60 | 5 | 55,466 | 0,18 | -3,56 |
| 80 | 5 | 55,473 | 0,2 | -4,73 |
| 100 | 5 | 55,375 | 0,02 | -5,94 |

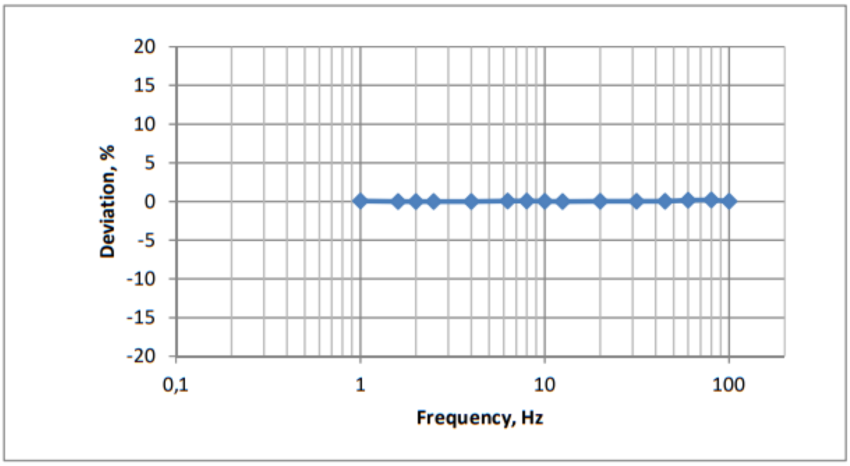

ASC GmbH, Ledererstraße 10, 85276 Pfaffenhofen, Germany
www.asc-sensors.de

Kalibrierlaboratorium
*Calibration laboratory*

| 35588 Y |
|---|
| ASC GmbH |
| 2021-02 |

# Werkskalibrierschein
*Factory Calibration Certificate*

| | |
|---|---|
| Gegenstand<br>*Object* | **Accelerometer** |
| Hersteller<br>*Manufacturer* | **ASC GmbH** |
| Typ<br>*Type* | **ASC OS-325MF-PG-005** |
| Fabrikat/Serien-Nr.<br>*Serial number* | **21-41733 Y** |
| Auftraggeber<br>*Customer* | **HS-Aalen, ZOT**<br>**Anton-Huber-Straße 21**<br>**DE -73430 Aalen** |
| Auftragsnummer<br>*Order No.* | **AB21-0007** |
| Anzahl der Seiten des Kalibrierscheines<br>*Number of pages of the certificate* | **4** |
| Datum der Kalibrierung<br>*Date of calibration* | **18.02.2021** |

Dieser Kalibrierschein dokumentiert die Rückführung auf nationale Normale zur Darstellung der Einheiten in Übereinstimmung mit dem Internationalen Einheitensystem (SI).

Für die Einhaltung einer angemessenen Frist zur Wiederholung der Kalibrierung ist der Benutzer verantwortlich.

*This calibration certificate documents the traceability to national standards, which realize the units of measurement according to the international Systems of Units (SI).*

*The user is obliged to have the object recalibrated at appropriate intervals.*

Dieser Kalibrierschein darf nur vollständig und unverändert weiterverbreitet werden. Auszüge oder Änderungen bedürfen der Genehmigung des ausstellenden Kalibrierlaboratoriums. Kalibrierscheine ohne Unterschrift und Stempel haben keine Gültigkeit.

*This calibration certificate may not be reproduced other than completely except with permission of the issuing company. Calibration certificates without signature and seal are not valid.*

| Stempel<br>*Seal* | Datum<br>*Date* | geprüft durch<br>*reviewed by* | Bearbeiter<br>*Person in charge* |
|---|---|---|---|
| | 18.02.2021 | Dr. Robert Diemer | Julia Maas |

## 1. Object of Calibration

Object: **Accelerometer**
Manufacturer: **ASC GmbH**
Type: **ASC OS-325MF-PG-005**
Serial number: **21-41733 Y**

## 2. Calibration Method

Calibration was performed using the method of comparison according to Directive "DKD-R 3-1 Blatt 3 Stand 2010". The transducer was exposed to sinusoidal acceleration which was applied by means of an electrody-namic vibration exciter. The transducer was calibrated by comparing the output of the transducer under test with that of a reference acceleration transducer.

## 3. Environmental Conditions

Environmental temperature of the test object: **(21,0 ± 1) °C**
Relative humidity: **(39 ± 5) %**

## 4. Test Conditions

Position of exciting axis (axes) relative to the earth gravity: **horizontal**
Temperature of test object: **(21,0 ± 2) °C**

Attachment of test object to vibration exciter: **glued**
Tightening torque: **-**

Technical data of the connecting cable (cable of the laboratory)
Manufacturer: **Kabeltronik**
Type: **Sensocord-M/D**
Length: **2,5 m**

## 5. Measurement Uncertainty

These are the total relative measurement uncertainties at selected values:
- for determination of the transfer coefficient at 8 or 16 Hz 1,0%/1,1°
- for determination of the amplitude-frequency response in the frequency range

| | | |
|---|---|---|
| 0,4 Hz bis | <1 Hz | 1,5% / 1,5° |
| 1 Hz bis | 63 Hz | 1,25%/ 1,25° |
| >63 Hz bis | 160 Hz | 1,25% / 1,5° |

The specified values are the extended measurement uncertainties obtained by multiplying the standard measurement uncertainties by extension factor k = 2. They were ascertained in line with DKD-3. The values of the measuring quantity fall into the assigned intervals with a probability of 95 %.

## 6. Components of the Reference Measuring Equipment

| | Manufacturer | Type | Serial number |
|---|---|---|---|
| Vibration exciter | APS Dynamics Inc. | 113AB | 2150 |
| Ref. standard transducer | Honeywell | QA1400 | 1618 |
| Calibration system | SPEKTRA GmbH Dresden | SRS 35 | 200712 |

Calibration system DKD-K-08665 2020-08 and Ref. Standard transducer DKD-K-06671-2019-09
The listed components are traced back to national standards.

## 7. Results

### 7.1 Determination of the Transfer Coefficient

| | | | |
|---|---|---|---|
| Frequency: | **16 Hz** | | |
| Acceleration (peak): | **5 m/s²** | | |
| Offset: | **-10 mV** | | |
| Standard deviation: | **0,0039 mV/(m/s²)** | **0,001 %** | |
| Mean value: | **55,363 mV/(m/s²)** | **542,93 mV/g** | |
| Supply voltage: | **10 VDC** | | |

(acceleration due to gravity $g_n$ = 9,80665 m/s²)

**7.2 Amplitude-Frequency Response (relative to 16 Hz)**

| Frequency<br>Hz | Acceleration<br>m/s² pk | Transfer coefficient<br>mV/(m/s²) | Deviation<br>% | Phase shift<br>degree |
|---|---|---|---|---|
| 1 | 1,39 | 55,369 | 0,01 | -0,07 |
| 1,6 | 3,59 | 55,343 | -0,04 | -0,1 |
| 2 | 5,08 | 55,347 | -0,03 | -0,12 |
| 2,5 | 5,07 | 55,346 | -0,03 | -0,15 |
| 4 | 5,08 | 55,349 | -0,03 | -0,24 |
| 6,3 | 5,08 | 55,395 | 0,06 | -0,38 |
| 8 | 5,08 | 55,375 | 0,02 | -0,48 |
| 10 | 5,06 | 55,368 | 0,01 | -0,6 |
| 12,5 | 5,05 | 55,349 | -0,02 | -0,77 |
| 20 | 5 | 55,308 | -0,1 | -1,2 |
| 31,5 | 5 | 55,449 | 0,16 | -1,97 |
| 45 | 5 | 55,339 | -0,04 | -2,65 |
| 60 | 5 | 55,821 | 0,83 | -3,73 |
| 80 | 5 | 56,028 | 1,2 | -4,55 |
| 100 | 5 | 55,258 | -0,19 | -6 |

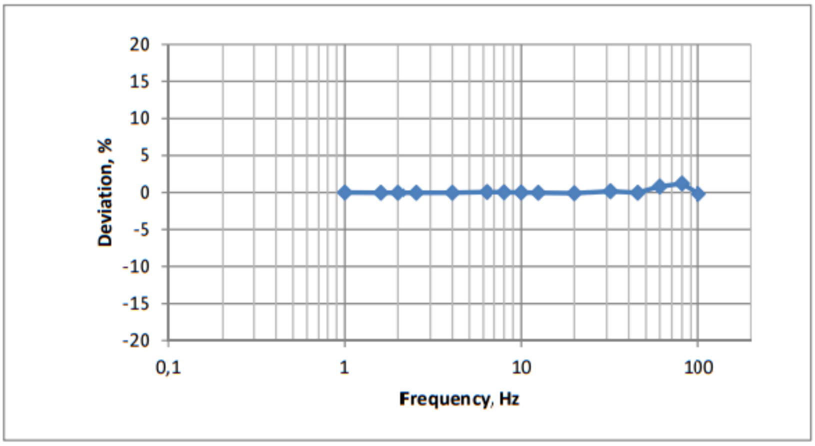

ASC GmbH, Ledererstraße 10, 85276 Pfaffenhofen, Germany
www.asc-sensors.de

Kalibrierlaboratorium
*Calibration laboratory*

| 35588 Z |
|---|
| ASC GmbH |
| 2021-02 |

# Werkskalibrierschein
*Factory Calibration Certificate*

| | |
|---|---|
| Gegenstand *Object* | **Accelerometer** |
| Hersteller *Manufacturer* | **ASC GmbH** |
| Typ *Type* | **ASC OS-325MF-PG-005** |
| Fabrikat/Serien-Nr. *Serial number* | **21-41733 Z** |
| Auftraggeber *Customer* | **HS-Aalen, ZOT**<br>**Anton-Huber-Straße 21**<br>**DE -73430 Aalen** |
| Auftragsnummer *Order No.* | **AB21-0007** |
| Anzahl der Seiten des Kalibrierscheines *Number of pages of the certificate* | **4** |
| Datum der Kalibrierung *Date of calibration* | **18.02.2021** |

Dieser Kalibrierschein dokumentiert die Rückführung auf nationale Normale zur Darstellung der Einheiten in Übereinstimmung mit dem Internationalen Einheitensystem (SI).

Für die Einhaltung einer angemessenen Frist zur Wiederholung der Kalibrierung ist der Benutzer verantwortlich.

*This calibration certificate documents the traceability to national standards, which realize the units of measurement according to the international Systems of Units (SI).*

*The user is obliged to have the object recalibrated at appropriate intervals.*

Dieser Kalibrierschein darf nur vollständig und unverändert weiterverbreitet werden. Auszüge oder Änderungen bedürfen der Genehmigung des ausstellenden Kalibrierlaboratoriums.
Kalibrierscheine ohne Unterschrift und Stempel haben keine Gültigkeit.

*This calibration certificate may not be reproduced other than completely except with permission of the issuing company. Calibration certificates without signature and seal are not valid.*

| Stempel *Seal* | Datum *Date* | geprüft durch *reviewed by* | Bearbeiter *Person in charge* |
|---|---|---|---|
| | 18.02.2021 | Dr. Robert Diemer | Julia Maas |

## 1. Object of Calibration

| | |
|---|---|
| Object: | **Accelerometer** |
| Manufacturer: | **ASC GmbH** |
| Type: | **ASC OS-325MF-PG-005** |
| Serial number: | **21-41733 Z** |

## 2. Calibration Method

Calibration was performed using the method of comparison according to Directive "DKD-R 3-1 Blatt 3 Stand 2010". The transducer was exposed to sinusoidal acceleration which was applied by means of an electrody-namic vibration exciter. The transducer was calibrated by comparing the output of the transducer under test with that of a reference acceleration transducer.

## 3. Environmental Conditions

| | |
|---|---|
| Environmental temperature of the test object: | **(21,0 ± 1) °C** |
| Relative humidity: | **(39 ± 5) %** |

## 4. Test Conditions

| | |
|---|---|
| Position of exciting axis (axes) relative to the earth gravity: | **horizontal** |
| Temperature of test object: | **(21,0 ± 2) °C** |
| Attachment of test object to vibration exciter: | **glued** |
| Tightening torque: | **-** |

Technical data of the connecting cable (cable of the laboratory)

| | |
|---|---|
| Manufacturer: | **Kabeltronik** |
| Type: | **Sensocord-M/D** |
| Length: | **2,5 m** |

| | | | | |
|---|---|---|---|---|
| Seite 3 | zum Kalibrierschein vom | 18.02.2021 | | **35588 Z** |
| *Page* | *of calibration certificate dated* | | | **ASC** |
| Transducer: | | | | **GmbH** |
| **Manufacturer: ASC GmbH** | **Type: ASC OS-325MF-PG-005** | **S/N: 21-41733 Z** | | **2021-02** |

## 5. Measurement Uncertainty

These are the total relative measurement uncertainties at selected values:

- for determination of the transfer coefficient at 8 or 16 Hz 1,0%/1,1°
- for determination of the amplitude-frequency response in the frequency range

| | | |
|---|---|---|
| 0,4 Hz bis | <1 Hz | 1,5% / 1,5° |
| 1 Hz bis | 63 Hz | 1,25%/ 1,25° |
| >63 Hz bis | 160 Hz | 1,25% / 1,5° |

The specified values are the extended measurement uncertainties obtained by multiplying the standard measurement uncertainties by extension factor k = 2. They were ascertained in line with DKD-3. The values of the measuring quantity fall into the assigned intervals with a probability of 95 %.

## 6. Components of the Reference Measuring Equipment

| | Manufacturer | Type | Serial number |
|---|---|---|---|
| Vibration exciter | APS Dynamics Inc. | 113AB | 2150 |
| Ref. standard transducer | Honeywell | QA1400 | 1618 |
| Calibration system | SPEKTRA GmbH Dresden | SRS 35 | 200712 |

Calibration system DKD-K-08665 2020-08 and Ref. Standard transducer DKD-K-06671-2019-09
The listed components are traced back to national standards.

## 7. Results

### 7.1 Determination of the Transfer Coefficient

| | | | | |
|---|---|---|---|---|
| Frequency: | **16** | **Hz** | | |
| Acceleration (peak): | **5** | **m/s²** | | |
| Offset: | **-7** | **mV** | | |
| Standard deviation: | **0,0042** | **mV/(m/s²)** | **0,001** | **%** |
| Mean value: | **55,39** | **mV/(m/s²)** | **543,19** | **mV/g** |
| Supply voltage: | **10** | **VDC** | | |

(acceleration due to gravity $g_n$ = 9,80665 m/s²)

| 35588 Z |
|---|
| ASC GmbH |
| 2021-02 |

Transducer:

**Manufacturer: ASC GmbH** **Type: ASC OS-325MF-PG-005** **S/N: 21-41733 Z**

## 7.2 Amplitude-Frequency Response (relative to 16 Hz)

| Frequency Hz | Acceleration m/s² pk | Transfer coefficient mV/(m/s²) | Deviation % | Phase shift degree |
|---|---|---|---|---|
| 1 | 1,39 | 55,416 | 0,05 | -0,06 |
| 1,6 | 3,59 | 55,385 | -0,01 | -0,1 |
| 2 | 5,08 | 55,39 | 0 | -0,12 |
| 2,5 | 5,07 | 55,387 | 0 | -0,15 |
| 4 | 5,08 | 55,391 | 0 | -0,24 |
| 6,3 | 5,08 | 55,434 | 0,08 | -0,37 |
| 8 | 5,09 | 55,417 | 0,05 | -0,47 |
| 10 | 5,06 | 55,408 | 0,03 | -0,6 |
| 12,5 | 5,05 | 55,36 | -0,05 | -0,81 |
| 20 | 5 | 55,385 | -0,01 | -1,18 |
| 31,5 | 5 | 55,446 | 0,1 | -1,91 |
| 45 | 5 | 55,366 | -0,04 | -2,63 |
| 60 | 5 | 55,536 | 0,26 | -3,58 |
| 80 | 5 | 55,61 | 0,4 | -4,57 |
| 100 | 5 | 55,413 | 0,04 | -5,94 |

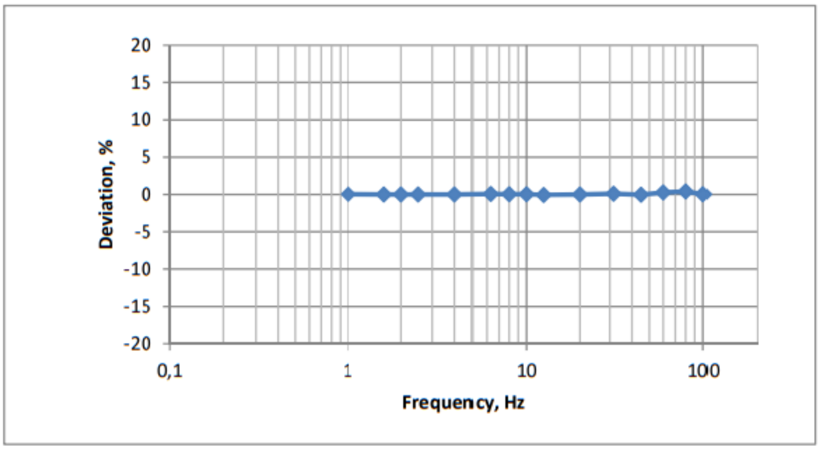

## Appendix G – Trials results

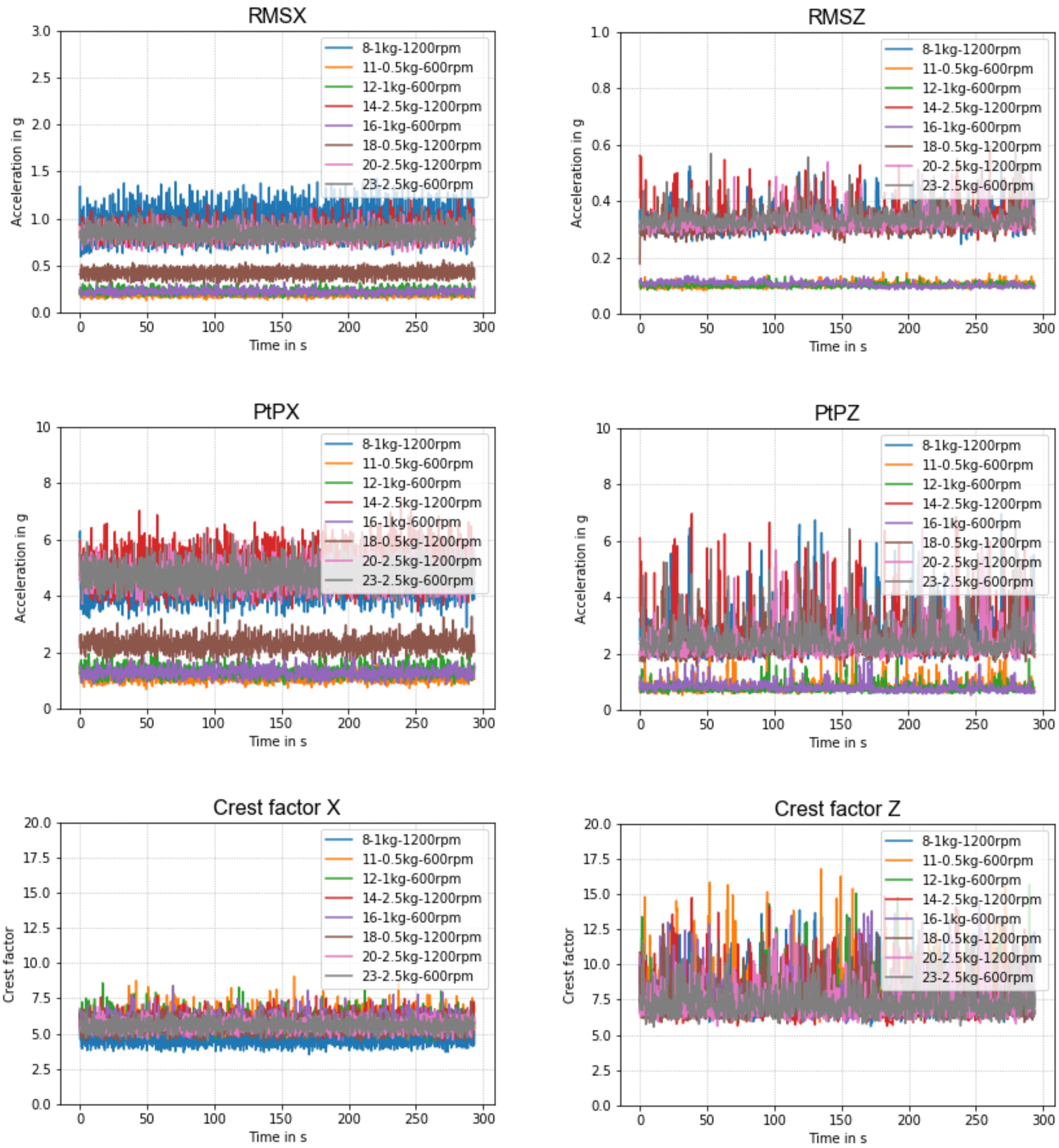


First trials in the test bench with new bearing with BALLUFF sensor

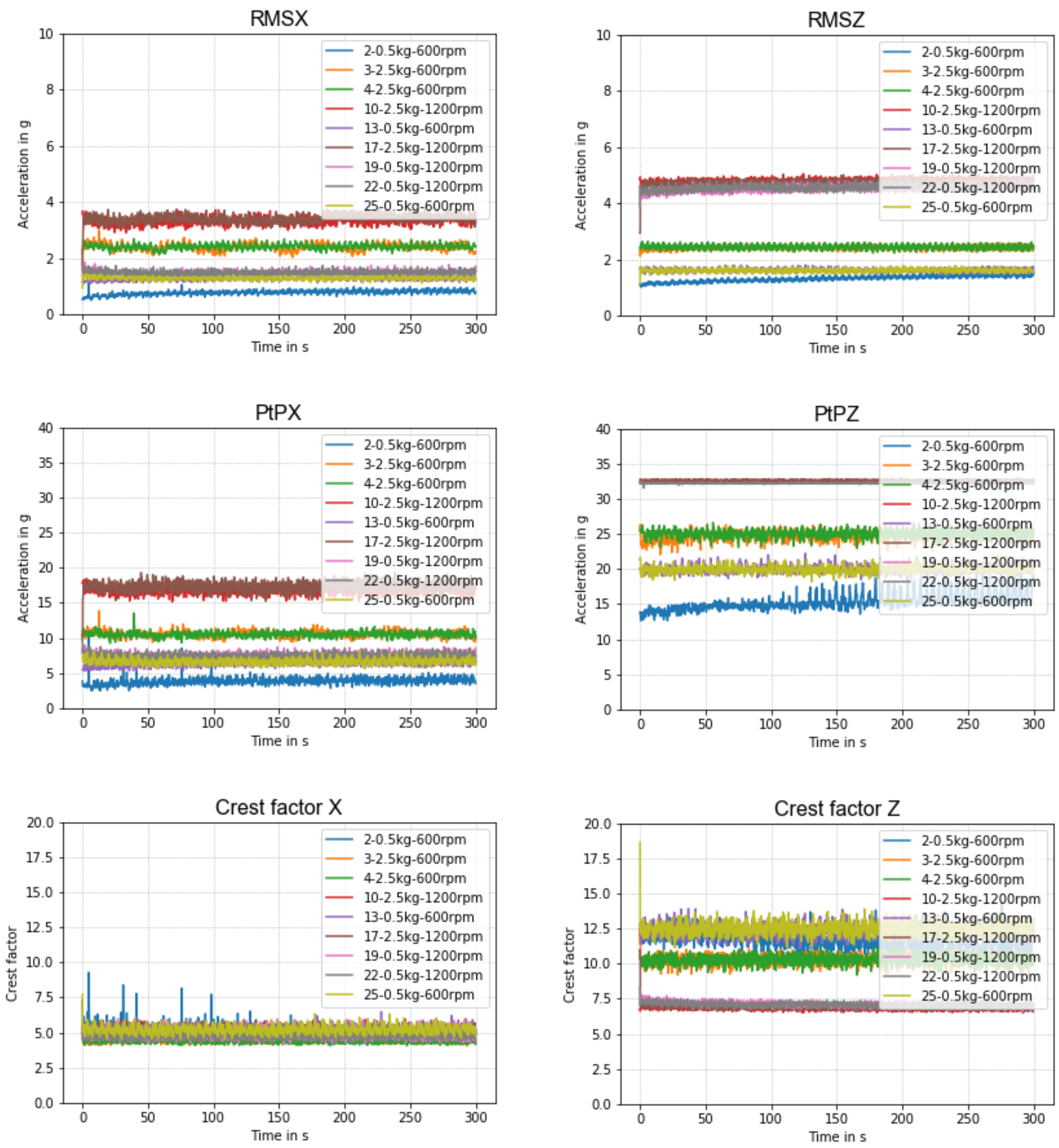


First trials in the test bench with milled bearing with BALLUFF sensor

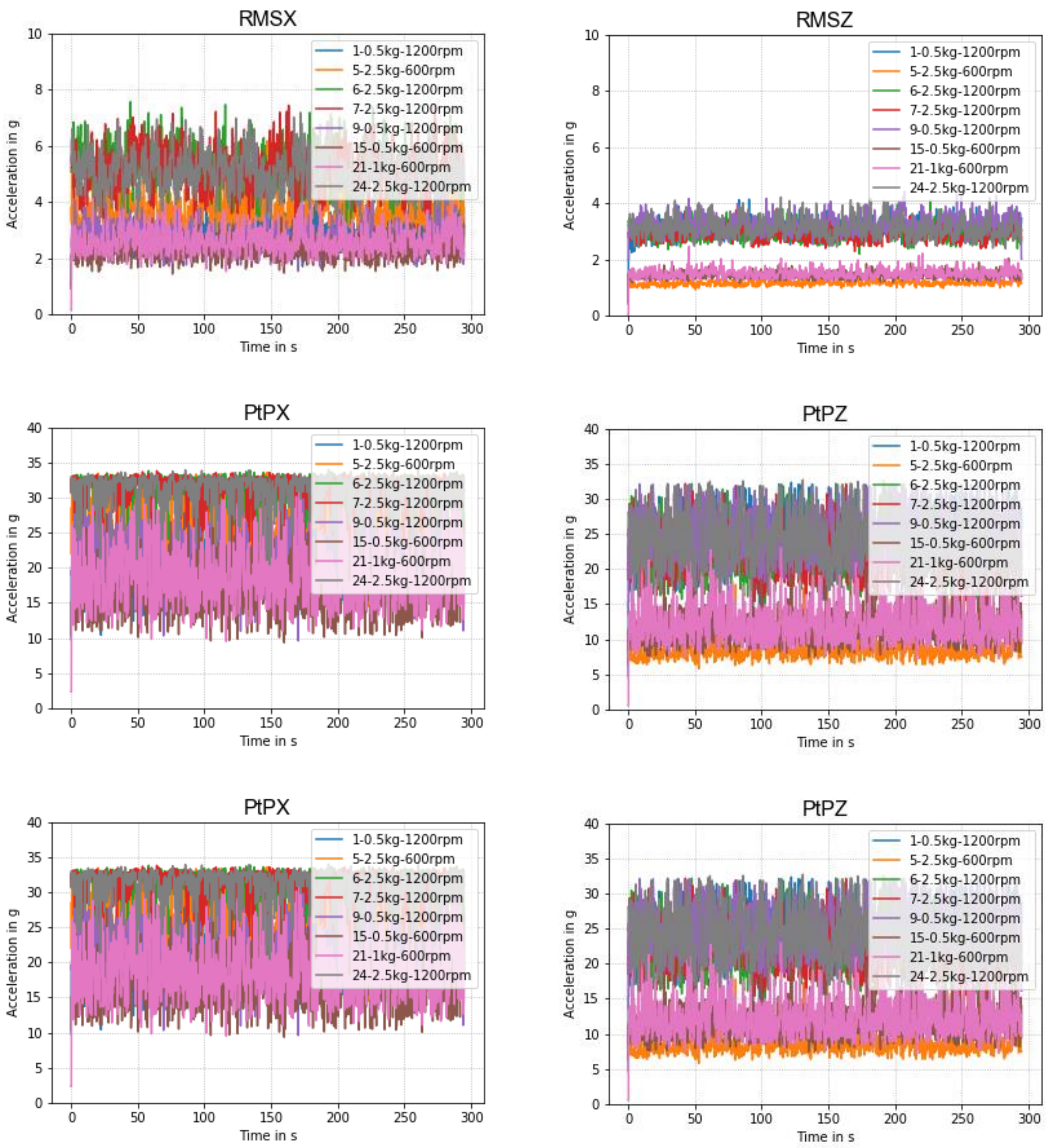


First trials in the test bench with corrosive bearing with BALLUFF sensor

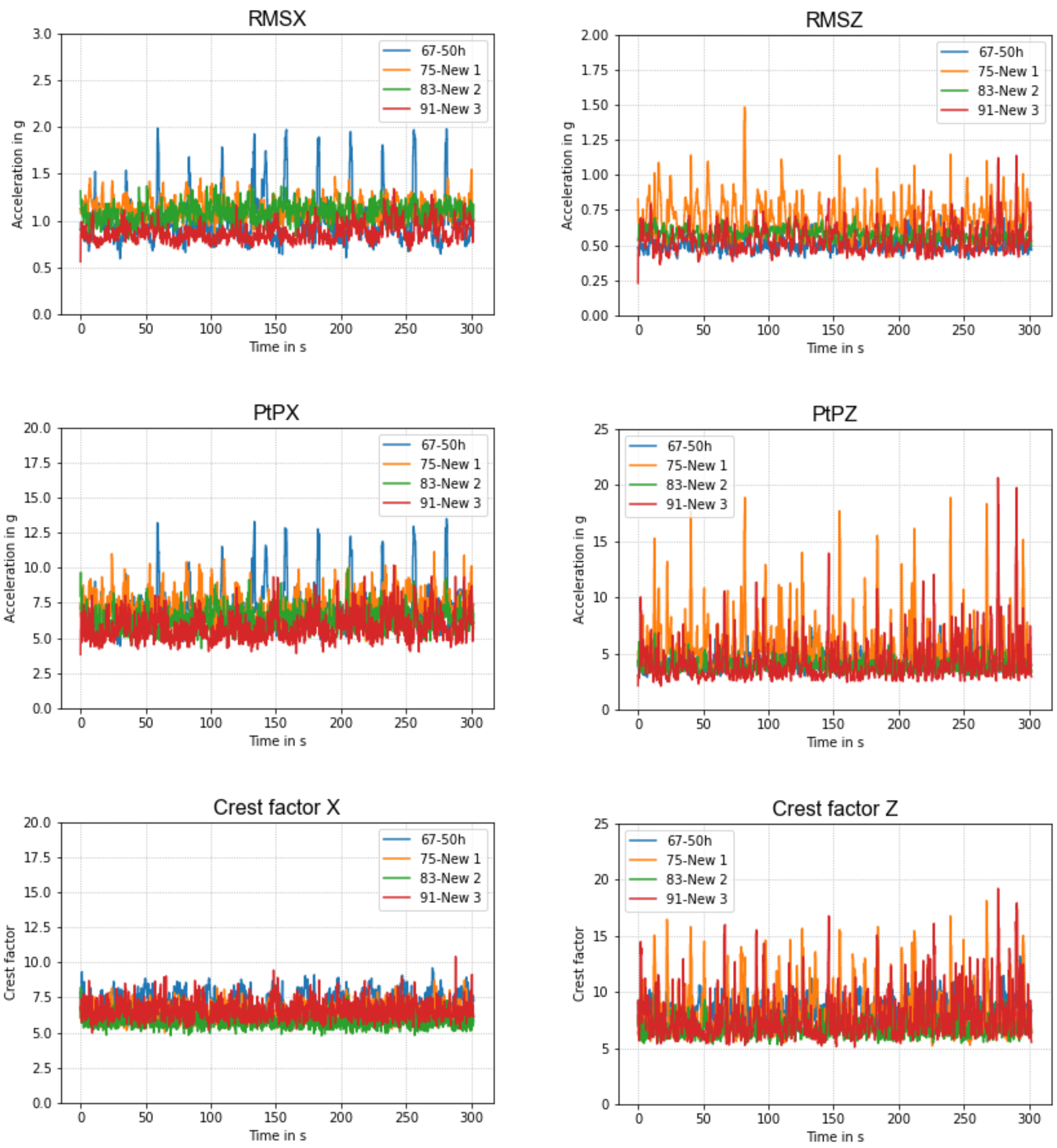


Second trials in the test bench with corrosive bearing with BALLUFF sensor (1200rpm)

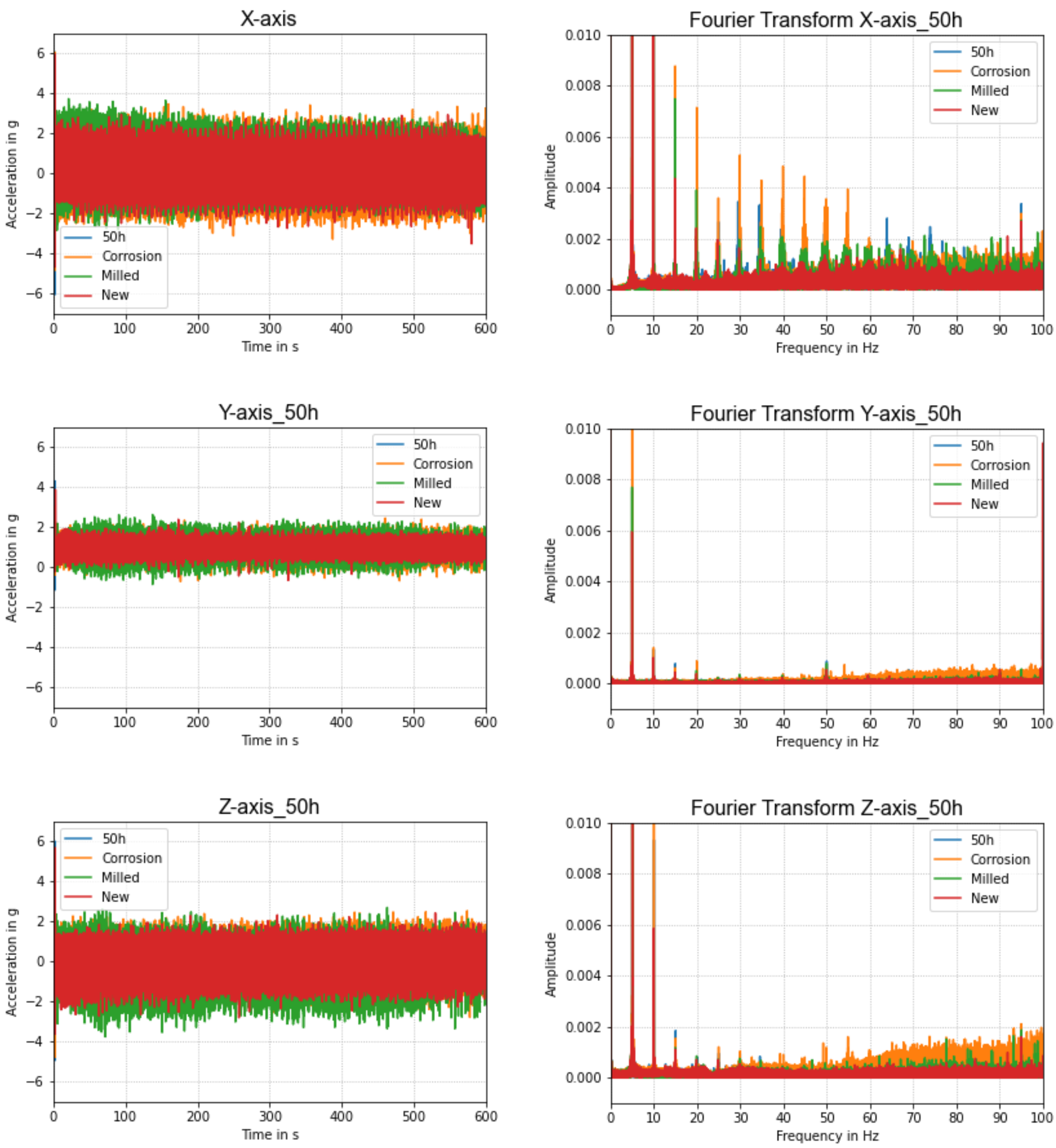


Last trials in the polishing head robot with ASC-325 sensor (300rpm)

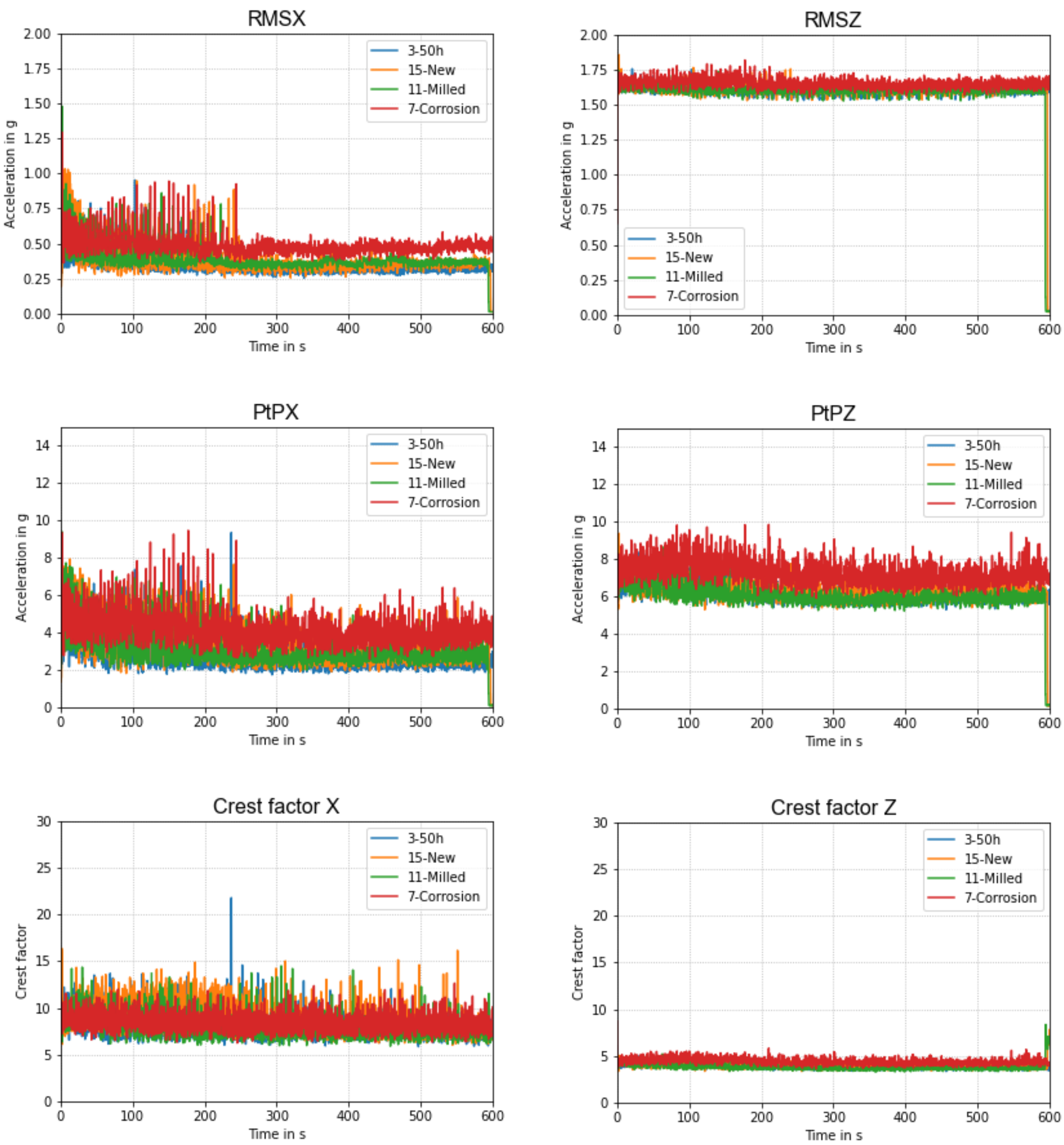


Last trials in the polishing head robot with ASC-325 sensor (300rpm)